

**EXPLORING THE ROLE OF ELEVATED LIPID PEROXIDATION AND
GLUTATHIONE PEROXIDASE 4 IN METABOLIC SYNDROME AND
CARDIAC REMODELING IN OBESITY**

By

Lalage Adalaide Katunga

May, 2016

Director of Dissertation: Dr. Ethan J. Anderson

Department of Pharmacology and Toxicology, Brody School of Medicine, East Carolina
University

ABSTRACT

Cardiovascular disease continues to be a leading cause of global mortality. Metabolic perturbations including obesity, hyperlipidemia and type II diabetes arising from a western style diet and a more sedentary lifestyle are significant contributors to this phenomenon. Diabetic patients are at a significantly higher risk of developing heart disease. Approximately 50% of diabetic patients suffer from cardiomyopathy and they are twice as likely to develop congestive heart failure. Importantly, this cardiomyopathy is often independent of hypertension and coronary artery disease, suggesting that factors inherent to the metabolic disease are pathogenic to the heart. Mitochondrial dysfunction is a mechanism that is has been postulated to have an etiological role in the

development of diabetic cardiomyopathy and heart failure. Studies on diabetic hearts reveal these mitochondria have increased reactive oxygen species (ROS) emission, reduced ATP production and oxidative damage. At a gross scale, an early histological finding in the hearts of a sub-set of both diabetic and obese patients is increased collagen deposition and an infiltration of fibroblasts which over time leads to reduced cardiac compliance/ relaxation and ultimately diastolic dysfunction.

Lipid peroxides and reactive aldehyde derivatives (LPPs) are derived from ROS peroxidation of cellular polyunsaturated fatty acids and have been linked to cardiometabolic disease. The objective of this study was to test the hypothesis that LPPs underlie cardiometabolic derangements in obesity. This hypothesis was tested using glutathione peroxidase 4 haploinsufficient (GPx4^{+/-}) mice. GPx4 is one of the few enzymes specialized to neutralize lipid peroxides. GPx4^{+/-} mice were fed a high fat, high sucrose (HFHS) diet to investigate cardiometabolic derangements in a model of increased LPP production. Our research revealed that greater carbonyl stress, exacerbated glucose intolerance, dyslipidemia, and liver steatosis occurred in GPx4^{+/-} mice compared to wild-type (WT) on a high fat high sucrose diet (HFHS). Although normotensive, cardiac hypertrophy was evident with obesity, and cardiac fibrosis was more pronounced in obese GPx4^{+/-} mice. Mitochondrial dysfunction manifesting as decreased fat oxidation capacity and increased reactive oxygen species was also present in obese GPx4^{+/-} but not WT hearts, along with up-regulation of pro-inflammatory and pro-fibrotic genes. Biochemical analysis was also performed on samples of human atrial myocardium revealed patients with diabetes and

hyperglycemia exhibited significantly less GPx4 enzyme and greater HNE-adducts in their hearts, compared with age-matched non-diabetic patients.

The pathogenic role of LPPs was further investigated using carnosinol (CAR), an LPP scavenger that preferentially binds and sequesters reactive aldehydes. In this follow-on study, CAR was administered via drinking water (40mg/kg) starting mid-way through the HFHS diet. In WT mice, CAR improved whole body glucose tolerance, blood lipid profiles and insulin sensitivity. CAR treatment also mitigated HFHS- diet induced cardiac hypertrophy and hepatic steatosis. Levels of 4-HNE adducts were reduced in the cardiac mitochondria, liver and whole heart following treatment. Mitochondrial oxidative phosphorylation efficiency (OxPhos) in the heart was also improved with CAR in WT mice fed HFHS diet, although no effect on mitochondria in the GPx4^{+/-} mice was observed. Collectively, the data presented in this dissertation provide evidence that lipid peroxides and their reactive aldehyde derivatives are a distinct form of oxidative stress that has an etiological role in human cardio-metabolic disease. It establishes that GPx4 is an adaptive response to oxidative stress in obesity, and that deficiency in this important enzyme accelerates the pathogenic effect of the condition. Furthermore, it provides support for the development of a novel class of aldehyde scavenging compounds to ameliorate the cardio-metabolic disease and associated comorbidities common with obesity.

**EXPLORING THE ROLE OF ELEVATED LIPID PEROXIDATION AND
GLUTATHIONE PEROXIDASE 4 IN METABOLIC SYNDROME AND
CARDIAC REMODELING IN OBESITY**

A Dissertation

Presented To

The Faculty of the Department of Pharmacology and Toxicology

The Brody School of Medicine at East Carolina University

In Partial Fulfillment

of the Requirements for the Degree

Doctor of Philosophy in Pharmacology and Toxicology

By

Lalage Adalaide Katunga

May, 2016

© Copyright 2016

Lalage A. Katunga

**EXPLORING THE ROLE OF ELEVATED LIPID PEROXIDATION AND
GLUTATHIONE PEROXIDASE 4 IN METABOLIC SYNDROME AND
CARDIAC REMODELING IN OBESITY**

By

Lalage A. Katunga

APPROVED BY:

DIRECTOR OF

DISSERTATION: _____

(Ethan J. Anderson, PhD)

COMMITTEE MEMBER: _____

(Abdel A. Abdel-Rahman, PhD)

COMMITTEE MEMBER: _____

(Jacques Robidoux, PhD)

COMMITTEE MEMBER: _____

(Jitka Virag, PhD)

COMMITTEE MEMBER: _____

(Saame Raza Shaikh, PhD)

CHAIR OF THE DEPARTMENT

OF (Pharmacology and Toxicology): _____

(David Taylor, PhD)

DEAN OF THE

GRADUATE SCHOOL: _____

Paul J. Gemperline, PhD

ACKNOWLEDGEMENTS

I am eternally grateful to my mother and father for pouring themselves into me and teaching me to be bold and relentless in the pursuit and attainment of my dreams. Emma and Victor you have been my anchor, you have offered the strength and encouragement to face the challenges of a new research day. Yatina thank-you for reminding me to seek out the simple pleasures in each day it has made the journey worthwhile.

My dissertation committee Drs Virag, Abdel- Rahman, Robidoux and Shaikh have been invaluable in the creation of an environment conducive for my growth and at different times have each have played a significant role in the development of my scientific thought process and technical abilities. I would like to thank my mentor Dr Ethan Anderson for creating a perfect incubator for my metamorphosis into an independent investigator. Your enthusiasm for science is contagious and thank-you for believing in me.

Finally the microcosm of people that have made my graduate experiences all the richer, the other members of my laboratory Margaret, Cherese and Preeti. Drs Efird and DeWitt who have played a critical role in shaping my identity as a scientist.

TABLE OF CONTENTS

LIST OF TABLES.....	ix
LIST OF FIGURES.....	x
LIST OF SYMBOLS AND ABBREVIATIONS	xii
CHAPTER ONE: INTRODUCTION.....	1
Metabolic Syndrome and Diabetes.....	2
Diabetes and Heart Disease.....	3
Lipid peroxidation and cellular Damage.....	3
Formation of LPPs and aldehydes in mitochondria	5
Mitochondria as a primary target	7
LPP effects on cellular membranes	8
LPP effects on cellular proteins	10
Compensatory mechanisms for adaptation to LPPS and Carbonyl Stress	
Glutathione peroxidase 4.....	14
GPx4 in metabolic disease and aging studies	15
Aldehyde metabolizing enzymes	16
Carbonyl Stress, chronic inflammation and profibrotic signaling in the obese/diabetic heart	18
Advanced Glycation End-products, a unique type of carbonyl stress with therapeutic potential	19
Pharmacological Intervention and Tools.....	21
Carnosine and its derivatives.....	21
Conclusion.....	23

CHAPTER TWO: OBESITY IN A MODEL OF *GPX4* HAPLOINSUFFICIENCY
UNCOVERS A CAUSAL ROLE FOR LIPID-DERIVED ALDEHYDES IN HUMAN
METABOLIC DISEASE AND CARDIOMYOPATHY 30

Abstract.....	31
Introduction.....	34
Methods	35
Mouse model and study design.....	35
Patient enrollment and myocardial tissue collection.....	36
Metabolic parameters.....	36
Assessment of cardiovascular function.....	37
Liver and cardiac histology.....	37
Preparation of permeabilized cardiac myofibers and mitochondrial function.....	37
Real-time qPCR of gene expression	38
Mitochondrial Isolation	39
Immunoblot and enzyme-linked immunosorbent assay (ELISA)	39
Hydrazide labeling of carbonyl- modified proteins	40
Results	41
Lipid peroxidation and carbonyl stress.....	41
Cardiac structural remodeling.....	42
Mitochondrial abnormalities, inflammatory and pro-fibrotic pathways.....	43

4-Hydroxynonenal adducts and relative risk for diabetes

in humans 45

Discussion46

CHAPTER THREE: A NOVEL CARBONYL SCAVENGING COMPOUND MITIGATES
MITOCHONDRIAL DYSFUNCTION AND CARDIOMETABOLIC PERTURBATIONS IN
OBESE WT AND GPX4+/- MICE..... 71

Abstract.....72

Introduction..... 73

Methods75

Experimental model and study design.....75

Metabolic parameters 75

Assessment of cardiac function...76

Liver and cardiac histology..... 76

Preparation of permeabilized cardiac myofibers and
mitochondrial function..... 76

Mitochondrial Isolation..... 76

Immunoblot analysis of protein content77

Statistical analysis..... 77

Results77

Glucose tolerance and insulin sensitivity77

Whole body indirect calorimetry..... 78

Lipid peroxidation and hepatic steatosis..... 78

Cardiac remodeling78

Cardiac Gpx4 protein levels and 4-HNE adducts.....	79
Mitochondrial efficiency and carbonyl adducts	79
Discussion.....	80
FINAL DISCUSSION.....	99
REFERENCES.....	103
APPENDIX A.....	141

LIST OF TABLES

Table 2.1	Body composition and metabolic parameters.....	52
Table 2.2	Patient Clinical and Demographic Characteristics	53
Table 2.3.	Multivariable analysis of GPx4 and HNE-adducts in human heart.....	54
Table 3.1	Body composition and metabolic parameters	84

LIST OF FIGURES

Figure 1.0	Primary sites of ROS formation in mitochondria, and reaction scheme for peroxidation of cardiolipin in outer- and inner-mitochondrial membrane	25
Figure 1.2	The major lipid peroxidation product detoxification systems present in the mitochondria and cytosol.	27
Figure 1.3	The structure of carnosine and hydrolysis of carnosinase	28
Figure 1.4	Three-step mechanism carnosine reaction with HNE.....	29
Figure 2.1	Glycemic control and liver biochemistry/pathology.....	55
Figure 2.2	Cardiac structural and functional parameters.....	57
Figure 2.3	Cardiac GPx4, protein carbonylation and redox signaling.....	59
Figure 2.4	Cardiac mitochondrial GPx4 and functional parameters.....	61
Figure 2.5	Cardiac inflammatory and pro-fibrotic/hypertrophic gene expression.....	63
Figure 2.6	GPx4 content and HNE-adducts in human myocardium.....	65
Suppl fig. 1	67
Suppl fig. 2	68
Suppl fig. 3	69
Figure 2.7	Overview	70
Figure 3.1	Body composition, glycemic control and insulin resistance.....	85
Figure 3.2	Whole body O ₂ and CO ₂ exchange.....	87
Figure 3.3	Liver histology	89

Figure 3.4	Cardiac histology.....	91
Figure 3.5	Cardiac function parameters.....	93
Figure 3.6	Cardiac GPx4 and protein carbonylation.....	95
Figure 3.7	Mitochondrial respiratory capacity and function in cardiac muscle following HFHS diet	97
Figure 4.0	Schematic of the two approaches used to test the effect of LPPS on the heart in diet-induced obesity.....	102

LIST OF SYMBOLS AND ABBREVIATIONS

4-HNE	4-Hydroxynonenal
ADP	Adenosine Diphosphate
AGE	Advanced glycation end-products
ALDH	Aldehyde dehydrogenase
ANOVA	Analysis of variance
AOX	Aldehyde oxidase
ApoE	Apolipoprotein E
ARE	Antioxidant/anti-inflammatory response elements
ATP	Adenosine triphosphate
AU	Arbitrary Units
AUC	Area under the curve
BMI	Body mass index
BSA	Bovine Serum Albumin
Ca-ATPase	Calcium ATPase
CABG	Coronary artery bypass graft
CAD	Coronary Artery Disease
CAR	Carnosinol
CL	Cardiolipin
CNTL	Control
CoA	Coenzyme A
Coll1a1	Collagen, type I, alpha
Coll4a1	Collagen, type IV, alpha 1
Complex I	NADH: ubiquinone oxidoreductase

Complex II	Succinate dehydrogenase
Complex III	Coenzyme Q: cytochrome c — oxidoreductase
Complex IV	Cytochrome c oxidase
Complex V	Mitochondrial ATP synthase
COX	Cytochrome C Oxidase
COX-IV	Cytochrome C oxidase, isoform IV
CYP450	Cytochrome P450
Cys	Cysteine
EDL	Extensor Diftorum longus muscle
EDTA	Ethylenediaminetetraacetic acid,
EF	Ejection fraction
EGTA	Ethylene-bis(oxyethylenitrilo)tetraacetic acid
eNOS	Endothelial nitric oxide
ETS	Electron transfer system
EF	ejection fraction
FAD	Flavin adenine dinucleotide
FMN	Flavin mononucleotide
FS	Fractional shortening
GPx	glutathione peroxidase
GPx4	Glutathione peroxidase 4
GSH	glutathione
H2O2	hydrogen peroxide
HDL	High-density lipoprotein
HEPES	4-(2-hydroxyethyl)-1-piperazineethanesulfonic acid
HFHS	High fat, high sucrose

HfpEF	Heart failure with preserved ejection fraction
HHE	4-hydroxy-2-Hexanal
HRP	Horse radish peroxidase
I/R	Ischemia/Reperfusion
IL-1 β	Interleukin-1 beta
IL-6	Interleukin-6
IMM	Inner Mitochondrial Membrane
iNOS	Inducible nitric oxide synthase
JH2O2	Mitochondrial H2O2 emission/production rate
JNADH	NADH production rate
JO2	Mitochondrial oxygen consumption rate
kDa,	Kilodalton
KHB	Krebs-Henseleit buffer
LDL	Low Density Lipoproteins
LPO	Lipid Peroxidation
LPPs	Lipid peroxidation end products
LV	Left Ventricle
M	Malate
MAO	Monoamine oxidase
MDA	malondialdehyde
MDA	Malondialdehyde
MIM	mitochondrial isolation medium
MnSOD	Manganese Superoxide Dismutase
MPTP	Mitochondrial Permeability Transition Pore
mtDNA	Mitochondrial DNA

MTP	mitochondrial permeability transition pore
Na ⁺ /K ⁺ ATPase	sodium-potassium adenosine triphosphatase
NADH	Reduced nicotinamide adenine dinucleotide
NEM	N-ethylmaleimide
	the nuclear factor kappa-light-chain-enhancer of activated
NFκB	B cells
nNOS	Neuronal nitric oxide synthase
NNT	Nicotinamide nucleotide transhydrogenase
NO•	Nitric oxide radical
NOS	nitric oxide synthase
Nrf2	Nuclear factor (erythroid-derived 2)-like 2
O ₂ ⁻ •	Superoxide radical
O ₂ K	Oroboros oxygraph-2 k
OH•	Hydroxyl radical
OM	Outer Membrane
ONOO• ⁻	Peroxynitrate radical
OXPHOS	Oxidative Phosphorylation
PA	phosphatidic acid
PBS	Phosphate Buffered Saline
PC	Palmitoyl-L-carnitine
PDH	Pyruvate dehydrogenase
PepT 1	Peptide transporter 1
PHGPx	Phospholipid Hydroperoxide Glutathione Peroxidase
PI	phosphatidylinositol
PLA	Phospholipase A

PPAR	peroxisome proliferator activated receptor
PS	phosphatidylserine
PTM	Post Translational Modification
PUFA	Polyunsaturated Fatty Acids
PVDF	Polyvinylidene fluoride
Pyr	Pyruvate
RAGE	Receptor for Advanced Glycation End Products
RNS	Reactive nitrogen species
ROS	Reactive oxygen species
RT-PCR	Real time polymerase chain reaction
S	Succinate
-S-	Thioether
S.E.M.	Standard error mean
SDS	Sodium dodecyl sulfate
SDS-PAGE	Sodium dodecyl sulfate polyacrylamide gel electrophoresis
-SH	Thiol
SNP	single nucleotide polymorphism
SOD	Superoxide dismutase
SOD	Superoxide Dismutase
State I	Respiration supported by mitochondria alone
State II	Respiration supported by ADP alone
State III	Respiration supported by substrates and ADP
State IV	Non-phosphorylating respiration
STZ	streptozotocin
TCA cycle	Tricarboxylic acid cycle

TG	Triglycerides
Tg	Transgenic
TG	Triglycerides
TGF- β 2	Transforming growth factor beta 2
TGF- β	Transforming growth factor beta
TGF- β 1	Transforming growth factor beta 1
TIIDM	Type II Diabetes Mellitus
TNF- α	Tumor necrosis factor- α
TxnRd2	thioredoxin reductase-2
WT	Wild type
β -MHC	β Myosin heavy chain

CHAPTER 1: INTRODUCTION

With sections as published in

Katunga LA and Anderson EJ. Carbonyl Stress as a Therapeutic Target for Cardiac Remodeling in Obesity/Diabetes. *Austin J Pharmacol Ther.* 2014; 2 (9).4

Alleman RJ, **Katunga LA**, Nelson MA, Brown DA, Anderson EJ.

The "Goldilocks Zone" from a redox perspective-Adaptive vs. deleterious responses to oxidative stress in striated muscle.*Front Physiol.* 2014 Sep 18;5:358.

Anderson EJ, **Katunga LA**, Willis MS. Mitochondria as a source and target of lipid peroxidation products in healthy and diseased heart.

Clin Exp Pharmacol Physiol. 2012 Feb;39(2):179-93.

Metabolic syndrome and diabetes

The global prevalence of obesity is almost 30% (1, 2). Epidemiological forecasts project this increase to continue making obesity one of the most significant public health concerns (3). According to the World Health Organization (WHO), obesity is defined as having a BMI of $\geq 30 \text{ kg/m}^2$. This increase in obesity prevalence is attributed largely to global dietary transition to a more western style diet in and a decline in physical activity (4). Obesity is part of a constellation of conditions, which include visceral adiposity, hyperglycemia, elevated serum triglycerides and high blood pressure (5). The manifestation of this cluster of conditions is called metabolic syndrome. Other risk factors for metabolic syndrome include age and race (6).

Obesity is also one of the most important risk factors that are associated with the development type II diabetes (TIIDM) later in life (6, 7). In TIIDM, there is a reduced sensitivity of the body's tissues particularly key glucose uptake organs such as the liver, skeletal muscle and adipose tissue to insulin. The hormone insulin is produced by the β -cells of the pancreas and once it binds to insulin receptors in peripheral tissues it stimulates increased uptake of glucose (8). In the early stages of TIIDM disease progression known as insulin resistance or prediabetes there is a progressively more suppressed tissue response to insulin stimulation and to compensate, the pancreas produces greater amounts of insulin in a positive feedback loop (9-12). It must be noted that not all patients who present with insulin resistance progress to TIIDM, indeed there is a subset of patients known as healthy obese where this characteristic appears to be protective (13). Insulin resistance as a pathology is a complex tissue specific interplay of the deleterious effects of chronically elevated levels of glucose and insulin. In the 1950s the association between diabetes and heart disease was first identified through ecological studies and coined diabetic cardiomyopathy (14, 15).

Diabetes and Heart Disease

The hallmarks of diabetic cardiomyopathy are ventricular hypertrophy and diastolic dysfunction (16-18). Early diabetic cardiomyopathy is characterized by cardiac stiffness from excess fibrotic deposition and this is often evident early in the progression of disease (19). Increased cardiac stiffness leads to decreased compliance of the left ventricle resulting in a reduction in end-diastolic volume (20). Furthermore, complete ventricular relaxation requires sequestration of Ca^{2+} molecules at the end of excitation-contraction cycle in the cardiomyocyte. This process requires energy supplied from adenosine triphosphate (ATP) hydrolysis. Numerous studies have demonstrated compromised both Ca^{2+} handling and bioenergetic capacity in both human and murine diabetic hearts (21-24). Ultimately in many patients the symptoms result in symptomatic heart failure, which called Heart Failure with preserved ejection fraction (HfpEF). Patients with hypertension, angina or coronary arterial disease are at a high risk of developing this particular form heart failure. Diastolic dysfunction progresses over time as demonstrated in the Olmsted County Heart Function Study (OCHFS) therefore older patients are at higher risk (2.85 greater odds) and many often progress to heart failure (20). In a study of approximately 1000 patients with an average age of 62 years, diastolic dysfunction was positively associated with HOMA-IR and metabolic syndrome (16). The mechanisms that under the link between diabetes and the progression to clinical cardiomyopathy and eventually heart failure are poorly understood however one prominent finding is the metabolic perturbations observed in the diabetic heart.

Lipid peroxidation and cellular damage

The heart is a post-mitotic, highly oxidative organ in which cell turnover rates are virtually absent, so products formed from oxidative damage of tissue and cellular material accumulate with time. The accumulation of these oxidative products is now a well-recognized causative factor in aging

and age-related diseases such as diabetes and cardiovascular disease (25). In fact, for all diseases where acute and chronic oxidative stress is either a causative factor or deleterious consequence, lipid peroxides are starting to take center stage as the most potent, persistent and physiologically relevant agents of this stress (25-27).

Oxidation of membrane phospholipids, and other polyunsaturated fatty acids (PUFAs) that are stored or otherwise located in cardiomyocytes, is one of the most prominent manifestations of oxidative stress in the heart. Indeed, with their long, chain-like structure and large number of unsaturated carbon-carbon bonds, PUFAs are some of the most readily oxidized chemicals in nature, occurring through enzymatic or non-enzymatic pathways. Non-enzymatic peroxidation of PUFAs, particularly those contained within membrane phospholipids, is typically initiated by electrophilic attack on one of the methylene carbons contained within the fatty acid side-chains. Reactive oxygen (ROS) and nitrogen species (RNS) are the electrophiles most commonly involved in lipid peroxidation, and if allowed to proceed unchecked this reaction results in formation of both stable and unstable lipid peroxidation products (LPPs). Of all the LPPs formed in this manner, reactive aldehydes have been shown to have regulatory roles in physiological systems, and have been implicated to play important roles in cardiovascular disease (28).

Because of the insatiable appetite for nutrients and oxygen required to meet its energetic demands, the heart contains a very high mitochondrial content relative to other organs. Mitochondria are the largest source of intracellular ROS in cardiomyocytes (29), as superoxide ($O_2^{\bullet-}$) is continuously formed at sites within the electron transport system during oxidative phosphorylation (OxPhos). Furthermore, mitochondria are double membrane-bound organelles that have an enormous amount of unsaturated phospholipids contained within their inner and outer membranes, notably cardiolipin, a phospholipid exclusive to mitochondria that is highly unsaturated and prone to peroxidation (30, 31). Thus, due to these characteristics mitochondria

are ostensibly the largest endogenous source of LPPs in the heart. To offset the formation of LPPs, mitochondria have a vast network of antioxidant and detoxification systems, ensuring that lipid peroxidation and levels of reactive aldehydes are kept at subtoxic levels. Over time, however, and under various pathological states, these antioxidant and aldehyde detoxification systems become compromised and/or lost, and the subsequent accumulation of LPPs and aldehydes has profound consequences for the function of mitochondria, the cardiomyocyte and the heart.

Formation of LPPs and aldehydes in mitochondria.

It has been known for decades that mitochondria generate ROS as a by-product of OxPhos (32). Mitochondrial $O_2^{\bullet-}$ is formed when electrons 'leak' from the electron transfer system (ETS) in the mitochondria and are taken on by molecular oxygen (33). The exact sites of $O_2^{\bullet-}$ formation within the ETS are controversial but there is broad consensus that redox reactions within Complex I + III are both capable of producing $O_2^{\bullet-}$ (shown in detail in **Figure 1A**), although which of these is the predominant site *in vivo* is far from clear (34, 35). Most of this $O_2^{\bullet-}$ is immediately converted to H_2O_2 by superoxide dismutase enzymes in either the mitochondrial matrix (MnSOD) or cytosol (Cu/ZnSOD). In addition to the ETS, mitochondria also generate H_2O_2 from monoamine oxidase (MAO) bound to the outer membrane (33, 36). MAO is the enzyme responsible for metabolism of catecholamines, and has recently been shown to be a substantial source of H_2O_2 and oxidative stress in heart failure (37). MAO's unique orientation relative to the ETC provides the ability for MAO to interfere with mitochondrial function and cellular energetics, although very little is known about the potential contribution of MAO-derived ROS in cardio-metabolic diseases. One study reported that MAO-derived ROS led to diminished state 3 and state 5 respiration (38). Furthermore, Hauptmann and colleagues showed that MAO-derived H_2O_2 can introduce mutations in mitochondrial DNA (mtDNA). Their results

demonstrated that H_2O_2 , produced from MAO exposure to tyramine, can readily diffuse through the inner mitochondrial membrane and produce a significant increase in mtDNA single strand breaks (36). Because of MAO's proximity to the mitochondrial oxidative phosphorylation system, ROS produced by MAO could conceivably disrupt the ATP-dependent electrochemical and contractile functions of cardiomyocytes, given the heavy reliance on mitochondria for ATP in these cells (39, 40)

Nitric oxide, as it exists with its unpaired electron (NO^\bullet), is also a free radical and can frequently react with $O_2^{\bullet-}$ to form peroxynitrite $ONOO^{\bullet-}$. Peroxynitrite is considered to be the chief RNS formed in physiological systems (41), and it is a highly reactive electrophile responsible for nitration and nitrosylation reactions with hydroxyl and thiol groups in proteins during periods of oxidative stress. Though still a matter of some debate, several studies have reported the presence of a nitric oxide synthase (NOS) isoform within mitochondria, distinct from other established isoforms of NOS such as eNOS, nNOS and iNOS (42, 43). The presence of NOS within mitochondria, coupled to continuous $O_2^{\bullet-}$ formation by the ETS would suggest that tight regulation of $ONOO^{\bullet-}$ formation and the presence of $ONOO^{\bullet-}$ scavenging systems are critical to maintaining homeostasis.

Ultimately it is $ONOO^{\bullet-}$, in addition to hydroxyl radical OH^\bullet , formed via Fenton reaction of Fe^{2+} or Cu^{2+} with H_2O_2 , that initiates lipid peroxidation by electrophilic attack on mitochondrial phospholipids. Outlined in the dashed box in **Figure 1** is the general reaction scheme of non-enzymatic lipid peroxidation in mitochondria with initial step coming from OH^\bullet attack of unsaturated fatty acids contained within cardiolipin (step 1). Following initiation by OH^\bullet , an unstable lipid radical is formed which can continue to abstract allylic hydrogens from nearby unsaturated fatty acids (step 2), or react with molecular O_2 (step 3) to form a lipo-peroxyl radical that either continues on to react with another fatty acid forming a new radical, or reacts with itself to form a lipid peroxide (step 4). Formation of lipid peroxides from cardiolipin has been

suggested to be partly responsible for the altered cardiac function seen in the aged heart (44), likely through disruption in membrane order and dynamics in mitochondria leading to destabilization of cytochrome c and complexes within the ETS, all of which have profound effects on cell energetics and vitality (45, 46).

If they are not neutralized by endogenous antioxidants, lipid peroxides will fragment and decompose to form reactive aldehydes such as di-aldehydes (malondialdehyde, MDA) and α,β -unsaturated aldehydes (acrolein; 4-hydroxynonenal, HNE; and 4-hydroxyhexenal, HHE) (47). The 4-hydroxyalkenals formed from PUFA oxidation (HNE from n-6 PUFAs, HHE from n-3 PUFAs) are highly reactive electrophiles capable of covalently modifying proteins, DNA and other macromolecules, similar to the ROS/RNS that spawned them, though they also have unique properties endowing them with distinct roles in biological systems. They are uncharged, lipophilic and chemically stable molecules capable of readily diffusing through membranes. In addition, some of the less hydrophobic aldehydes such as MDA, acrolein and HHE are able to diffuse fairly long distances from their sites of origin, enabling them to act as signaling mediators within cells and tissues under various physiological and pathological contexts (28).

Mechanisms for scavenging LPPs and aldehydes. Mitochondria are endowed with such a highly concentrated and layered antioxidant network that they can be considered to not only be primary 'sources' of ROS/RNS within cells, but also primary 'sinks' (33, 48). This network includes glutathione and thioredoxin systems, along with peroxidases, catalase, superoxide dismutase, glutaredoxin, sulfiredoxin, peroxiredoxin, and others. (48-50).

Mitochondria as a primary target of LPPs in heart

To date, the majority of research directed at identifying molecular targets of LPPs has been conducted in models of cancer, neuronal disease or in purely cytotoxic (i.e. supra-physiological) conditions. This complicates extrapolation of these findings to other organs or to systems where

lipid peroxidation may be a constitutive process that is fundamental to maintaining homeostasis, such as the heart (39). Studies of the effects of lipid peroxidation in cardiac tissue are sparse, even though this tissue may easily be considered to have the highest capacity for this process. Cardiomyocytes possess the highest mitochondrial density of all tissues in the body, therefore a higher capacity for ROS production. In addition to the high PUFA content distributed across the mitochondrial membrane, there is also an omnipresent pool of free fatty acids, the preferred substrate of cardiac mitochondria. This pool closely reflects dietary intake. According to some estimates the n-6: n-3 PUFA ratio approaches 10:1 in the archetypal Western diet (40). Hence, HNE would be expected to constitute a much higher proportion of LPPs in individuals on such a diet. Approximately 2-8% of HNE(41) produced is involved in largely irreversible cell conjugation reactions with both cellular and mitochondrial proteins. The following sections shall discuss the resultant mitochondrial component damage and aberrations in homeostasis.

LPP effects on cellular membranes.

The primary source of ROS in cardiomyocytes is the electron transport system located in the mitochondrial inner membrane (42). Thus, the most immediate target of the 4-hydroxyalkenals are the lipids present in the phospholipid bilayer (43, 44) and its associated proteins (45). The reaction of 4-hydroxyalkenals with the mitochondrial membrane results in altered lipid-lipid and protein-lipid interactions. This occurs through a variety of mechanisms which include cross-linking of the lipid tails which limits mobility of phospholipids in the bilayer (46). Of singular importance, the inner mitochondrial membrane mosaic contains a phospholipid, cardiolipin that is specifically localized to this compartment. Its presence ensures the efficient function of a battery of mitochondrial components such as the electron transport chain complexes, adenine nucleotide transporter and the acylcarnitine carrier, among others (47, 48). Cardiolipin levels diminish dramatically in robust lipid peroxidation conditions (49), and diminished levels of

cardiolipin have been observed in many pathological conditions including aging, Barth syndrome, heart failure, ischemia and reperfusion, diabetes and neurodegenerative disease (47). The mitochondrial membranes contain a high density of polyunsaturated fatty acids (PUFAs) and phospholipids, which are susceptible to peroxidation (52, 53).

Phosphatidylethanolamine and phosphatidylcholine are the most abundant phospholipids and comprise ~40% and ~ 30% of total mitochondrial phospholipids, respectively. Cardiolipin and phosphatidylinositol (PI) account for ~ 10–15% of phospholipids, whereas phosphatidic acid (PA) and phosphatidylserine (PS) comprise ~ 5% of the total mitochondrial phospholipids. Cardiolipin is concentrated in the inner mitochondrial membrane in close proximity to the ETS. Although it comprises a relatively a low percentage of total membrane phospholipid, its peroxidation is directly associated with a decline in activity of respiratory complexes III and IV, and the release of cytochrome c which initiates apoptotic signaling (54-56). This is significant because cardiolipin is especially susceptible to peroxidation.

In the event that 4-hydroxyalkenals migrate to the cell membrane, the high number of conjugated unsaturated carbon bonds in the cholesterol molecule make it an attractive target for attack (50). Collectively, studies on the effects on lipid peroxidation on membrane physiology demonstrate a marked reduction in membrane fluidity (46, 51, 52) and an increase in membrane permeability (53, 54). Moreover, the production of 4-hydroxyalkenals via lipid peroxidation gives rise to a chain reaction. The products formed from electrophilic attack by the 4-hydroxyalkenals degrade to generate more aldehydes which serve to propagate the cycle (55). Some of the more stable products include isoprostanes and neuroprostanes following cyclization of the fatty acid tails (45).

LPP effects on cellular proteins.

Enzymatic, structural and signaling proteins present in the phospholipid bilayer and mitochondrial matrix are a key target of 4-hydroxyalkenals. Like all electrophiles, they have characteristic affinity for sulfhydryl groups (e.g. cysteine, methionine), although lysine and histidine are also subject to covalent modification in their amide groups (56-58) via Michael addition reactions (55). HNE augments the accumulation of damaged proteins by interfering with normal proteolysis pathways (59, 60). A recent proteomic study of the relative levels of adducted proteins in rat cardiac mitochondria treated with a spectrum of LPPs including HNE and HHE revealed that proteins of the electron transport chain constituted the greatest percentage of altered proteins. Moreover, this group observed that cysteine constituted an overwhelmingly high percentage of total modified residues (85%), while histidine accounted for 12% and lysine less than 5% (61). Adduct levels for both HHE and HNE were relatively similar. This study underscores the high propensity that LPPs exhibit towards attacking protein components involved in cellular respiration (41, 62-64) (57), expanding our current knowledge of the negative impact of the LPPS on mitochondrial homeostasis.

In addition to their direct effects, the 4-hydroxyalkenals are also indirectly capable of affecting mitochondrial homeostasis by disturbing the balance of ions (65, 66). HNE attacks the sulfhydryl groups of the Na⁺/K⁺ ATPase (67) resulting in diminished activity and elevated intracellular concentrations of free calcium. Both HNE and HHE have been implicated in inducing Ca²⁺ overload in cardiomyocytes (68); activation of uncoupling proteins (69) and premature opening of the mitochondrial permeability transition pore (MTP) (70) thus increasing the risk of heart failure (3, 71).

LPP effects on DNA and other cellular targets. The role of the 4-hydroxyalkenals in DNA adduct formation during mutagenesis is well documented with respect to HNE. HNE displays a differential affinity for the respective bases with the highest reactivity toward

guanosine ⁽⁷²⁾, cytosine, adenine, and least toward thiamine ⁽⁷³⁾. The cell machinery is capable of repairing damage to the DNA inflicted by LPPs by excising the damaged portion, although long-term exposure to LPPs leads to an accumulation of damaged DNA. In addition to its well-documented reactivity with DNA, HNE is both directly and indirectly involved in the upregulation of several cell signaling pathways including Protein Kinase C, Mitogen Activated Protein Kinases, I κ B Kinase Complex, Tyrosine receptor Kinases, Serine/ Threonine Kinase, C-Jun H-Terminal Kinases ^(57, 71, 74-78).

Compensatory Mechanisms for Adaptation to LPPs and Carbonyl Stress

The diagram in **Figure 1.2** shows the major enzymatic and non-enzymatic endogenous systems present in mitochondria and cytosol specific for neutralizing LPPs and aldehydes (i.e. scavenging LPPs and aldehydes once they have already been formed). In most cell types, including heart, the major enzyme responsible for neutralizing lipid peroxides is glutathione peroxidase 4 (GPx4), also known as phospholipid hydroperoxide glutathione peroxidase ^(27, 28). This enzyme resides in cytosol, nucleus, and the inner membrane of mitochondria, where it utilizes glutathione (GSH) to reduce lipid peroxides to their corresponding alcohol. GSH not only provides the reducing power for a large number of redox enzymes capable of reducing ROS ⁽²⁹⁾, but it is also capable of neutralizing electrophilic lipids, such as HNE, after they are formed ⁽³⁰⁾. Esterbauer's group showed that in heart, the conjugation of glutathione to HNE is catalyzed by the enzyme glutathione-transferase, resulting in export of this conjugate from the cell and into the systemic circulation ⁽³¹⁾. The aldehyde dehydrogenase (ALDH) family of enzymes is also capable of neutralizing LPPs. In particular, the cytosolic enzyme ALDH3a1, also called fatty aldehyde dehydrogenase (FALDH) ⁽³²⁾, and ALDH2 ⁽³³⁾, a mitochondrial matrix enzyme, are the 2 isoforms of ALDH that are most likely to be the enzymes responsible for detoxification of LPPs *in vivo* (circled in blue in **Figure 1.2**), though other isoforms may also play

a role. ALDH converts aldehydes to acetate, rendering them far less reactive and virtually benign.

In addition to the endogenous systems, chemical agents that have been demonstrated to have the capacity to neutralize LPPs and aldehydes are also presented in **Figure 1.2**. Lipophilic antioxidants such as vitamin E, α -lipoic acid and co-enzyme Q10 have all been repeatedly shown to have the capacity to inhibit lipid peroxidation and prevent adverse downstream effects (34, 35). Agents that have been demonstrated to effectively neutralize and/or remove aldehydes in both experimental models of metabolic and cardiovascular diseases as well as clinical studies include taurine (36), histidine analogs (37), and carnosine (38). These agents provide a number of different options for stand-alone or supplemental therapy in treating diseases where suppression or removal of LPPs is desired.

Carbonyl stress arising from PUFA peroxidation is known to activate genes involved in phase I and II antioxidant/detoxification, mitochondrial biogenesis, and other pathways, all of which serve to restrain the further production of PUFA-derived aldehydes and suppress their toxic effects. A primary adaptive response pathway that is activated by oxidative and carbonyl stress involves NF E2-related factor-2 (Nrf2). Electrophiles such as LPPs and PUFA-derived aldehydes generated during periods of oxidative stress activate Nrf2 by liberating it from its tethering protein Keap1 in the cytosol, allowing it to translocate to the nucleus where it binds to antioxidant/anti-inflammatory response elements (AREs) in promoter regions of genes/proteins involved in glutathione synthesis and phase II detoxification (58). Studies have shown that HNE induces nuclear accumulation of Nrf2 and up-regulates many GSH-synthesizing enzymes and proteins (reviewed in (59)). Indeed, pre-conditioning of the heart by retro-orbital injection of HNE induces cardioprotection from ischemia/reperfusion injury via Nrf2, and this cardioprotection is lost in Nrf2^{-/-} mice (60). The roles and regulation of Nrf2, and other transcription factors that activate the ARE, are discussed in a number of review articles (61-63).

In addition to Nrf2, recent evidence has implicated members of the peroxisome proliferator activated receptor (PPAR) family in the cellular response to ROS. Several reports have documented a key role for PPAR α and PPAR γ in augmenting the antioxidant capacity of liver (64-66) and vascular tissue (67, 68) in response to oxidized PUFAs. Our group recently completed a small clinical trial and observed that a concentrated dose of fish oil n-3 PUFA's was associated with up-regulation of several antioxidant enzymes, particularly mitochondrial-localized thioredoxin reductase-2 (TxnRd2), and this was accompanied by increased nuclear transactivation of PPAR γ , in atrial myocardium of patients undergoing cardiac surgery (69). This finding is particularly intriguing given the emerging evidence that TxnRd2 is critical for maintaining mitochondrial redox balance in multiple cell types and tissues, including the heart (70-72). These articles and other recent literature documenting the beneficial adaptations to ROS in striated muscle under various physiological contexts are listed in Table [1](#). Another key adaptive response to ROS includes activation of cellular quality control pathways in myocytes, namely autophagy and mitophagy. These pathways are a very active and rapidly expanding area of research, and well beyond the scope of this work. The role of autophagosome formation in the adaptive response to ROS in myocytes and is the topic of a number of thorough reviews (73-75)

LPP detoxification occurs at two main stages. The first is at the site of lipid peroxidation itself (membrane-localized), and the second is in the cytosol. Following their formation, LPPs may undergo phase I biotransformation where they are conjugated to antioxidant molecules (i.e., glutathione). Alternatively, LPPs are converted by phase II detoxification enzymes such as aldehyde dehydrogenase (76), which converts LPPs to their corresponding alcohols. Below we discuss some of the major enzymes involved in the detoxification of LPP-derived aldehydes. It is important to note for many of these enzymes, their enzymatic efficiency is itself decreased by aldehydes, which may be key factor in the limitation of antioxidant capacity. A list of the major

enzymes responsible for detoxifying LPPs, along with the reaction catalyzed by the enzyme, can be viewed in Box [1](#).

Glutathione peroxidase 4.

GPX4, which is also known as Phospholipid Hydroperoxidase, is a member of the glutathione peroxide family of selenoenzymes. GPx4 was first identified in 1982 by Ursini et al (77). GPX4 prevents the initiation step in free radical attack of the lipid membrane this has been demonstrated to occur specifically in the mitochondria (78). Unlike other members of the GPx family of enzymes, which are tetramers, GPx4 is a 20-22kDa monomer (79).

In addition to being able to neutralize small hydroperoxides such as H_2O_2 , it is one of only a few enzymes capable of neutralizing complex and bulky hydroperoxides (e.g., cholesterol hydroperoxides) (80-83). GPX4 is unique in that unlike other GPXs, it is not limited to glutathione as a substrate (83). Its protein thiols can perform the function of GSH, and as a result, GPX4 may function as either a glutathione peroxidase or a thiol peroxidase adapting to perform its functions depending on cellular redox conditions. The catalysis of GPx4 occurs through a tert- ping-pong mechanism (84), which is similar to other members of the GPx4 family. The primary studies conducted by Ursini et al. reported that although GPx4 could metabolize H_2O_2 molecules like other members of the family, it did possess a higher affinity for “lipophilic, interfacial substrates” compared to other members of the GPx4 family (85, 86).

There are 3 major isoforms of GPX4: cytosolic, mitochondrial and nuclear (87). GPx4 is synthesized as a long form, which contains a peptide, which directs it to the mitochondria and a short-form that is present in other cellular compartments such as cytosol, nucleus and endoplasmic reticulum. GPx4 activity is has been observed in both the inner and external mitochondrial membranes. Many studies have overexpressed GPx4 in vivo in order to elucidate the physiological role of GPx4. Overexpression in a number of cellular models protects against

insults presented by lipid peroxide species including phosphatidyl choline, linoleic acid as well as inhibitors such as rotenone and cyanide. In the mitochondria, GPX4 over-expression has been shown to protect against cytochrome c release, generation of H₂O₂ and loss of membrane potential following ischemia/reperfusion injury (88). In diabetic mice, over expression of mitochondrial GPX4 was protective against cardiac ischemia reperfusion injury and preserves mitochondrial integrity (89-93). GPx4 is under the regulation of a number of transcription factors including Nrf-2, Guanine rich sequence-binding factor 1 (GRSF-1) (94), p-53 and SP-1. Disruption of the GPx4 gene in mouse models has been conducted independently by a number of different groups. GPx4 is embryonic lethal at E7.5. Tamoxifen induced knockouts are lethal within two weeks of treatment (95).

In addition, to its antioxidant action, GPx4 has been shown to have an important role in preventing apoptosis in a variety of models (96). In a study that compares markers of liver apoptosis following diquat exposure GPx4 was shown to modulate the release of apoptotic proteins from the mitochondria and prevent cardiolipin oxidation (97, 98). Work from Ran et al. demonstrates that the cross talk between GPx4 and apoptosis may be complex. This group shown that in GPx4 heterozygote knockouts, although there is greater apoptosis, these mice in fact have that have a longer lifespan. (99). GPx4 exerts a significant influence on lipoxygenase metabolism (100, 101), which is important in light of the contribution of chronic low-grade inflammation to metabolic syndrome.

GPx4 in metabolic disease and aging studies

ROS are thought to be a major mechanism through which aging occurs therefore it follows that GPx4 content and levels important in counteracting aging. According to studies conducted in rats the general trend appears to be GPx4 activity is lowest in the tissues of younger animals, this increases adult animals however from this point on the trend is very tissue specific. For

instance in the liver, GPx4 activity increased by 25%, in the liver and kidney it remains about the same whether as in the heart there is a slight decrease (102). In contrast that of other GPx enzymes is almost 2 fold lower in aged compared to adult rats (102). Human studies that investigate potential roles of GPx4 in disease are sparse but have grown in number in recent years. A single nucleotide polymorphism (SNP) in a small group of 66 patients has demonstrated to have an impact on lipoxygenase metabolism (103). GPx4 polymorphisms have also been demonstrated to predispose endothelial dysfunction (104). GPx4 is responsive to ischemia reperfusion (Beckman 1991). GPX4 levels increase after reperfusion the kidney within an hour in response to ischemia. More recently in the context of metabolic syndrome GPx4 polymorphisms have been associated with obesity in children (105).

Glutathione S-transferase (GST). The GSTs conjugate electrophilic aldehydes with GSH to yield a less reactive conjugate that is eliminated from the cell by glutathione S-conjugate efflux pumps, this process not only increases the solubility of conjugated compounds but also marks these structures for elimination from the cell (106). ROS regulate the expression of GST via c-fos and c jun signaling (107). A study in rat hepatocytes reported that for HNE, metabolism by GST is responsible for the majority of HNE removal (~60%); a little is metabolized by the alcohol and aldehyde dehydrogenases (10%) leaving ~24% of 4-HNE clearance for other mechanisms (108).

Aldehyde-metabolizing enzymes.

Aldehyde dehydrogenase. The ALDHs are particularly relevant in the mitochondria as metabolizers of aldehydes generated from PUFAs and monoamine oxidase, as it has been demonstrated that inhibiting ALDH activity has a direct impact on the metabolism of amines by MAO (109, 110). There are 19 known isoforms of the ALDH enzyme with ALDH2 as the major

mitochondrial isoform (111). In human populations, individuals with a polymorphism for ALDH2 had higher levels of the biomarker C-reactive protein following myocardial infarction (112). In the SAPPHIRe prospective cohort study patients with ALDH2 genetic variants with a possessed two-fold greater risk of progression to clinical hypertension (113). ALDH3A2 also was found to be important in redox-related pathologies stemming from nutritional overload. It is expressed in both the heart and skeletal muscle and displays substrate specificity for aldehydes of various long and short chain fatty acids.

Molybdenum hydroxylases. There are two main enzymes in this class (1) Aldehyde oxidase (AOX): This enzyme oxidizes aldehydes to carboxylic acids and it is relatively nonspecific and its endogenous role is not well understood. (2) Xanthine Oxidase: exists as xanthine dehydrogenase-metabolism of aldehydes by xanthine oxidase generates radicals. These two enzymes share some amino acid sequence homology and both contain molybdenum and iron as well as Flavin adenine dinucleotide (FAD) as co-factors.

Carbonyl reductases. Carbonyl reductases are part of short chain dehydrogenases/reductases (SDR) family of proteins. These enzymes are ubiquitous and are largely localized to the cytosol with some isoforms in the mitochondria and peroxisomes (114).

Aldo-ketoreductases. The aldose reductases metabolize lipid aldehydes and their glutathione conjugates (115). AKR1 specifically metabolizes aldehydes produced by MAO using NADPH. The mitochondrial isoform accounts for 5% of cell activity and metabolizes 4-HNE. AKR1B uses both NADH and NADPH and is also localized in the cytosolic fraction (116). It is highly expressed in the cardiovascular system, appears to be partly responsible for reducing aldehydes such as 4-HNE, and its activity is potentiated when the substrate is conjugated to glutathione.

Carbonyl stress, chronic Inflammation and profibrotic signaling in the obese/diabetic heart

Elevated LPPs may in fact be responsible for shifting the dynamic equilibrium in favor for AGE formation by increasing the stabilization of the Amadori product thus augmenting profibrotic remodeling (117, 118). The most prominent histopathologic finding in the hearts of Type II Diabetes patients is fibrosis, as damaged myocardium is infiltrated by fibroblasts (15, 119). Myocyte death, collagen deposition and development of fibrotic lesions are visible even before decreased cardiac performance is observed (120, 121). Upon initial onset, fibrosis is a compensatory response that adds increased tensile strength to counteract pressure overload in the heart. The transition to maladaptation occurs gradually as muscle fibers are encased in extracellular matrix, leading to ventricular wall stiffening and ultimately decompensation, which manifests as diastolic dysfunction (122).

Over-production of extracellular matrix has physical effects on the microstructure as well as changes in physiological environment through the release of factors such as Transforming growth factor beta (TGF- β) (123). The most notable change in cellular physiology is the transformation of fibroblasts to myofibroblasts. Myofibroblasts are crucial in the normal response to injury and there is evidence to suggest the processes that trigger this transformation are tissue dependent (19, 124). Myofibroblasts are highly specialized for the secretion of extracellular matrix. Furthermore, they are more responsive to stimulation by factors such cytokines (125). In certain patients this transition in phenotype to a myofibroblast-predominant population of cells may increase risk of adverse cardiac events (126, 127). For example, as poor transmitters of electric potential this change in phenotype may directly account for increased risk of ventricular arrhythmias. Studies show that hyperglycemia/ insulin resistance promotes fibroblast - myofibroblasts transformation (19). Furthermore in the context of lipid peroxidation it is intriguing that *in vitro* treatment of human fibroblasts with carbonyl

modified proteins produces a similar phenotype transition (120). Carbonyl scavengers such as carnosine may mitigate this effect and it is postulated that inhibition of the TGF- β pathway may serve as a potential mechanism (128). These observations are not confined to patients with metabolic syndrome, in fact in a subset of 'healthy' obese patients with a relatively normal metabolic profile (normotensive, euglycemic), the early stages of irreversible fibrotic cardiac remodeling have been observed (129).

Advanced Glycation End-products, a unique type of carbonyl stress with therapeutic potential

The Receptor for Advanced Glycation End-products (RAGE) is a 35KDa receptor that belongs to the immunoglobulin G family of receptors (130, 131). RAGE does not recognize a primary amino acid sequence or arrangement. It is essentially a Pattern Recognition Receptor (PRR) that displays affinity to a wide variety of glycated proteins (132). Since in many cases lipid peroxidation end-products (LPPs) and advanced glycation end products (AGE) often share structural homology, proteins modified with LPPs (e.g., HNE, MDA) may serve as candidate ligands for RAGE. The importance of RAGE in diabetic pathologies (retinopathy, neuropathy) is an established and active area of study. In the context of carbonyl stress RAGE may serve as a key mediator of carbonyl stress in cardiometabolic disease. Formation of AGE occurs through the Maillard reaction, which is discussed extensively elsewhere. Aldehydes contribute in the conversion of the unstable Schiff Base intermediate in an irreversible rearrangement reaction to a stable Amadori product (133-135). Therefore in conditions of elevated carbonyl stress, it is plausible that increased cross-linking of Amadori products would shift the dynamic equilibrium even more in favor of the formation AGE according to Le Chatelier's principle. This would, in theory, increase the concentration of RAGE ligand.

RAGE signaling activates numerous pathways but two are of key interest in relation to cardiac remodeling (136, 137). In this context, increased localized RAGE tissue expression and activation may serve as a form of localized 'metabolic memory' through which previous insults are sustained through lingering signals (130). RAGE gene translation is regulated by the nuclear factor kappa-light-chain-enhancer of activated B cells (NFκB) transcription factor (130). Conversely, NFκB is also activated by RAGE signaling. The RAGE/ NFκB axis is unique in that it typically overwhelms endogenous auto-regulatory feedback inhibition loops. In other words, once RAGE switches NFκB on, it is difficult to switch off. Carbonyl stress may contribute to chronic low-grade inflammation through this mechanism (138). Chronic low-grade inflammation is a mechanism that underlies many diseases associated with metabolic syndrome (139). The cyclic pattern of RAGE/ NF-κB activation is consistent with these observations. This may explain in part why deterioration of cardiac function persists even after onset of anti-hyperglycemic therapy. Interestingly, treatment with the antioxidant selenium, which induces the expression of many glutathione-dependent antioxidant enzymes, has been shown to reduce both RAGE expression and NF-κB activation in diabetic rats (140). RAGE is a well-known activator of the TGF-β pathway (133, 139, 141, 142). The TGF-β proteins are pleiotropic and have been implicated in diverse mechanisms, which include cell differentiation and proliferation. TGF-β receptors type I and II (TGFβRI and TGFβRII) are present in virtually all mammalian cells TGF-β1, the major isoform in heart, is expressed in cardiac fibroblasts and cardiac myocytes (CMs) and stimulates transformation to myofibroblasts and proliferation, as well as ECM production. Active TGF-β1 binds membrane receptors that activate downstream signaling molecules Smad2 and Smad3, which are phosphorylated on the C-terminal serine residues. Phosphorylated Smad2 and Smad3 (pSmad2 and pSmad3) bind to Smad4 and translocate to the nucleus. The Smad complex then binds to response elements in the promoter regions of the ECM genes and activates pro-fibrogenic factors by up-regulating gene transcription (143). TGF-β increases the

abundance of mRNA for collagen types I and III in the whole heart and enhances collagen type I. Models of TGF β 1 overexpression in mice suggest that Smad2 is the isoform involved in cardiac remodeling involving hypertrophy and fibrosis (139, 141, 142). In human fibroblasts, HNE suppresses the TGF- β mediated production of elastin, which compromises ventricular elasticity (144).

Pharmacological Intervention and Tools

Relatively few studies have tested compounds that target lipid peroxidation and or neutralize LPPs. Viable drug candidates need to be sufficiently lipophilic in order to enter cellular compartments, as well as nucleophilic enough for carbonyl species to preferentially react with it, or alternatively break the covalent bond formed. It is imperative that the drug is only moderately reactive (which would be selectively beneficial in obese/diabetic patients) since many groups have demonstrated that 'over-scavenging' can potentially interrupt the normal redox cell signaling pathways and can be detrimental to health. A brief description of drugs that have been explored in this capacity is provided below in Box 1.2 with information pertinent to cardiometabolic disease included where available. In addition, other compounds relevant to this discussion but not included in this table include Angiotensin converting enzyme inhibitors, AT1 angiotensin receptor inhibitors, N-acetyl cysteine and antioxidants such as Tocopherol- α and, resveratrol (25).

Carnosine and its derivatives

Carnosine, discovered in 1900, was the first member of the family of histidine containing dipeptides identified (145). Carnosine is a β - alanyl-L- histidine dipeptide present in extraordinarily high concentrations in skeletal muscle, particularly in white muscle, which can contain up to 0.6% wet weight. The heart contains derivatives of carnosine and other members of the peptide family anserine, acetylcarnosine and acetylserine (146). The exact role of these

compounds is not well understood. Muscle often possesses a mixture of these compounds concentrated around synapses (145).

Metabolism: Dietary meat consumption is the largest source of carnosine (147).

Carnosine uptake in the small intestine occurs through via a proton dependent oligotransporter called the HPepT1 (148). Carnosine is hydrolyzed by two enzymes, carnosinase which is highly specific and homocarnosinase (149). These enzymes are found in the in the plasma, and tissues such as the liver and kidney and comparatively low levels in skeletal muscle and this may account for the extremely high levels of carnosine in this tissue (145). Carnosine enters muscle tissue only when it is contracting (145). Carnosine possesses a high buffering capacity and this points towards its possible role in muscle (145).

Function: In some muscles carnosine accounts for up to a third of buffering capacity at neutral pH (150) (Davey, 1968). It also chelates metal ions. Carnosine has been shown to increase the activity of metabolic enzymes such as glyceraldehydes 3 phosphate dehydrogenase. Carnosine increases the activity of the ATPases, Na⁺ /K⁺ ATPase and Ca-ATPase (145). It improves the efficacy of reactions by reducing activation energy and increasing coupling of reactions. Interestingly enough these effects are only observed in compromised membrane preparations. This brings us to a major functional role of carnosine and this is preserving membrane function (151). Carnosine is known to preserve membrane integrity by reducing lipid peroxidation in a concentration dependent manner. These properties of carnosine are thought to be linked to the pH by protonation of the imidazole ring in the molecule (145). At physiological pH carnosine inhibits the initiation and chain reaction of lipid peroxidation. Furthermore it is known that as the lipid membrane is modified the distortion of lipids allows for greater penetration of carnosine into the intermembrane space. Carnosine reacts directly with ROS such as hydroxyl radical, superoxide anions (147, 152). Carnosine has a synergistic effect with other antioxidants that target lipid peroxidation such as a-tocopherol (153). Interestingly

levels of carnosine are not changed by training therefore this suggests that there may be significant benefit gained from therapeutic administration of this drug since natural means e.g. exercise do not affect its levels (150).

A significant limitation to the clinical application of carnosine as a therapeutic is that it is rapidly hydrolyzed. A number of approaches have been used to circumvent this one of these is the use of the D-enantiomer of carnosine, however it has low bioavailability (152) since its configuration is incompatible with that of the transporters (148). Following these studies d-carnosine octylester was synthesized to improve bioavailability (154). In the ApoE mouse fed a western diet, d-carnosine octylester mitigated atherosclerosis (155). It has also been shown to improve dyslipidemia and renal function (156). The development of more potent derivatives is currently an active area of research.

Conclusion

Despite the overwhelming amount of literature available in support of the significant role of LPPs in cardiometabolic disease there are few studies that have attempted to elucidate this relationship. This dissertation will seek to address this deficiency in the knowledge base using high fat high sucrose fed models of elevated (GPx4 mice) and diminished carbonyl stress (carnosine derivative treated) mice to test the central hypothesis: LPPs are responsible for reduced mitochondrial efficiency and cardiac fibrosis associated with diet induced obesity. Using this dual approach we have conducted a series of studies that will serve as a foundation for future studies on of the lipid peroxides in cardiometabolic disease as a target for therapeutic intervention.

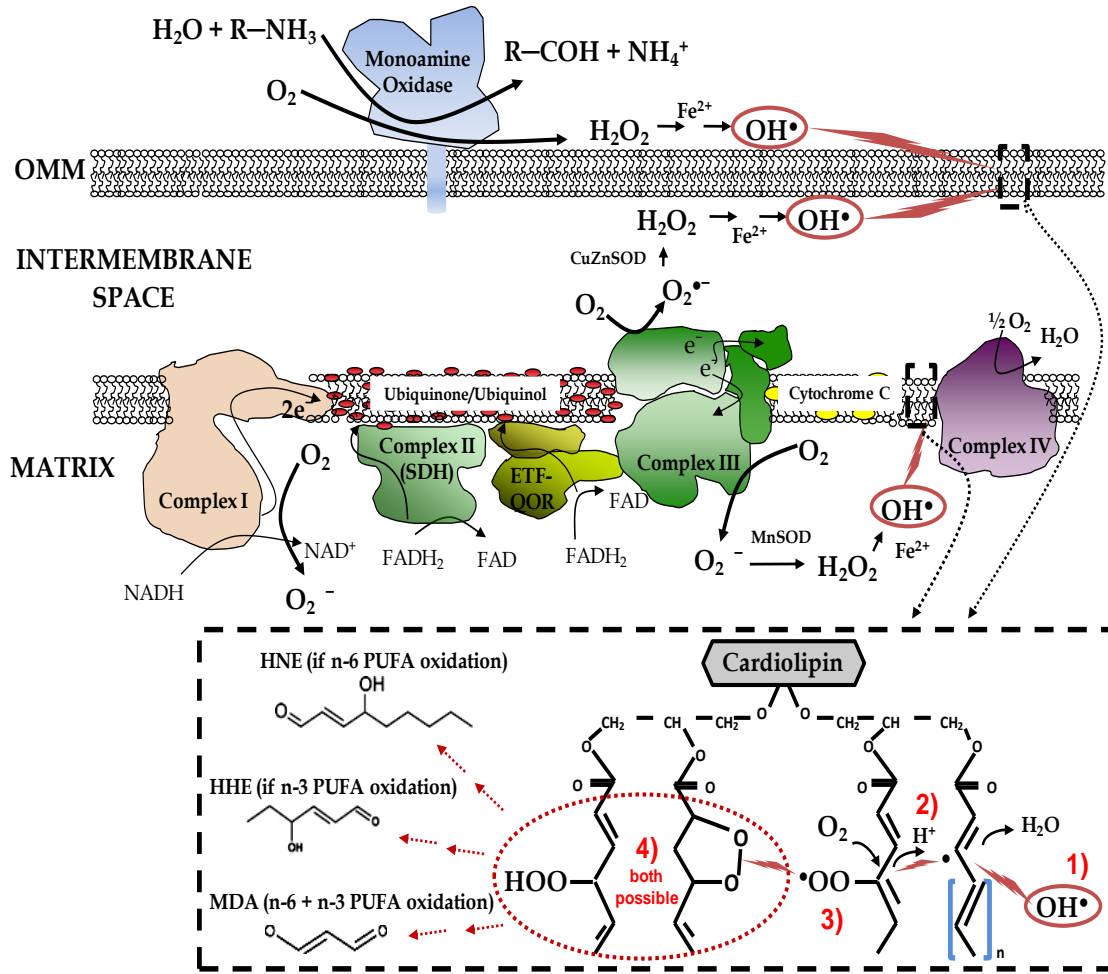


Figure 1.0 Top: Primary sites of ROS formation in mitochondria, and reaction scheme for peroxidation of cardiolipin in outer- and inner-mitochondrial membrane (51). Sites of ROS formation at Complex I and III are depicted, with the formation of hydroxyl radical (OH^{\bullet}) circled in red. Electrophilic attack on cardiolipin from OH^{\bullet} initiates lipid peroxidation by abstracting hydrogen from a methylene carbon in cardiolipin fatty acyl side-chain. Stepwise reaction scheme and products formed are outlined in dashed box. **Dashed box:** The general reaction scheme of non-enzymatic lipid peroxidation in mitochondria with initial step coming from OH^{\bullet} attack of unsaturated fatty acids contained within cardiolipin (step 1). Following initiation by OH^{\bullet} , an unstable lipid radical is formed, which can continue to abstract allylic hydrogens from nearby unsaturated fatty acids (step 2), or react with molecular O_2 (step 3) to form a lipo-peroxyl radical that either continues on to react with another fatty acid forming a new radical, or reacts with itself to form a lipid peroxide (step 4).

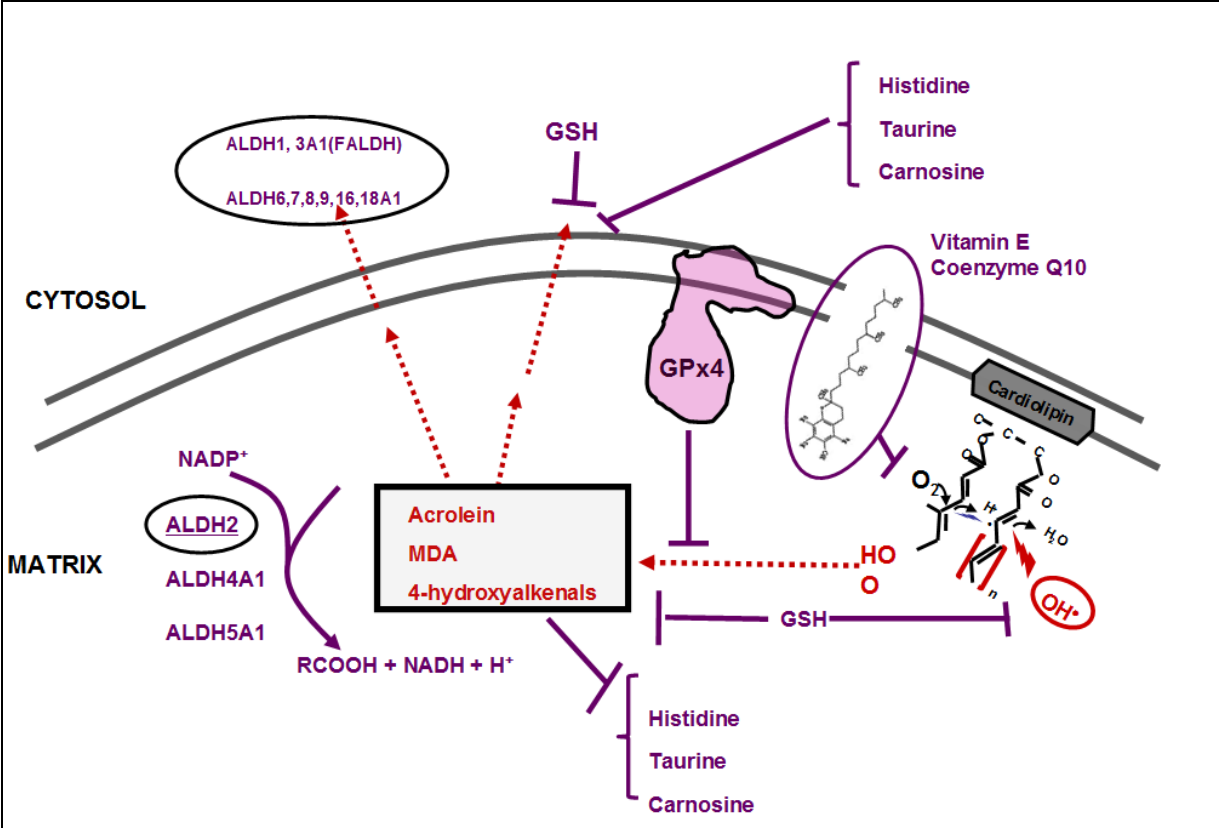


Figure 1. 2. The major lipid peroxidation product detoxification systems present in the

mitochondria and cytosol. (51) Lipid peroxidation can be blunted directly by GSH removal of $\text{OH}^{\bullet-}$ prior to initiation of lipid peroxidation. GSH is also used by the enzyme glutathione peroxidase 4 (GPx4), also known as phospholipid hydroperoxide glutathione peroxidase, to neutralize lipid peroxides as they are formed in mitochondrial membrane. Once aldehydes are formed (examples in box), the most physiologically relevant enzyme in neutralizing these electrophiles is the aldehyde dehydrogenase (ALDH) family, with ALDH2 and ALDH3a1 as most likely candidate enzyme for removal of aldehydes in mitochondrial matrix and cytosol, respectively. Exogenous agents known to suppress lipid peroxidation and/or neutralize aldehydes are listed in purple text.

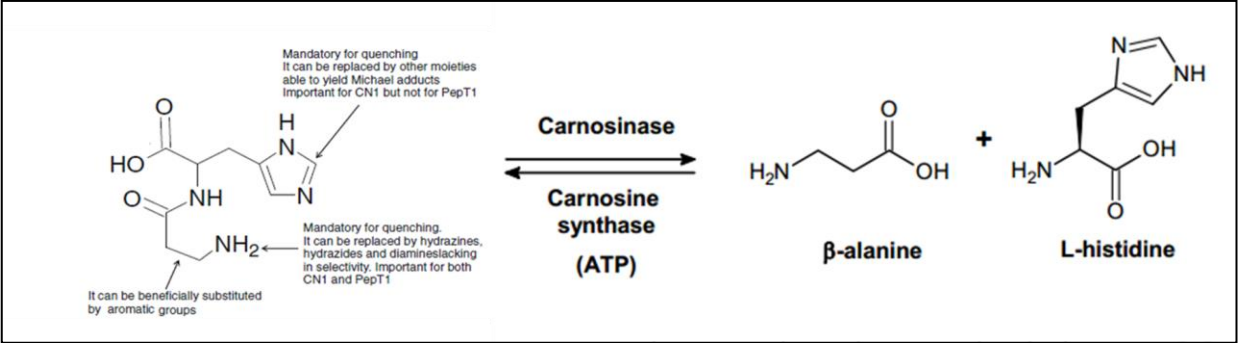


Figure 1.3 The structure of carnosine and hydrolysis of carnosinase

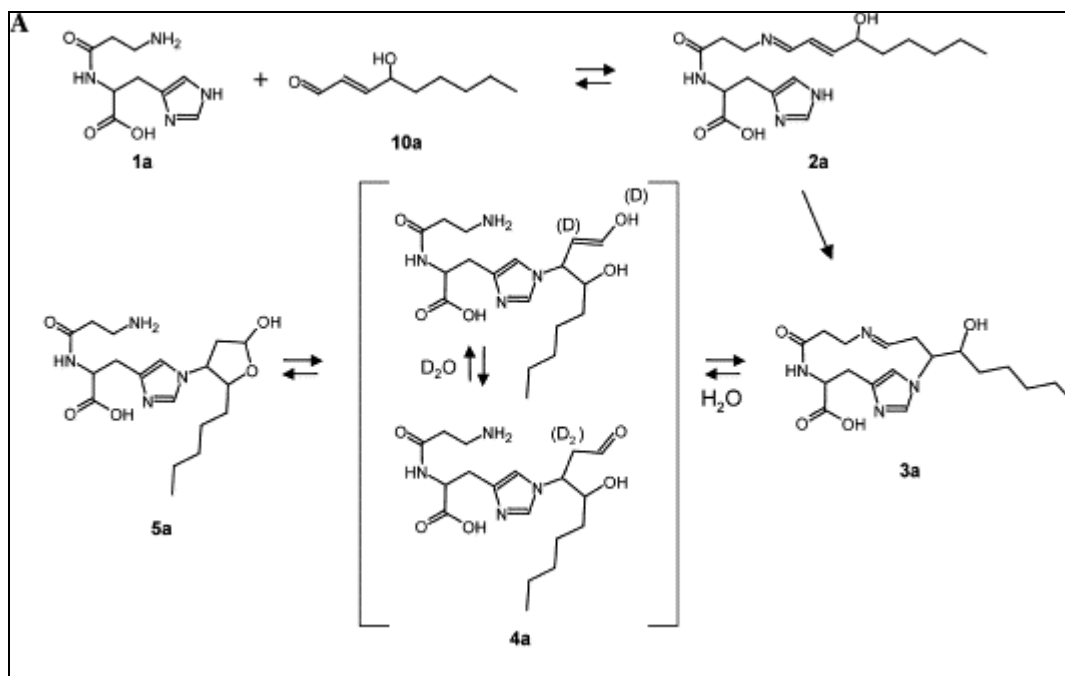


Figure 1.4 Three-step mechanism carnosine reaction with HNE. (147)

CHAPTER TWO

Obesity in a model of *gpx4* haploinsufficiency uncovers a causal role for lipid-derived aldehydes in human metabolic disease and cardiomyopathy

As published in:

Katunga LA, Gudimella P, Efird JT, Abernathy S, Mattox TA, Beatty C, Darden TM¹, Thayne KA, Alwair H, Kypson AP, Virag JA, Anderson EJ. Obesity in a model of *gpx4* haploinsufficiency uncovers a causal role for lipid-derived aldehydes in human metabolic disease and cardiomyopathy. 2015. *Molecular Metabolism*. In Press

ABSTRACT

Objective - Lipid peroxides and their reactive aldehyde derivatives (LPPs) have been linked to obesity-related pathologies, but whether they have a causal role has remained unclear. Glutathione peroxidase 4 (GPx4) is a selenoenzyme that selectively neutralizes lipid hydroperoxides, and human *gpx4* gene variants have been associated with obesity and cardiovascular disease in epidemiological studies. This study tested the hypothesis that LPPs underlie cardio-metabolic derangements in obesity using a high fat, high sucrose (HFHS) diet in *gpx4* haploinsufficient mice (GPx4^{+/-}) and in samples of human myocardium.

Methods Wild-type (WT) and GPx4^{+/-} mice were fed either a standard chow (CNTL) or HFHS diet for 24 weeks, with metabolic and cardiovascular parameters measured throughout. Biochemical and immuno-histological analysis was performed in heart and liver at termination of study, and mitochondrial function was analyzed in heart.

Biochemical analysis was also performed on samples of human atrial myocardium from a cohort of 103 patients undergoing elective heart surgery.

Results Following HFHS diet, WT mice displayed moderate increases in 4-hydroxynonenal (HNE)-adducts and carbonyl stress, and a 1.5-fold increase in GPx4 enzyme in both liver and heart, while *gpx4* haploinsufficient (GPx4^{+/-}) mice had markedly greater carbonyl stress in these organs accompanied by exacerbated glucose intolerance, dyslipidemia, and liver steatosis. Although normotensive, cardiac hypertrophy was evident with obesity, and cardiac fibrosis more pronounced in obese GPx4^{+/-} mice. Mitochondrial dysfunction manifesting as decreased fat oxidation capacity and increased reactive oxygen species was also present in obese GPx4^{+/-} but not WT hearts, along with up-regulation of pro-inflammatory and pro-fibrotic genes. Patients with diabetes and

hyperglycemia exhibited significantly less GPx4 enzyme and greater HNE-adducts in their hearts, compared with age-matched non-diabetic patients.

Conclusion These findings suggest LPPs are key factors underlying cardio-metabolic derangements that occur with obesity and that GPx4 serves a critical role as an adaptive countermeasure.

KEYWORDS:

glutathione peroxidase 4; lipid peroxidation; obesity; mitochondria; inflammation; human heart

ABBREVIATIONS

PUFA	Polyunsaturated fatty acids
LPPs	Lipid peroxidation end products
GPx4	Glutathione peroxidase 4
HFHS	High fat, high sucrose
WT	Wild type
CNTL	Control
BMI	Body mass index
4-HNE	4-Hydroxynonenal
ROS	Reactive oxygen species
RNS	Reactive nitrogen species
HDL	High-density lipoprotein
TG	Triglycerides
EF	Ejection fraction
FS	Fractional shortening
Nrf2	Nuclear factor (erythroid-derived 2)-like 2
IL-1 β	Interleukin-1 beta
IL-6	Interleukin-6
TNF- α	Tumor necrosis factor- α
iNOS	Inducible nitric oxide synthase
RAGE	Receptor for Advanced Glycation End Products
Coll1a1	collagen, type I, alpha
Coll4a1	Collagen, type IV, alpha 1
β -MHC β	Myosin heavy chain
TGF- β 1	Transforming growth factor beta 1
TGF- β 2	Transforming growth factor beta 2

1. INTRODUCTION

The prevalence of obesity is rapidly spreading throughout the world with over 28% of adults having a body mass index (BMI) of $\geq 25\text{kg/m}^2$ ((1, 2)). In addition to the increased risk for type 2 diabetes, a growing number of studies have reported a high prevalence of cardiomyopathy in obese patients (~40% by some estimates) ((18)), with 'preclinical' myocardial damage ((157)) and diastolic dysfunction already evident in young adult ($\leq 35\text{yrs}$) obese/diabetic patients ((158)) and even children ((159)). Importantly, these cardiac derangements appear in the absence of detectable coronary disease or hypertension. Together, these findings strongly indicate a need for more careful examination of potential mechanisms that underlie cardiomyopathy in obese individuals.

Polyunsaturated fatty acids (PUFAs) are continuously oxidized *in vivo* through both enzymatic and non-enzymatic reactions ((160, 161)), forming lipid peroxidation end products (LPPs) such as isoprostanes, isofurans, thromboxanes, and α , β -unsaturated aldehydes ((162)), all of which have biological effects ((163-166)). These aldehydes cause post-translational modifications of proteins through Michael addition with lysines and histidines, and through covalent modification of sulfhydryl groups (e.g., cysteines) to form carbonyl adducts ((167, 168)). Due to this high degree of reactivity, many of these aldehydes have been proposed to be etiologic agents in disease ((160, 169) (57, 167, 169-173)). 4-hydroxynonenal (HNE) is a α , β -unsaturated aldehyde derived from n-6 PUFA peroxidation, and HNE levels increase proportionally with ROS/RNS levels ((47)). One recent report showed that HNE-modified albumin is significantly increased in the serum of type 2 diabetic patients ((174)).

Mitochondrial membranes are abundant with unsaturated fatty acids, which are prone to peroxidation ((54-56)). The mitochondrion is also the primary source of cellular ROS, making it a major source of LPPs ((51)). As a countermeasure, mitochondria contain an elaborate system of antioxidant and LPP-detoxifying enzymes. One of these is glutathione peroxidase 4 (GPx4), which resides in the mitochondrial inner membrane (in addition to nucleus and cytosol) to

specifically scavenge lipid hydroperoxides ((80, 83, 88)). GPx4 is one of a few antioxidant enzymes known to neutralize both simple and complex lipid hydroperoxides (e.g., Cholesterol hydroperoxide) ((175, 176)). It is the only member of the GPx super-family that is indispensable during development, with embryonic lethality of GPx4 null mice occurring at stage E7.5 ((177-179)). In recent genetic and epidemiological studies, variants of *gpx4* that result in diminished content and/or catalytic activity have been associated with obesity ((105)), cardiovascular disease ((104, 180)) and inflammation ((181, 182)). However, no experimental studies to date have explored GPx4 in the context of obesity or its related pathologies, and this may be a significant oversight given the well-known association between mitochondrial-derived oxidative stress and metabolic disease ((24, 183)). In this study, we tested the hypothesis that LPPs are a causal factor underlying cardio-metabolic derangements in obesity by investigating the effect of a long-term high fat, high sucrose (HFHS) diet in a mouse model of *gpx4* haploinsufficiency (GPx4^{+/-}) and in samples of human atrial myocardium obtained from non-diabetic and diabetic patients undergoing elective heart surgery.

2. METHODS

2.1. Mouse Model and Study Design. Animal care and experimental procedures were performed with approval from the Institutional Animal Care and Use Committee of East Carolina University and were in compliance with the National Institutes of Health's Guide for Care and Use of Laboratory Animals. C57BL6/J female mice (Jackson Laboratory) were crossed to male GPx4^{+/-} mice and pups were genotyped by polymerase chain reaction (PCR) using primers described in ((82)). At 8-12 weeks, WT and GPx4^{+/-} male and female age-matched littermates (n=6) were randomly assigned to groups and individually housed. Mice were fed either control (CNTL-TD110367) or high fat high sucrose (HFHS-TD110365) diet from Harlan-Teklad Laboratories (Madison, WI) *ad libidum* for 25 weeks. The composition of this diet was a special formulation consisting of mixed saturated and n-6 PUFA (44.6% kcal/g fat),

with high sucrose (34% kcal/g) content ((72)). Mice were housed at controlled temperature and a 12hr light/dark cycle was maintained. At the end of the diet period, all live animal metabolic and echocardiographic measurements were made 1-2 weeks prior to tissue collection to allow for a 'wash-out period' to minimize artifact attributable to additional stress that may have been introduced by these procedures.

2.2. Patient enrollment and myocardial tissue collection. The Institutional Review Board of the Brody School of Medicine at East Carolina University approved all aspects of this study. Adult patients undergoing primary, non-emergent elective coronary artery bypass graft (CABG) or CABG/valve surgery between January 2011 and December 2014 were enrolled for this study. Demographic and clinical variables for these patients, including preoperative cardiovascular and metabolic drugs, are listed in **Table 2** according to diabetes status. Those having prior cardiac surgery, history of arrhythmia, or severely enlarged atria (>4.0 cm) were excluded from the study. Atrial appendage biopsies were obtained from each patient as previously described ((224)), directly prior to institution of cardiopulmonary bypass. Myocardium was dissected from the endocardial side of the biopsy, rinsed briefly and frozen in liquid N₂. All samples were rapidly processed this way to minimize protein and mRNA degradation across patients.

2.3. Metabolic Parameters. Body weight of the mice was recorded on a weekly basis throughout HFHS diet. Body composition was analyzed by nuclear-MRI (EchoMRI 700 Echo Medical Systems, Houston, TX). An oral glucose tolerance test (dose-0.5g/kg) was performed following a ~4 hour fast in week 22 of the HFHS diet period. Glucose levels were measured using a standard glucometer (OneTouch UltraMini, LifeScan, Milpitas, CA) in blood collected from a tail nick. Serum cholesterol, high-density lipoprotein (HDL), and triglycerides (TG) were analyzed using UniCel DxC 600 (Beckman Coulter, Indianapolis, IN).

2.4. Assessment of Cardiovascular Function. At end of the diet intervention, blood pressure was determined by non-invasive tail-cuff plethysmography (SC1000, Hattaras Instruments, Cary, NC). Mice were acclimated to the procedure for 3 days, and the average of blood pressure readings made over 3 consecutive days was recorded. A single recording was an average of 10 measurements after 5 acclimatization cycles, with duration no longer than 10 minutes, at approximately the same time every day. Also at this time, high-resolution echocardiography was performed on fully conscious mice using a 30 MHz transducer (Vevo 2100, VisualSonics, Toronto, ON) to assess cardiac function and structural parameters *in vivo*. Parasternal long- and short-axis views were captured in M-mode and recordings analyzed using system software.

2.5. Liver and Cardiac Histology: Mice were anesthetized with isoflurane. Hearts (n=2/group) were stopped with KCl, fixed in Zinc Fixative then embedded in paraffin. Next, they were cut cross-sectionally, stained in Hematoxylin and eosin or picosirus red (collagen), then viewed under polarized light. Livers from these animals were fixed, embedded and stained in a similar fashion, with the exception that oil red O was used for liver triglycerides. Images of each heart were captured at 20X. The cardiomyocyte diameter of 8-10 myocytes from 5 captured images per animal was analyzed using Image J (<http://imagej.nih.gov/ij/>) by an individual blinded to the treatment group.

2.6. Preparation of permeabilized cardiac myofibers and mitochondrial function measurements. All procedures for these measurements have been described in detail by our group previously ((22-24, 72)). The mice were anesthetized with isoflurane and rapidly euthanized by pneumothorax. Blood was collected for serum analysis via cardiac puncture. Whole hearts were dissected, weighed, and a small portion of the left ventricle (LV) was cut for preparation of permeabilized myofibers (~30 mg) and placed in Buffer X containing (in mM):

7.23 K₂EGTA, 2.77 CaK₂EGTA, 20 Imidazole, 20 Taurine, 5.7 ATP, 14.3 Phosphocreatine, 6.56 MgCl₂·6H₂O and 50 MES (pH 7.1, 295 mOsm). Of the remaining LV/septum, one portion was used for standard mitochondrial isolation, and another was snap frozen in liquid N₂ and stored at -80°C for further biochemical analysis. Following permeabilization in 50 µg/ml saponin for 30 minutes, fibers were transferred to Buffer Z containing (in mM): 110 K-MES, 35 KCl, 1 EGTA, 5 K₂HPO₄, 3 MgCl₂·6H₂O, and 5 mg/ml BSA (pH 7.4, 295 mOsm) and remained in Buffer Z with 20µM Blebbistatin on a rotator at 4°C until analysis (<1.5 hours). Fibers were then transferred to an Oroboros O2K (Oroboros Instruments, Innsbruck, Austria) where respiration was recorded in Buffer Z + 20µM Blebbistatin, 20 mM Creatine at 30°C. Respiration (*J*O₂) measurements were performed following addition of 125µM palmitoyl-carnitine + 1mM malate followed by 4mM ADP. H₂O₂ emission was measured using a spectrofluorometer (Photon Technology Instruments, Birmingham, NJ) in Buffer Z + 20µM Blebbistatin, 10µM Amplex Red, 1 U/ml horseradish peroxidase, 25 U/ml superoxide dismutase. For H₂O₂ measurements, respiratory substrates used were 125 palmitoyl-carnitine, 2mM Malate + 100 µM ADP, 5 mM glucose and 1 U/ml hexokinase (i.e., phosphorylating state) followed by sequential addition of 5mM glutamate then 5mM succinate. Once mitochondrial experiments completed, fibers were collected, rinsed in ddH₂O to remove excess salts, and lyophilized (Labconco, Kansas City, MO). Fibers were then weighted on a microbalance (Mettler Toledo, Denver, CO) and mitochondrial *J*O₂ (oxygen consumption rate) and *J*H₂O₂ (peroxide emission rate) were normalized to dry weight.

2.7. Real-time qPCR of gene expression. Cardiac samples (~10mg) were homogenized in glass grinders (Kimble Chase, Vineland, NJ) then subjected to Proteinase K digestion. All materials used in RNA extraction were provided in RNeasy® Fibrous Tissue Mini Kit (Qiagen Inc, Valencia, CA cat# 74704). Reverse Transcription was performed using the iScript™ cDNA Kit (Biorad Laboratories, Hercules, CA cat# 170-8891). The SsoAdvanced™ SYBER® Green

reaction cocktail was used in the amplification and detection of DNA in RT-PCR. All protocols were performed according to product specifications unless otherwise stated. Cycle threshold (C(t)) values were converted to relative gene expression levels using the $2^{-\Delta\Delta C(t)}$ method and normalized to the level of 18S ribosomal RNA. Data are reported as fold-change in gene expression (arbitrary units) \pm S.E.M. relative to WT-CNTL mice (n=4-5 per group). The sequences and references for the primers used in qRT-PCR are listed in **Supplemental Table 1**.

2.8. Mitochondria Isolation. The technique applied has been modified from methods previously described ((225, 226)). Briefly, ~100 mg of cardiac tissue was excised and added to a petri dish with ice. The tissue was minced for 4-5 minutes, until it could pass through a pipette, and subjected to a brief (2 minutes) trypsin incubation. The mixture was transferred to a 50mL conical tube and allowed to settle. The supernatant was removed and discarded. The remaining mixture was resuspended in 3mL of Mitochondria Isolation Medium (MIM) (300mM Sucrose, 10mM Na-HEPES, 0.2mM EDTA) with BSA, then transferred to a pre-chilled Dounce homogenizer and slowly homogenized for a total of ~10-12 counts. The homogenate was then subjected to a series of differential centrifugation steps. The fractions of isolated mitochondria obtained (mixed subsarcolemmal and intermyofibrillar) were resuspended in a small volume of MIM+BSA and frozen at -80° for biochemical analysis.

2.9. Immunoblot and enzyme-linked immunosorbent assay (ELISA). Cardiac tissue was homogenized in TEE-T Buffer (10 mM Tris, 1 mM EDTA, 1 mM EGTA + 0.5% Triton X-100), and then loaded on 4-20% pre-cast polyacrylamide SDS gel (Biorad, Hercules, CA) under reducing conditions. Protein was transferred to PVDF membranes (Millipore, Bellerica, CA) and incubated with primary antibodies for GPx4 and α -tubulin (Abcam, Cambridge, UK), COX IV and β -actin (Cell Signaling Technology, Danvers MA), and HNE-adduct (Percipio Biosciences). Membranes were incubated using infrared fluorophore-conjugated secondary antibodies (LiCor Biosciences, Lincoln, NE), scanned using Odyssey Clx Infrared Imaging System (Li-Cor) and analyzed by

densitometry using Image J (NIH). The absolute quantities of GPx4 and HNE-modified protein adducts in human cardiac tissue was determined by a quantitative ELISA approach developed in our lab, as described previously ((72)). Fixed concentrations of HNE-adducts were made by incubating 4-hydroxynonenal (Cayman Chemical, Ann Arbor, MI) with BSA. A standard curve of both recombinant GPx4 (AbFrontier, Seoul, Korea) and HNE-modified BSA were then incubated on immunolon-coated 96-well assay plate (Fisher Scientific) along with diluted cardiac protein. Samples were incubated overnight at 4°C, and subsequently washed with PBS+0.05% Tween-20 and blocked for 2 hours with BSA or NB4025 (NOF America, White Plains, NY) at 37°C. Samples were then incubated with primary antibodies for GPx4 and HNE adduct for 2 hours at 37°C. Samples were washed with PBS+0.05% Tween-20 and incubated with HRP-conjugated secondary antibody for 2 hours at 27°C. Following this incubation, samples were washed as before and incubated with Amplex Red (10 µM). Concentrations of GPx4 and HNE-adducts in the samples were determined by fitting to the standard curve within each plate and normalized to total protein concentration.

2.10. Hydrazide labeling of carbonyl-modified proteins: Hydrazide Cy5.5 dye (GE Healthcare Bio-Sciences, Pittsburgh, PA) was diluted in dimethyl sulfoxide (DMSO) at a stock concentration 1mg/ml. Tissue was homogenized under an anaerobic chamber (Coy Laboratory Products, Grass Lake, MI) in 10mM sodium phosphate buffer, containing 0.1% Triton X-100, and de-gassed using dry vacuum pump (Welch No. 25228-01, Monroe, LA). Dye was added to half of the homogenate (1:10). The samples were left under anaerobic conditions for 2 hours and incubated overnight on orbital shaker at 4C. The other aliquot of tissue homogenate was used to quantify protein content. Portions of the labeled cardiac tissue homogenate were subjected to SDS-PAGE on 10% SDS polyacrylamide gel. The gels were scanned using Odyssey Clx Infrared Imaging System (Li-Cor) and Cy5.5-labeled proteins were analyzed by densitometry using Image J (NIH).

2.11. Statistical Analysis. All animal data are presented as mean \pm SEM. Statistical analysis on mouse model variables were performed with Graph Pad Prism (Graph Pad Prism, La Jolla, Ca.). One-way ANOVA was performed on continuous variables followed by Newman-Keuls posttest, with $\alpha < 0.05$ considered statistically significant. In the human data analysis, categorical variables are presented as frequency and percentage and continuous variables were presented as mean \pm standard deviation, median, median and interquartile range. Fisher exact and Chi (χ^2) procedures were used to compute statistical significance of group comparisons for categorical variables. Deuchler-Wilcoxon was used for continuous variables. Biochemical variables were divided into quartiles (GPx4) or tertiles (HNE) and analyzed using a robust Poisson regression model (with relative risk as the measure of association). Missing values for all clinical and biochemical variable were imputed using the iterative expectation-maximization (EM) algorithm as described in a recent study ((224)). Variables that were statistically significant in the univariable analysis were included into the multivariable analysis. *P*-value was computed using Friedman's Nonparametric test for central tendency while adjusting for age. *P*_{trend} was computed using likelihood ratio trend test, adjusting for age and sex. Statistical significance was defined as $P < 0.05$. SAS Version 9.3 was used for all analyses of human biochemical and clinical variables.

3. RESULTS

3.1. GPx4 deficiency in obesity leads to enhanced lipid peroxidation and carbonyl stress in liver, exacerbating insulin resistance and steatosis.

To test our hypothesis that LPPs underlie obesity-related pathologies we used a GPx4-deficient (GPx4^{+/-}) mouse model. GPx4^{+/-} mice are phenotypically indistinguishable from WT in the absence of an exogenous stressor but more susceptible to damage from radiation and environmental toxicants ((82, 99)). The rationale for using this mouse model was that it mimics

the effect of previously identified *gpx4* gene variants on GPx4 enzyme levels and activity in human cells ((104, 105, 184)). Following HFHS diet no significant differences in adiposity or weight gain were observed between WT and GPx4^{+/-} mice, although obese GPx4^{+/-} mice had substantial dyslipidemia and fasting hyperglycemia with HFHS diet (Table 1). Whole body energy expenditure, determined by VO₂ and VCO₂ using indirect calorimetry, was not different between WT and GPx4^{+/-} mice, either with CNTL or HFHS diet (data not shown). Glucose intolerance was also exacerbated in the GPx4^{+/-} mice compared with WT (Figure 1A), and serum insulin levels were also significantly increased with HFHS diet (Figure 1B). GPx4 enzyme levels in liver of WT mice increased significantly as a result of HFHS diet, although GPx4^{+/-} mice contain significantly less enzyme than WT (Figure 1C and Supplemental Figure 1A). In parallel with the increase in GPx4, levels of HNE-adducts in liver increased in WT with HFHS diet but were significantly more pronounced in GPx4^{+/-} mice compared with WT. To determine whether the increased lipid peroxidation in the GPx4^{+/-} mice corresponded to a more severe liver pathology following HFHS diet, liver triglycerides and collagen were measured by oil red O and picrosirius red staining, respectively. GPx4^{+/-} mice displayed markedly greater liver steatosis (Figure 1D) and fibrosis (Figures 1E) than WT mice following HFHS diet.

3.2. Cardiac structural remodeling and fibrosis is exacerbated by GPx4 deficiency in obesity.

Previous studies have shown that HFHS diet-induced obesity causes significant cardiac hypertrophy and left ventricular (LV) diastolic dysfunction in rodent models ((185-187)). Here, HFHS diet caused an increase in cardiac mass to a similar extent between WT and GPx4^{+/-} mice (Figure 2A, E). However, compared with WT, GPx4^{+/-} mice display significantly greater cardiomyocyte diameter (Figure 2E, F) and fibrosis (Figure 2B, C) following HFHS diet. Obese mice also have increased levels of serum brain natriuretic peptide (BNP, Figure 2G), indicative of ventricular wall stress. This evidence of cardiomyopathy exists in the absence of any changes in

LV systolic function (Figure 2H), blood pressure (Figure 2I) or heart rate (Figure 2J) in the mice following HFHS diet, indicating that any cardiomyopathy which might be present in these mice is not due to increased afterload.

Recently, in two independent experimental models of cardiac hypertrophy it was observed that GPx4 and Thioredoxin Reductase (TxnRd) were the only antioxidant seleno-enzymes to increase in the heart, suggesting that they are critical for cardiac compensatory response to hypertrophic stimuli ((50, 188)). A significant increase in GPx4 mRNA (Figure 3A) and enzyme content (Figure 3B and Supplemental Figure 1B) in myocardium of WT mice with HFHS diet was observed. Conversely, GPx4^{+/-} mice had lower levels of mRNA that did not correspond to any changes in GPx4 enzyme levels following HFHS diet. Levels of HNE-adducts (Figure 3C) and protein carbonyls (Figure 3C) do increase moderately in WT hearts with HFHS diet, although GPx4 deficiency leads to a striking increase in this protein carbonylation with obesity. To determine if GPx4 deficiency and augmented carbonyl stress in obesity triggered a compensatory redox adaptive response in the heart, expression of a number of antioxidant genes were examined. GPx4^{+/-} mice were found to have increased expression of several antioxidant genes following HFHS diet (Figure 3D).

3.3. GPx4 deficiency causes mitochondrial abnormalities and up-regulation of cardiac inflammation and fibrosis signaling pathways with obesity.

Mitochondrial dysfunction, as characterized by decreased ATP and/or respiration combined with increased ROS, has been linked to several obesity-related pathologies, including insulin resistance and cardiomyopathy, and recent studies have implicated a role for mitochondrial protein carbonylation in mediating this dysfunction ((189-191)). Parameters of mitochondrial function in permeabilized LV myofibers were examined to assess the interrelationship between GPx4 deficiency, carbonyl stress, and mitochondria in the obese myocardium. Mitochondrial GPx4 enzyme content was measured in the mitochondrial fraction isolated from whole hearts.

GPx4 increased in cardiac mitochondria of WT mice with HFHS diet, while total levels of GPx4 were lower and remained that way following HFHS diet in the GPx4^{+/-} mice (Figure 4A and Supplemental Figure 2A).

It was expected that mitochondrial GPx4 deficiency would potentially lead to a greater degree of mitochondrial membrane lipid peroxidation and reactive aldehyde formation. Here, the amount of mitochondrial HNE-adducts were greater in GPx4^{+/-} hearts than WT, and the HFHS diet increased the relative amount of these adducts in both WT and GPx4^{+/-} mice (Figure 4B and Supplemental Figure 2B). These increased HNE-adducts may have functional consequences since recent studies have documented that mitochondrial HNE-adducts correspond to decreased oxidative phosphorylation in diabetic heart mitochondria ((192, 193)). Moreover, another report highlights the importance of mitochondrial fatty acid β -oxidation as a metabolic 'sink' for HNE ((194)). In WT hearts, both basal and maximal ADP-stimulated Palmitoyl-L-carnitine supported respiration was markedly increased following HFHS diet, while these rates were unchanged with HFHS diet in the GPx4^{+/-} mice (Figure 4B).

In a previous study we reported that the selenoenzyme thioredoxin reductase-2 (TxnRd2) increased in rat heart with HFHS diet ((72)), corresponding to a decreased rate of mitochondrial H₂O₂ emission in the obese rat heart. Other groups have also reported decreased mitochondrial ROS with obesity/diabetes in mouse ((195)) and rat models ((196)). Given our previous findings, combined with the fact that TxnRd2 expression was increased in GPx4^{+/-} hearts with HFHS diet (Figure 3E), we sought to ascertain whether a similar adaptation in redox buffering was occurring in cardiac mitochondria of these mice. Here, using paired H₂O₂ emission experiments in the absence and presence of the TxnRd2 inhibitor auranofin, a dramatic (~4-fold) increase in total H₂O₂ emission was observed in permeabilized myofibers prepared from obese GPx4^{+/-} mice fed HFHS diet, while a decrease in this ROS emission was observed in the obese WT mice following HFHS diet (Figure 4C). Auranofin exposure significantly increased the rate of mitochondrial ROS in the obese WT mice but not obese GPx4^{+/-} mice.

Chronic, low-grade inflammation in the obese heart is known to cause profibrotic and hypertrophic signaling. Although it has been difficult to fully ascertain the exact nature of the relationship between inflammation and cardiac remodeling, some investigators have proposed that activation of the receptor for advanced glycation end products (RAGE) may play a role. RAGE belongs to a family of pattern recognition receptors for AGE and has been studied extensively in the context of diabetes-related pathologies ((132, 197)). Increased expression of RAGE is present in the hearts of obese GPx4^{+/-} mice (Figure 5A), and this is consistent with the increased carbonyl stress present in these hearts since reactive aldehydes such as HNE are known to potentiate AGE formation ((198)). Activation of RAGE has been shown to induce chronic activation of nuclear factor kappa-light-chain-enhancer of activated B cells (NFκB), which, in turn, activates further inflammatory pathways. Furthermore, there is extensive crosstalk between the RAGE and Transforming Growth Factor-Beta (TGF-β) family of proteins ((123, 141, 199)). Notably, the hearts of obese GPx4^{+/-} mice also displayed greater pro-inflammatory cytokine expression and genes involved in fibrosis and hypertrophy compared with WT following HFHS diet, while only a modest increase in a few select genes was observed with HFHS diet in WT hearts (Figure 5A & B).

3.4. Cardiac GPx4 deficiency is associated with increased HNE-adducts and relative risk (RR) for diabetes in humans. Next, we sought to determine whether there is an association between GPx4 and lipid-derived carbonyl stress in human heart and, also, to examine whether there is a connection between these parameters and human metabolic disease. In a small pilot study of ~20 patients, we previously reported greater levels of HNE-protein adducts in the hearts of hyperglycemic type 2 diabetic patients, and these increased HNE-adducts were accompanied by depletion of cardiac glutathione and increased mitochondrial ROS production ((200)). Here, using samples of atrial myocardium obtained from patients (n=103) undergoing elective cardiac surgery (Table 2), we observed that diabetic patients had significantly less cardiac GPx4 than

non-diabetic patients (Figure 6A), and this corresponded with greater levels of HNE-adducts in the diabetic hearts (Figure 6B). A multivariable regression analysis was performed on quartiles of cardiac GPx4 and tertiles of HNE-adducts, and cardiac GPx4 was found to be negatively associated while HNE-adducts positively associated with RR for diabetes in these patients (Table 3). To determine if hyperglycemia was associated with cardiac GPx4 or HNE-adducts in these patients, a multiple linear regression model was applied, adjusting for sex. No significant association between cardiac GPx4 or HNE-adduct levels and HbA1c was observed in these patients (Table 3 and Supplemental Figure 1).

Similar to what was observed with the WT-HFHS mice, cardiac GPx4 content was positively correlated with cardiac HNE-adducts in these patients (Figure 6C), suggesting that GPx4 is an adaptive response of the tissue to persistent oxidative stress. Interestingly, the ratio of HNE-adducts/GPx4 was much higher in diabetic than non-diabetic hearts (Figure 6D), indicating that the GPx4 adaptive response has been over-whelmed or compromised in these patients.

4. DISCUSSION

Only an increased understanding of the mechanisms underlying obesity-related pathologies will enable physicians to better manage diseases associated with this emerging epidemic. Lipid peroxides and their reactive aldehyde derivatives have been postulated to play a causal role in obesity-related cardio-metabolic diseases, and emerging epidemiologic data has reported a link between polymorphisms and mutations in *gpx4* and human diseases, including obesity. Together, these previous findings suggest that GPx4 may be an adaptive component that serves a protective role against the persistent oxidative stress in obesity. The present study tested this hypothesis in a translational model of HFHS diet-induced obese GPx4^{+/-} (i.e. GPx4 deficient) mice, combined with cardiac tissue samples obtained from patients undergoing elective cardiac surgery. The findings from this study demonstrate that GPx4 deficiency with diet-induced obesity

leads to significant increases in lipid peroxide-derived aldehydes, corresponding to more severe cardio-metabolic derangements including glucose intolerance, dyslipidemia, liver steatosis, and cardiac hypertrophy and fibrosis. Abnormalities in mitochondrial function in hearts from the obese GPx4^{+/-} mice implicate a role for the enzyme in protecting that critical organelle from oxidative damage in obesity. Furthermore, the adverse cardiac remodeling observed in the obese GPx4^{+/-} mice was accompanied by up-regulation of genes involved in cardiac inflammation and remodeling, illustrating the importance of carbonyl stress as a causal factor in these pathways. Lastly, the relationship between decreased cardiac GPx4 and increased HNE-adducts and human metabolic disease was confirmed by studying cardiac tissue samples obtained from non-diabetic and diabetic patients. Collectively, these observations allow for a proposed model of GPx4 as a protective adaptation in obesity (as shown in the Graphical Abstract). Clearly, when HNE-adducts increase as a result of persistent lipid peroxidation in obesity/nutrient overload, GPx4 becomes upregulated to compensate (Figure 1 & 3). However, over time and possibly due to underlying genetic causes, GPx4 becomes overwhelmed in an obese individual and HNE-adducts increase. The consequence of this is increased inflammation, mitochondrial dysfunction (and likely potentiation of mitochondrial ROS), and the broad cardio-metabolic pathologies that are known to follow (e.g., diabetes, cardiomyopathy, liver disease).

These findings stand in contrast to preceding studies of diet-induced obesity in antioxidant-deficient models. One recent study of high fat-fed GPx1-deficient mice (whole body GPx1^{-/-}) found that systemic oxidative stress increased with obesity as expected, but these mice were actually protected from insulin resistance and liver steatosis (99). In a study using high fat diet in SOD2^{+/-} mice (also exhibiting greater oxidative stress), insulin sensitivity was again unchanged with obesity, although a modest effect on pancreatic β -cell release of insulin was observed (100). Another intriguing study used high fat diet in a glutathione-deficient (Gclm^{-/-}) mouse model. The authors found that despite a huge increase in systemic oxidative stress with the diet, these mice were also protected from increased adiposity, insulin resistance and

steatosis, possibly due to an increase in basal energy expenditure (101). Given these recent findings, the fact that GPx4 haploinsufficiency alone can induce such a dramatic effect on cardio-metabolic disease parameters with HFHS diet implies that lipid peroxides must play a very prominent etiological role in obesity-related cardio-metabolic diseases.

Deleterious effects of lipid-derived aldehydes in biological systems have been well known for many years. For example, nucleophilic attack of cysteine residues by aldehydes has negative ramifications on metabolic pathways in the cell ((167, 201)). A recent mass spectrometric analysis of cysteine oxidation status in hearts from mice fed a diabetogenic diet for 8 months showed that ~40% of total oxidized cysteines are mitochondrial in origin ((202)). Proteomic analysis of mitochondria from diabetic rat hearts reveals an increased formation of carbonyl adducts (e.g. HNE, MDA) with complexes of the electron transport chain and respiratory complexes, and these adducts correspond to a reduction in enzyme activity ((170)). Our data suggest that GPx4 protects against cardiac mitochondrial dysfunction with obesity as the obese GPx4^{+/-} mice had very high levels of carbonyl stress in their hearts (Figure 3), particularly HNE-adducts in the cardiac mitochondria (Figure 4B), accompanied by mitochondrial dysfunction, as compared with obese WT mice. Several studies have shown that GPx4 preserves ATP production and attenuates cytochrome c release in the mitochondria under oxidative stress ((203-205)). Cardiac-specific overexpression of mitochondrial GPx4 is protective in models of cardiac ischemia/reperfusion injury and in a streptozotocin (STZ)-induced diabetes model ((92, 206)). GPx4 exists as both short (i.e., mitochondrial-localized) and long (i.e., cytosolic-localized) isoforms, yet only deletion of the former is lethal in mice ((207)). Thioredoxin Reductase is the only other essential selenoenzyme identified to date, and this enzyme also has both mitochondrial (TxnRd2) and cytosolic (TxnRd1) isoforms ((208)). In the present study, increased mitochondrial H₂O₂ emission was observed in hearts of lean GPx4^{+/-} mice following the inhibition of TxnRd2 with auranofin (Figure 4C), although auranofin did not significantly affect the rate in the obese GPx4^{+/-} mice (which was already much greater than all other groups). This suggests

that mitochondrial lipid peroxide-scavenging with GPx4 and the thioredoxin redox couple are both important adaptive responses of cardiac mitochondria in obesity-related cardiac hypertrophy and that TxnRd2 cannot appropriately compensate for GPx4 deficiency within cardiac mitochondria if animals are obese.

A recent study showed that fatty acid β -oxidation is a novel HNE clearance pathway in heart (194). Considering the diminished rates of maximal Palmitoyl carnitine-supported respiration observed in the obese GPx4^{+/-} hearts, it is plausible that the elevated carbonyl stress observed in the hearts of these mice is a result of both increased mitochondrial ROS production (which initiates more lipid peroxidation) as well as a disruption of aldehyde detoxification pathways. The decreased GPx4 and correspondingly increased HNE-adducts seen here in myocardium of diabetic patients support our previous observations of decreased Palmitoyl-L-carnitine supported respiration and increased mitochondrial ROS in diabetic human hearts ((23, 24)). A link between mitochondrial HNE-adduct formation and decreased oxidative phosphorylation in diabetic heart mitochondria has recently been made ((192, 193)), and our findings suggest that GPx4 deficiency may underlie these oxidative modifications. High variability in dietary fat may also be a contributor to the greater levels of cardiac HNE-adducts in the diabetic patients, as it has been reported that diets consisting of high fat mixed with carbohydrate, or high fat alone, can lead to drastically different outcomes in HNE accumulation in oxidative tissues (102). Other studies directed at examining the role that alternative aldehyde-producing (e.g., monoamine oxidase) and detoxifying enzymes (e.g., aldehyde dehydrogenases) may have in pathologies of obese/diabetic hearts may also be useful ((201)). In addition, an improved understanding of the regulation of selenocysteine status may serve as a major clue to uncovering the mechanisms that govern the progression to maladaptive remodeling in hearts of patients with metabolic disease. Epidemiological studies of Keshan's disease, a cardiomyopathy endemic to regions of China, confirm that the heart is highly susceptible to injury resulting from disturbances to selenocysteine enzymes. Cardiomyopathy in Keshan's disease manifests as

acute cardiac fibrosis and mitochondrial dysfunction ((209)), a phenotype that is strikingly similar to the GPx4^{+/-} mice in the present study.

Aside from measurements of liver steatosis and serum lipids, our study did not explore the potential contribution of altered lipid metabolism that might exist in these mice. Lipotoxicity is a consistent feature of cardio-metabolic disease in both humans and animal models of obesity ((71, 210-214)) and therefore may contribute to the severe liver and cardiac pathology observed in the obese GPx4^{+/-} mice. The obese GPx4^{+/-} mice do not possess significantly greater adiposity than obese WT, as determined by % body fat. However, we cannot exclude that there may have been differences in adipose distribution between groups. It is also known that GPx4 directly modulates the lipoxygenase and cyclooxygenase II enzyme systems, and, when viewed in this context, the increased cardiac inflammation present in obese GPx4^{+/-} mice supports a potential role for prostaglandins and other oxidized lipids in mediating the severe metabolic pathologies in this model. Thus, we cannot exclude the contribution of these mediators in the obese GPx4^{+/-} mice. Other studies have documented that proteolysis and autophagy become compromised with carbonyl stress, and the diminished activity of these cellular processes may also explain the more severe phenotype observed in the obese GPx4^{+/-} hearts ((215, 216)). None of these alternative pathways were explored in the present study.

It is anticipated that these findings will serve to lay a foundation for future mechanistic studies directed at understanding how LPPs contribute to obesity-related pathologies and the adaptive role of GPx4. Considering that the most severe effects observed in the obese GPx4^{+/-} mice were evident in oxidative tissues (i.e., liver, heart, muscle), it will be very important in future studies to identify the cell- and tissue-specific role of GPx4 in mediating lipid peroxidation and carbonyl stress with obesity. Furthermore, our findings have clinical implications as they suggest that patients exhibiting decreased GPx4 expression and activity might be predisposed to obesity-related cardio-metabolic diseases. Indeed, clinical studies and human cell models have shown that GPx4 expression and activity vary widely in response to environmental and nutritional cues

((104, 184, 217-220)). Finally, although our understanding of the role of lipid-derived aldehydes and carbonyl stress in the etiology of obesity-related diseases is in its infancy, it is important to recognize that compounds that scavenge HNE and other lipid-derived aldehydes specifically, such as histidine-containing dipeptides, may be very useful in this regard ((154, 156), 103) and have experienced some success in pre-clinical testing and even clinical trials ((221-223)). Thus, further research into novel therapeutics targeting carbonyl stress will be important for mitigating the numerous cardio-metabolic diseases that accompany this rising epidemic of obesity.

ACKNOWLEDGEMENTS:

These authors would like to thank Amy Bullock for assistance with animal care and breeding and Joany Oswald Zary for assistance with histology.

FUNDING:

This research was supported by National Institutes of Health grants 1R21HL098780 and 1R01HL122863 to E.J.A

CONFLICT OF INTEREST:

The authors have no conflict of interest to declare.

TABLE 1: Body composition and metabolic parameters.

Variables	WT CNTL	WT HFHS	GPx4^{+/-} CNTL	GPx4^{+/-} HFHS	p-value
Terminal Body Weight (g)	34.5±1.3	48.0±2.2*	35.8±4.2	48.5±1.2*§	<0.0001
Fat Mass (g)	8.4±1.0	17.7±0.9*	10.0±2.9 [□]	19.4±0.8*§	0.0001
Lean Mass (g)	21.6±0.4	26.0±1.2*	22.3±1.4 [□]	24.9±0.4*	0.004
Body fat (%)	24.0±2.1	36.9±0.5*	31.3±3.0*	40.0±0.8*§	<0.0001
Fasting glucose (mg/dL)	141.3±4.1	168.6±14.2*	148.0±3.7	204.8±11.3* [□] §	0.007
Cholesterol (mg/dL)	51.0 ±8.6	72.8 ±6.5	34.0 ±8.7	103.5 ±17.8*§	0.01
Triglycerides (mg/dL)	46.8 ±6.3	44.0 ±10.6	55.5 ±1.5	99.5 ±11.3* [□] §	0.003
HDL Cholesterol (mg/dL)	74.9 ±8.0	96.7 ±7.2	53.1 ±9.4	118.4 ±14.4*§	0.009

All values expressed as mean ± S.E.M., n = 4- 6. * P<0.05 vs. WT-CNTL vs. [□] P<0.05 vs.

WT-HFHS. § P<0.05 vs. GPX4^{+/-} CNTL

Table 2. Patient Clinical and Demographic Characteristics

Variables	Diabetes n (%)	No Diabetes n (%)	p-value
Age			
Mean±SD	64±9.28	61±11	0.49
Median (IQR)	65 (16)	60 (17)	
Sex			
Female	7 (14)	1 (2)	0.026
Male	42 (86)	53 (98)	
Race			
White	41 (84)	47 (87)	0.78
Black	8 (16)	7 (13)	
BMI			
Mean±SD	31±6.6	30±5.3	0.46
Median (IQR)	30 (7.4)	29 (4.5)	
Preoperative Medications			
β-blockers	34 (69)	41 (76)	0.87
ACEi/ARBs	15 (31)	22 (41)	0.79
Diuretics	21 (43)	20 (37)	0.69
CCBs	10 (20)	13 (24)	0.89
Diabetic Medications	43 (88)	2 (4)	<0.0001
Insulin	32 (65)	2 (4)	
Metformin	15 (31)	0	
Sulfonylureas	4 (8)	0	
Glitazones	1 (2)	0	
GLP-1 agonist	2 (4)	0	
DDP-4 inhibitor	3 (6)	0	
Statins	41 (84)	46 (85)	0.94
Nitrates	19 (39)	32 (59)	0.65
Heart Failure	8 (16)	5 (9)	0.31
LVEF (%)	51.8 ± 3.9	53.6 ± 6.4	0.87

Sample size N = 103 for GPx4, N = 61 for HNE-adduct

Table 3. Multivariable analysis of GPx4 and HNE-adducts in human heart

GPx4 content (ug/ml)			
	Diabetes n (%)	No Diabetes n (%)	RR (95% CI)‡
Mean±SD	6.2±4.2	8.7±5.9	<i>P</i> =0.034†
Median (IQR)	6.0 (5.2)	6.7 (6.6)	
Q1 (≤3.9)	17 (35)	9 (17)	1.0 Referent
Q2 (>3.9 to 6.3)	10 (20)	15 (28)	0.65 (0.37 to 1.1)
Q3 (>6.3 to 9.4)	13 (27)	13 (24)	0.74 (0.47 to 1.2)
Q4 (>9.4)	9 (18)	17 (31)	0.58 (0.31 to 1.1)
			<i>P</i> _{trend} =0.063††
HNE content (mM)			
Mean±SD	18±8.3	14±9.8	<i>P</i> =0.028†
Median (IQR)	16 (11)	11 (12)	
T1 (≤9.0)	3 (10)	21 (47)	1.0 Referent
T2 (>9.0 to 17)	14 (47)	11 (24)	4.2 (1.4 to 13)
T3 (>17)	13 (43)	13 (29)	3.9 (1.2 to 12)
			<i>P</i> _{trend} =0.050††

‡ Relative Risk (RR) and 95% Confidence Interval (CI), adjusted for age and sex.

† *P*-value computed using Friedman's Nonparametric test for central tendency, adjusting age and sex.

†† *P*-value computed using the likelihood ratio trend test, adjusting for age and sex.

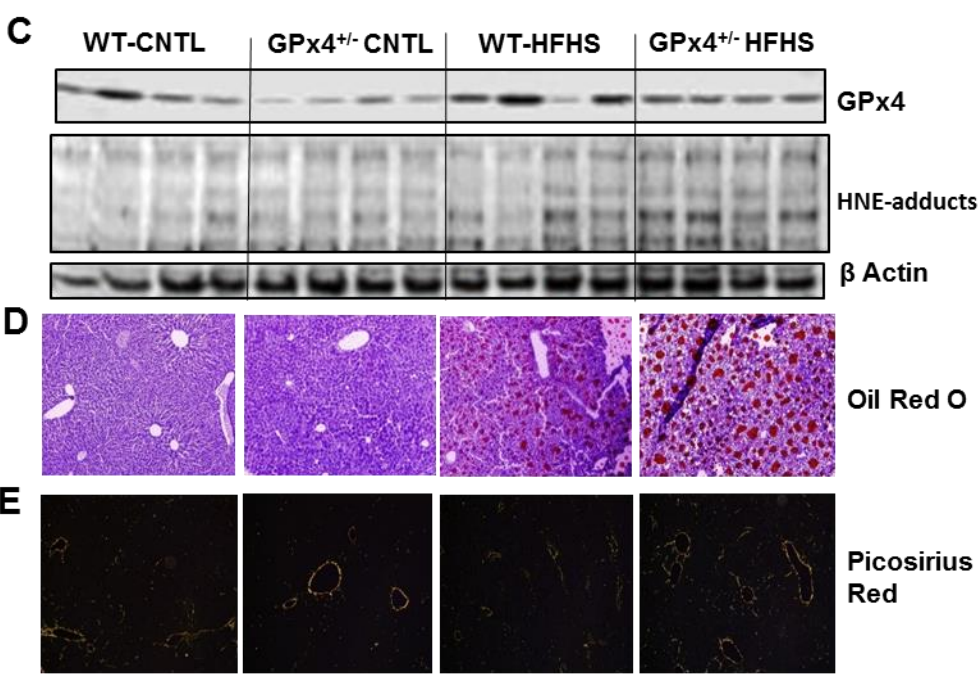
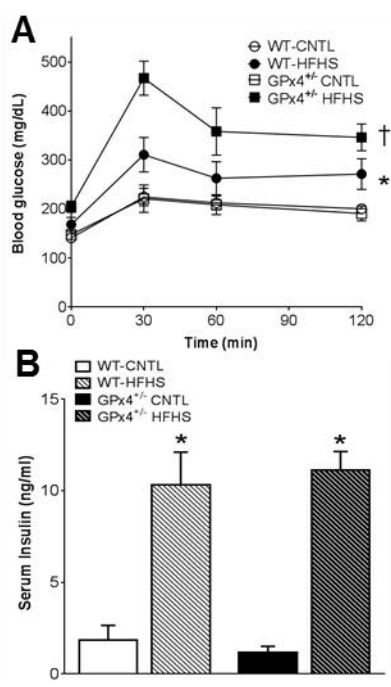


Figure 1. Glycemic control and liver biochemistry/pathology. Shown in **A** are oral glucose tolerance tests, along with fed-state serum insulin levels **B** after 24 weeks on the diet. In **C** are representative immunoblots of GPx4 and HNE-adducts in liver from 4 individual mice in each group, along with the corresponding β -actin loading control. Representative images of liver triglycerides stained with oil red O **D**, and collagen stained with picosirius red under polarized light **E** are shown for each group. Images are representative of 16 image fields captured per mouse, n=2-3 mice per treatment group. Data shown as mean \pm S.E.M., n = 7-8 mice per group. *P<0.05 vs. CNTL within genotype, † P<0.05 vs. WT-HFHS.

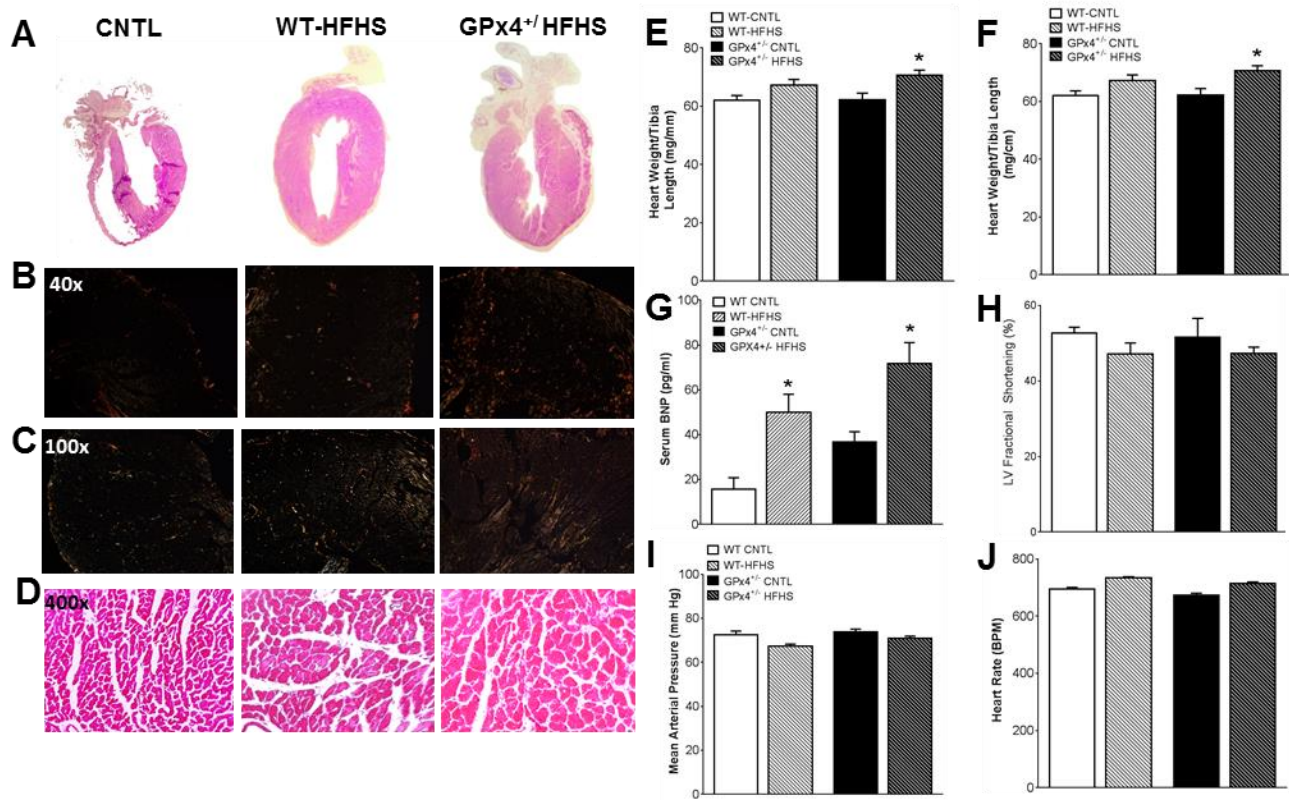


Figure 2. Cardiac structural and functional parameters. Panels shown are representative images of whole hearts **A**, cardiac collagen stained with picosirius red under polarized light **B,C**, and Masson's Trichrome stained cardiac tissue **D**, from mice within each study group. Shown in **E** are heart weight/tibia length ratio, cardiomyocyte diameter **F**, and serum BNP levels **G**. Cardiac contractility **H**, mean arterial pressure **I**, and heart rate **J** are shown for each group. Images are representative of 16 image fields captured per mouse, n=2-3 mice per treatment group. Data in **E-J** are shown as mean \pm S.E.M., n = 6-8 mice per group. *P<0.05 vs. WT-CNTL, † P<0.05 vs. WT-HFHS, § P<0.05 vs. GPx4^{+/-}-CNTL

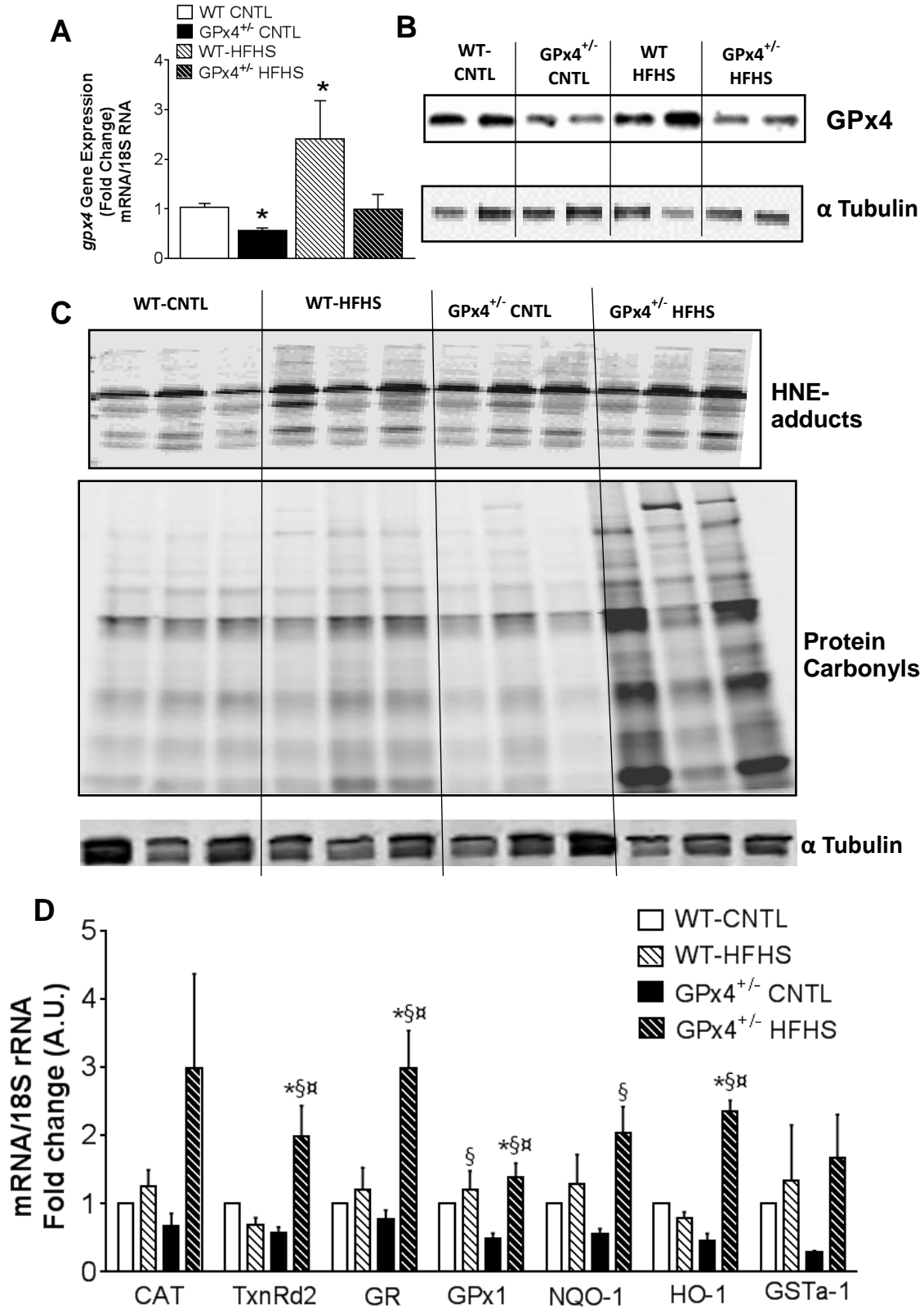


Figure 3. Cardiac GPx4, protein carbonylation and redox signaling. Shown here is GPx4 mRNA expression **A** and protein content **B** in whole hearts from mice used in this study. Representative immunoblot of HNE-adducts and hydrazide-labeled protein carbonyls **C** are shown from 3 individual mice in each group, Expression of redox and phase II detoxifying genes are shown in **D**. Data shown in **A & D** are means \pm S.E.M, n= 5-7 per group. *P<0.05 vs. WT-CNTL, $\#$ P<0.05 vs. WT-HFHS, \S P<0.05 vs. GPx4^{+/-}-CNTL. CAT-Catalase; TrxII- Thioredoxin reductase II; GR- Glutathione Reductase; GPX1- Glutathione Peroxidase1; NQO1- NAD(P)H:quinine oxidoreductase; HO-1- Heme oxygenase-1; GSTA1- glutathione s- transferase-1.

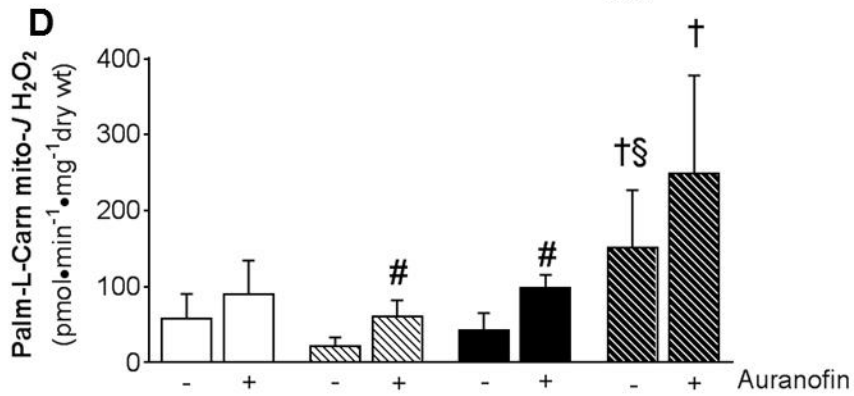
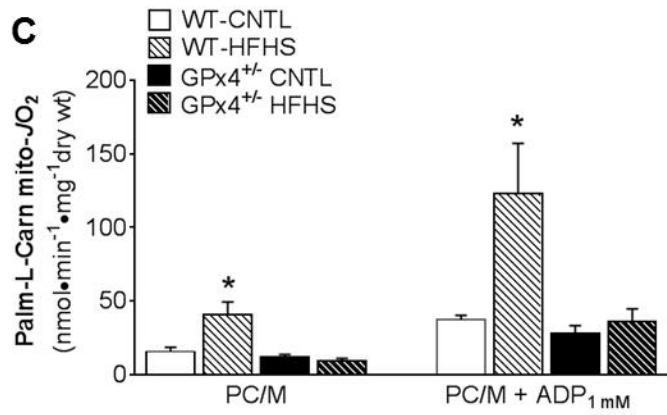
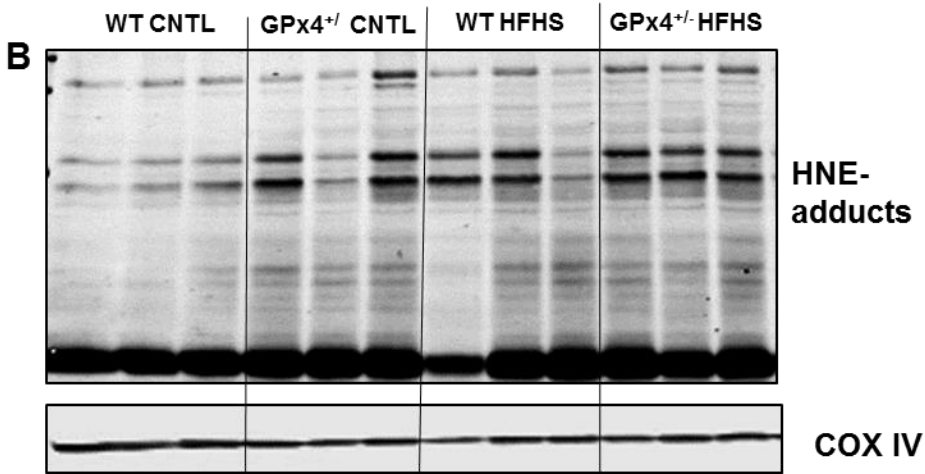
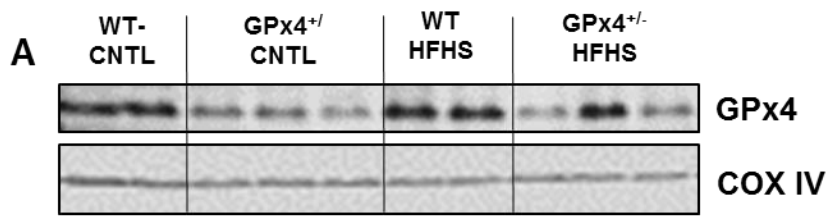


Figure 4. Cardiac mitochondrial GPx4 and functional parameters. A representative immunoblot of GPx4 protein **A** and HNE-adducts **B** along with corresponding COX IV loading control are shown of isolated cardiac mitochondria obtained from mice used in this study. In **C** are maximal ADP-stimulated rates of mitochondrial respiration (J_{O_2}) supported by Palmitoyl-L-carnitine in permeabilized cardiac myofibers from these mice. Shown in **D** are rates of mitochondrial H_2O_2 emission (mito- $J_{H_2O_2}$) in phosphorylating state supported by Palmitoyl-L-carnitine + 100 μ M ADP, in the absence (-) and presence (+) of the TxnRd2 inhibitor Auranofin. Data shown in **C & D** are means \pm S.E.M, N = 4-6 per group. * $P < 0.05$ vs. all other groups for each respiratory state, † $P < 0.05$ vs. WT-HFHS, § $P < 0.05$ vs. GPx4^{+/-}-CNTL, # $P < 0.05$ for Auranofin effect within group.

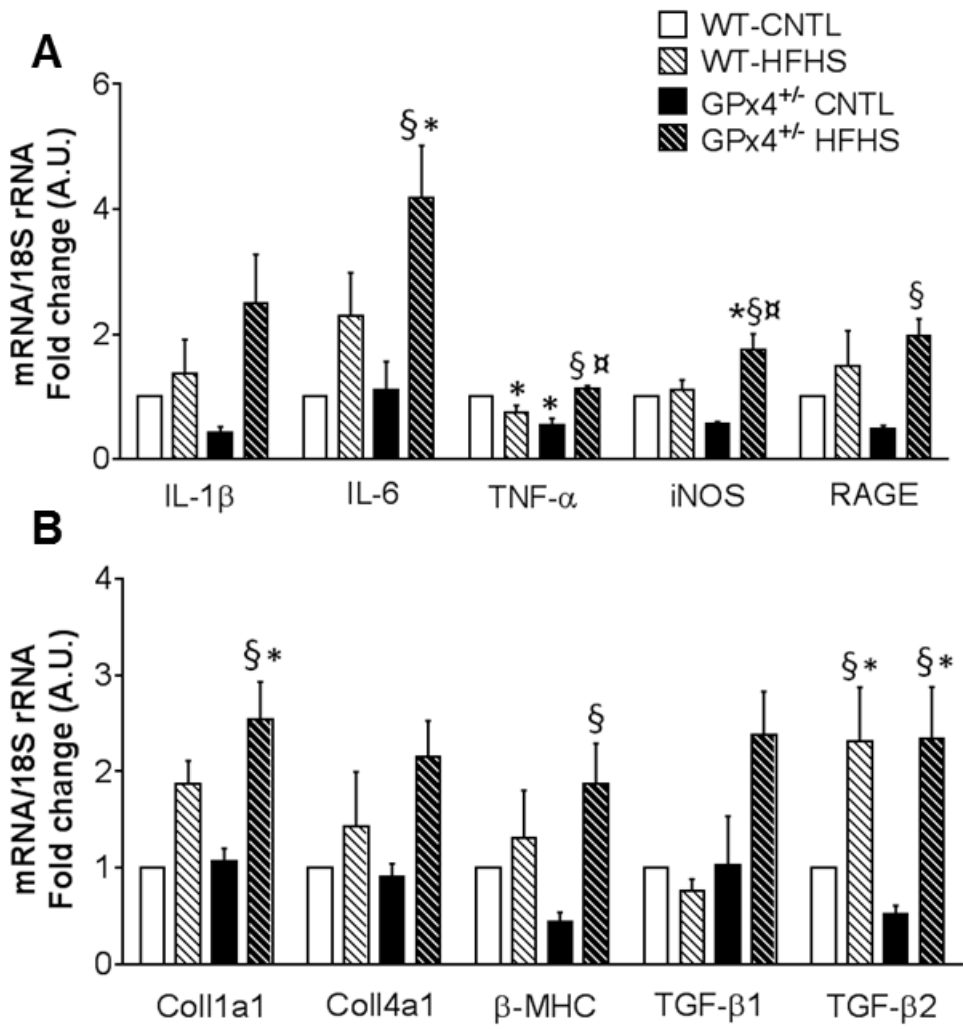


Figure 5. Cardiac inflammatory and pro-fibrotic/hypertrophic gene expression.

Expression of pro-inflammatory **A**, pro-fibrotic and hypertrophy genes **B** are shown in hearts from all four groups of mice in this study. B-MHC- β -Myosin Heavy Chain; Coll1a1-Collagen 1a1; Coll4a1-Collagen 4a1; TGF β 1 and 2 -Transforming Growth Factor β 1 and 2; IL- β -Interleukin-1 Beta; IL-6 -Interleukin -6; TNF- α -Tumor Necrosis Factor- alpha; iNOS-Inducible nitric oxide synthase; RAGE- Receptor for Advanced Glycation End Products. All target genes normalized to 18S ribosome RNA. Data shown are means \pm S.E.M, N = 4-6 per group. *P<0.05 vs. WT-CNTL, α P<0.05 vs. WT-HFHS, \S P<0.05 vs. GPx4^{+/-}-CNTL.

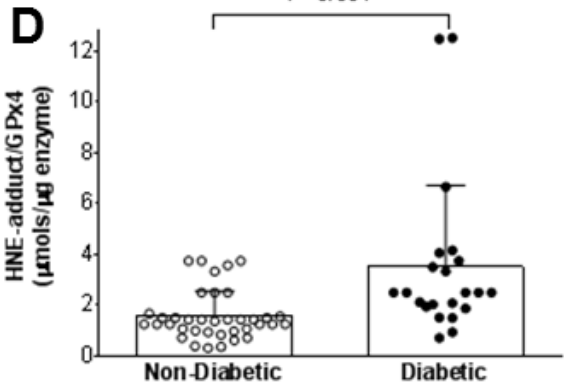
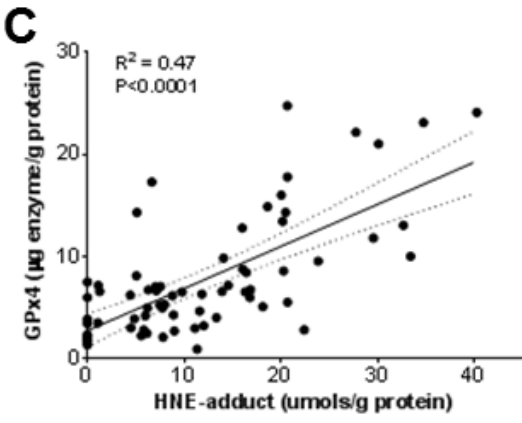
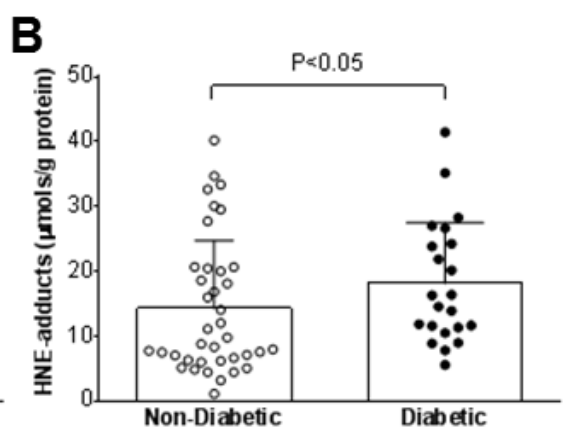
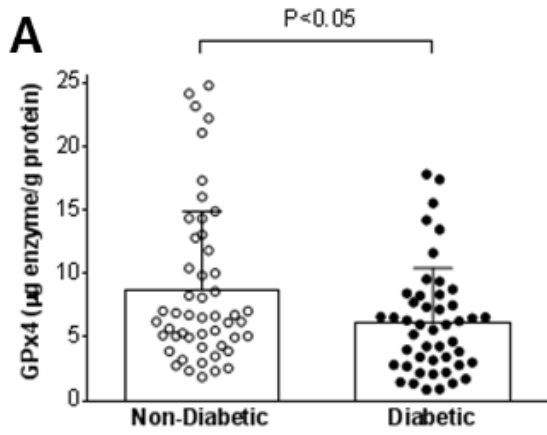
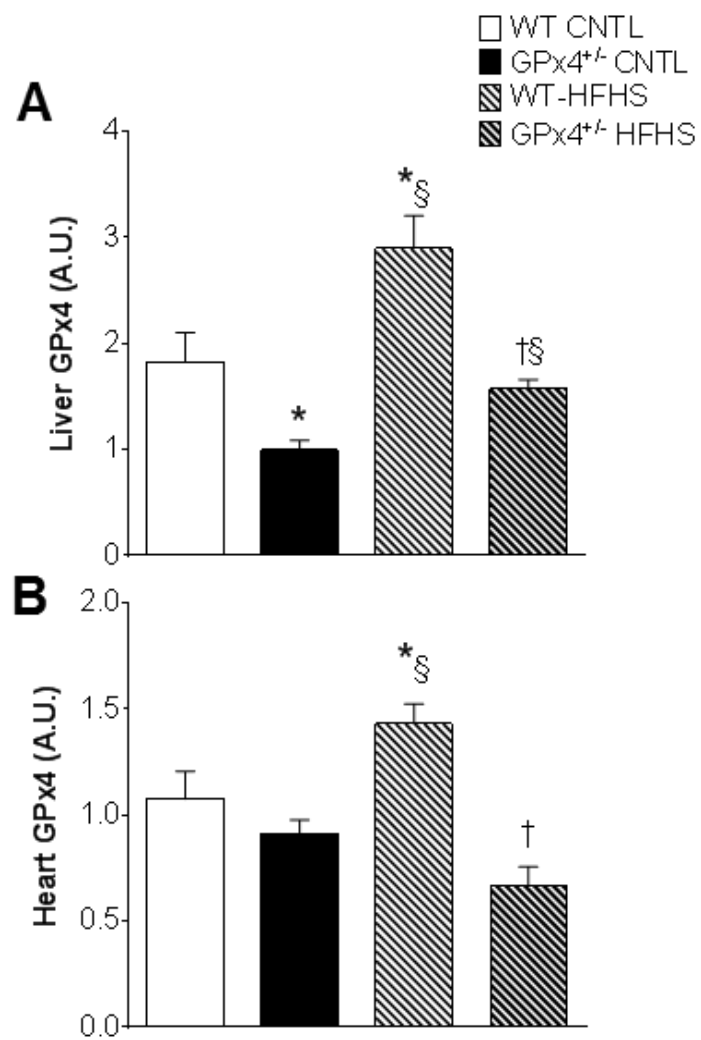
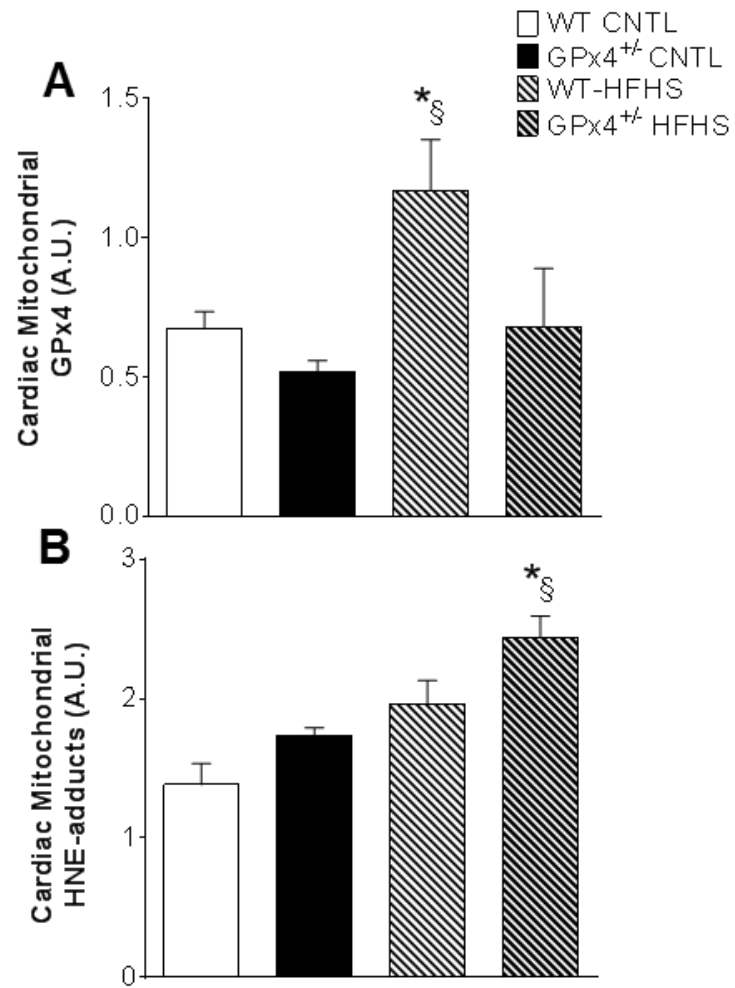


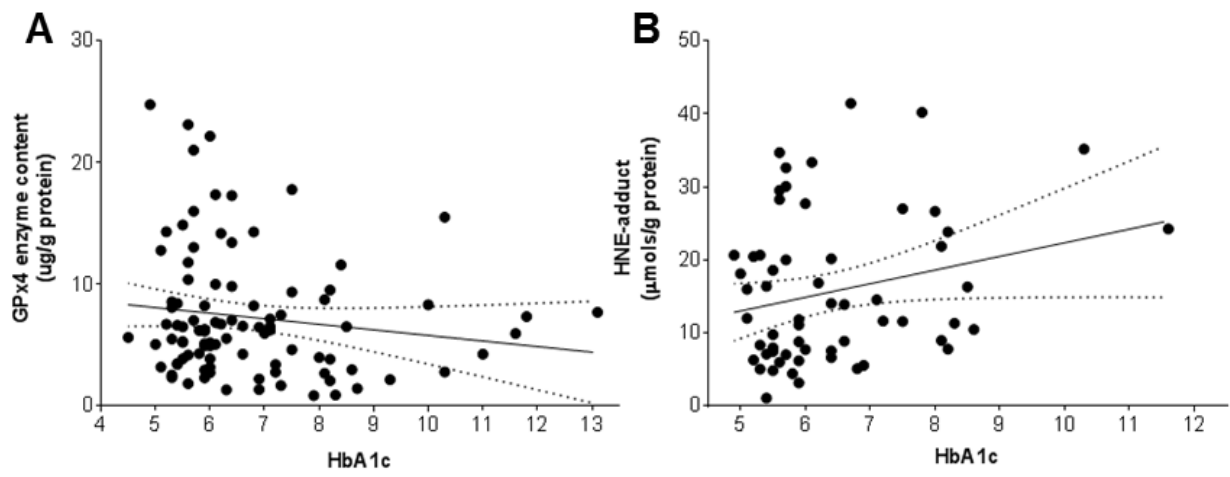
Figure 6. GPx4 content and HNE-adducts in human myocardium. Total GPx4 enzyme content **A** and HNE-adducts **B** are shown in atrial myocardium obtained from non-diabetic and diabetic patients undergoing elective heart surgery. Shown in **C** is association between HNE-adducts and GPx4 enzyme in these heart samples, and the ratio of HNE-adduct to GPx4 enzyme are depicted in **D**. Each symbol corresponds to one individual patient (N=103, see **Table 2** for demographics and clinical variables). *P*-value computed using Friedman's nonparametric test for central tendency, adjusting for age and sex.



Supplemental Figure 1



Supplemental Figure 2



Supplemental Figure 3

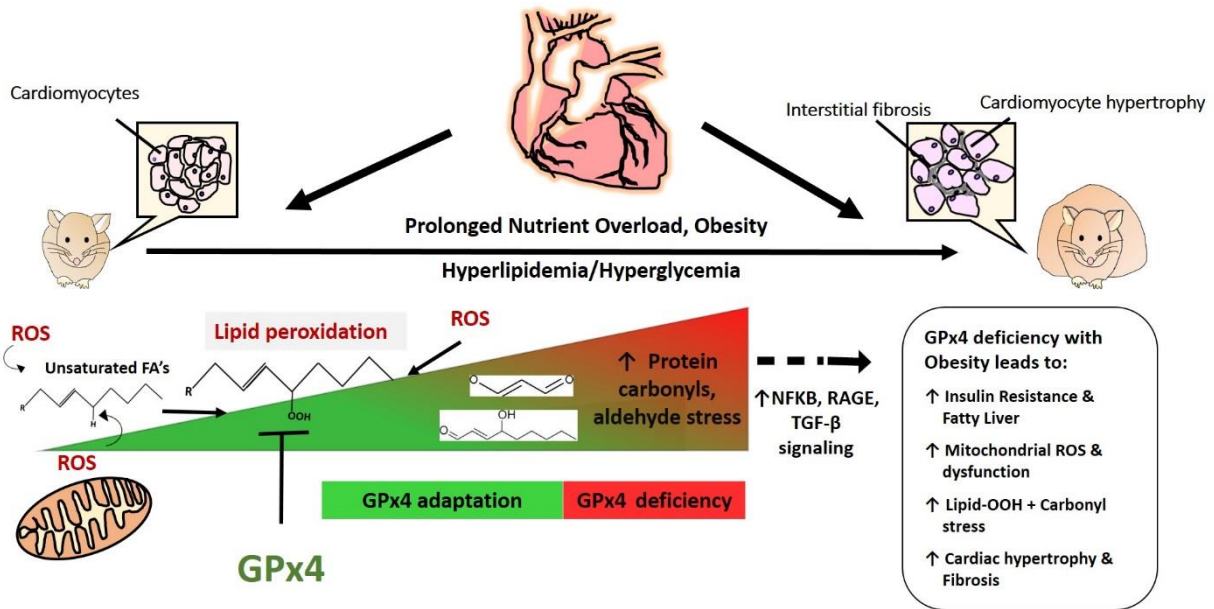


Figure 7. Overview Figure.

CHAPTER THREE

A novel carbonyl scavenging compound mitigates mitochondrial dysfunction and cardiometabolic perturbations in obese WT and GPx4^{+/-} mice

Adapted from

Lalage A. Katunga LA, Paran CW, Funai K, Beatty C., Mitchell HE, Aldini G, Anderson EJ. A novel carbonyl-scavenging compound mitigates mitochondrial dysfunction and cardiometabolic perturbations in obese WT and GPx4^{+/-} mice. 2015. In preparation.

ABSTRACT

In a previous study we reported that diet-induced obesity in a model of Glutathione Peroxidase 4 (GPx4)-deficiency leads to exacerbation of cardiometabolic disease and mitochondrial dysfunction in the heart. Carnosine is an endogenous alanyl-histidine dipeptide capable of neutralizing reactive aldehydes, however it is rapidly hydrolyzed by serum carnosinases and thus not suitable as a therapeutic. Here we used a novel carnosine derivative carnosinol (CAR), an orally bioavailable compound which possesses an additional hydroxyl group and greater aldehyde reactivity, to determine if the aldehydes were the causative factor underlying the cardiometabolic derangements observed in the previous study. .

Methods WT and GPx4^{+/-} mice littermates were fed a high fat high sucrose (HFHS) diet for 16 weeks. After 8 weeks on HFHS diet, half of the mice in each cohort were treated with CAR, a novel aldehyde-scavenging compound (40mg/kg in drinking water).

Results At the termination of the study, GPx4^{+/-} mice were substantially more insulin resistant compared to WT. CAR improved glucose tolerance by 60% and 22% in WT and GPx4^{+/-} respectively. In soleus muscle (SOL), insulin-stimulated glucose uptake (ISGU) was ~80% lower in GPx4-HFHS vs WT-HFHS mice, and CAR had no effect on ISGU in either genotype. In glycolytic extensor digitorum longus muscle (EDL), ISGU was not affected by genotype but CAR increased ISGU ~40% in both WT and GPx4 mice. Hepatic steatosis was present following HFHS diet in both WT and GPx4^{+/-}, although more pronounced in GPx4^{+/-} mice. CAR mitigated steatosis in both WT and GPx4^{+/-}, although treatment was more effective in WT. CAR improved cardiac mitochondrial efficiency – the ratio of ATP production to O₂ consumption and reduced H₂O₂ in WT groups. However, although mitochondrial respiration capacity was increased in GPx4^{+/-} HFHS, CAR group mitochondrial efficiency remained unchanged.

Conclusion Collectively, these findings suggest 1) lipid peroxidation and subsequent aldehyde stress are causal factors in the pathogenesis of insulin resistance and hepatic steatosis with

obesity, 2) GPx4 is a protective mechanism against this stress; and 3) aldehyde-scavenging compounds have clinical potential in obesity/diabetes.

1. INTRODUCTION

Lipid peroxidation of polyunsaturated fatty acids (PUFA) can lead to accumulation of α,β -unsaturated aldehydes including 4-hydroxynonenal (4-HNE), malondialdehyde (MDA), acrolein and 4-hydroxy-2-hexanal (HHE) (25, 47). Through mechanisms that involve the electrophilic attack of cellular components including enzymes and structural proteins, aldehydes have been implicated as key pathophysiological mediators of oxidative stress (25, 26, 47, 51, 227). The main mechanism for clearance of lipid peroxides is reduction, which is catalyzed by glutathione peroxidase 4 (GPx4) and to a far lesser extent through the phospholipase A-glutathione peroxidase 1 enzyme pathway (79, 86, 228, 229). Although the oxidative burden, which is classified by generation of oxidized glutathione (GSSG), is an order of magnitude greater with hydrogen peroxide (229), lipid peroxides induce prolonged effects on a cell. The aldehydes have a prolonged half-life and are capable of traversing cellular compartments. For this reason they have been called “toxic second messengers” (47). Nonetheless, aldehydes do have a critical role in normal signaling mechanisms. Therefore models such as the heterozygote GPx4 mice (GPx4^{+/-}) are useful to explore pathophysiological mechanisms that are triggered when reactive aldehyde species levels are elevated.

A number of studies have reported the involvement of LPPs specifically in cardiometabolic disease. Levels of aldehyde adducts are increased in both hearts of obese and diabetic human and murine models (23, 230). Aldehyde adducts are indeed biomarkers of oxidative stress, however in this capacity there is growing evidence to suggest these compounds play a causal role in disease (231).

The development of compounds to scavenge these reactive aldehydes is a growing area of research. L- carnosine is an endogenous alanyl-histidine dipeptide that has aldehyde scavenging properties (145, 232) . It is present in muscle at high concentrations and is thought to have aldehyde-sequestering function there, however its precise function remains unknown (145). Muscle carnosine levels are depleted in type II but not type I diabetic patients, suggesting that it may be involved in a compensatory response in metabolic diseases (233).The exploitation of the scavenging properties of carnosine in the body are limited by the fact that it is rapidly hydrolyzed by serum carnosinases (147, 149). A number of studies have utilized carnosine analogs in models of metabolic disease. In ApoE ^(-/-) mice, carnosine treatment stabilized atherosclerotic plaques (155). A D- carnosine octylester was shown to be protective against atherosclerosis and markers of renal disease in ApoE ^(-/-) (152). Although, the D-enantiomer is not recognized by serum carnosinases allowing for a longer half-life, it has extremely low bioavailability as it is not recognized by the intestinal drug oligopeptide transporter hPepT1 (147, 152). To address this problem, Carnosinol, orally bioavailable compound, which possesses an additional hydroxyl group and greater aldehyde reactivity, was used (147, 152, 234). The hydroxyl moiety, which shields carnosinol from hydrolysis from serum carnosinases. In addition, carnosinol has increased activity due to the higher nucleophilicity of the imidazole ring. Preliminary pharmacokinetic studies of carnosine demonstrate there it is associated with no cytotoxicity or induction of CYP450s, low plasma protein binding and high bioavailability (Data, not shown). In this study, we used this novel compound carnosinol, to test the hypothesis that scavenging LPPs would rescue cardiometabolic derangements in obesity by using a mouse model of diet-induced obesity in gpx4 haploinsufficient (GPx4^{+/-}) mice.

2. MATERIALS AND METHODS

2.1 Experimental Model and Study Design. Approval was obtained from the institutional animal care and use committee of East Carolina University for all procedures performed in compliance with the National Institutes of Health's Guide for Care and Use of Laboratory. C57BL6/J male mice (Jackson Laboratory) were crossed to GPx4^{+/-} females. (82). At 8-12 weeks, WT and GPx4^{+/-} male age matched littermates (n=8) were randomly assigned to groups and individually housed. Mice were fed either control (CNTL-TD110367) or two groups of high fat high sucrose (HFHS-TD110365) diet from Harlan-Teklad Laboratories (Madison, WI) *ad libidum* for 18 weeks. The composition of this diet has been described previously (72). Mice were housed at controlled temperature and a 12hr light/dark cycle was maintained. At 8 weeks one of the WT HFHS and GPx4^{+/-} HFHS groups were administered carnosinol at 40mg/kg in the drinking water *ad libidum*. 1-2 weeks before tissue collection all live animal metabolic and echocardiographic measurements were made to allow the animals to reacclimate to minimize the effect of stress that may have been introduced by these procedures.

2.2 Metabolic Parameters. Total body weight, food and water consumption was recorded on bi-weekly basis for the duration of the study Nuclear- MRI was used to assess body composition at 8 and 16 weeks (EchoMRI 700 Echo Medical Systems, Houston, TX). Following a ~4 hour fast at 8 and 16 weeks an oral glucose tolerance (dose-0.5g/kg) was performed on the cohorts. Blood was obtained as described previously standard glucometer (LifeScan, Milpitas, CA). Indirect calorimetry was performed. Mice were single housed in metabolic cages (TSE Systems) for 4 days after 16 weeks on the diet. TSE Software was set to record parameters including maximal O₂ consumption (VO₂), CO₂ production (VCO₂) at 20 minute intervals. The average of two complete light and dark cycles was calculated. Insulin stimulated 2-deoxyglucose (2-DOG) uptake was measured in soleus and extensor digitorum longus (EDL) skeletal muscles. Briefly,

muscles were incubated in Krebs-Henseleit buffer (KHB) in the presence of insulin. Muscles were then rinsed then incubated with KHB that contained 2-DOG. Muscles were incubated for 30 minutes then blotted and flash frozen. Muscle was homogenized then levels of 2-DOG were measured.

2.3 Assessment of Cardiac Function. Blood pressure was measured by non-invasive tail-cuff plethysmography (SC1000, Hattaras Instruments, Cary, NC). The detailed procedures have been described in the previous chapter.

2.4 Liver and Cardiac Histology: Mice were anesthetized with isoflurane. Hearts (n=2) were infused with paraformaldehyde then fixed with paraffin. Histological measurements were measured using (<http://imagej.nih.gov/ij/>) the details of processing and staining have been described in the previous chapter.

2.5 Preparation of permeabilized cardiac myofibers and mitochondrial function

measurements. Cardiac muscle was processed exactly as described in (22-24, 72) Katunga et al., in press. Fibers were weighed before experiments and once mitochondrial experiments completed, fibers were collected, rinsed, lyophilized (Labconco, Kansas City, MO) then weighted on a microbalance (Mettler Toledo, Denver, CO).

2.6 Mitochondria Isolation. Methods used were modified from (225, 226). Briefly, approximately 100 mg of cardiac tissues was excised, minced then incubated in trypsin. Remaining mixture was resuspended in 3mL of Mitochondria Isolation Medium (MIM) (300mM Sucrose, 10mM Na-HEPES, 0.2mM EDTA) with BSA then homogenized. The homogenate was then subjected to a series of centrifugation steps. The final mitochondrial fraction was frozen and stored at -80°C. Mitochondrial experiments conducted are described in the previous chapter.

2.7 Immunoblot analysis of protein content. Homogenized tissue was loaded in 12% polyacrylamide SDS gel (Bio-Rad, Hercules, CA). Protein was transferred to PVDF membranes (Millipore, Bellerica, CA) and incubated with primary antibodies for GPx4, COXIV, β -actin and α -tubulin (Abcam, Cambridge, UK) and 4 HNE (Peptisico). Membranes were incubated using infrared fluorophore-conjugated secondary antibodies (LiCor Biosciences, Lincoln, NE), scanned using Odyssey Clx Infrared Imaging System (Li-Cor) and analyzed by densitometry using Image J (NIH).

2.8 Statistical Analysis. Data are presented as mean \pm SEM. Statistical analysis were performed with Graph Pad Prism (Graph Pad Prism, La Jolla, CA). Two way ANOVA was performed on continuous variables followed by Sidak multiple comparison's test unless otherwise stated, with $\alpha < 0.05$ considered statistically significant.

3. RESULTS

3.1 Carnosinol improves glucose tolerance and insulin sensitivity in WT following a high fat diet. We have described the rationale behind the use of the GPx4 +/- mouse as model of increased LPPs in cardio-metabolic disease in the previous chapter. The goal of this study was to determine whether CAR could rescue cardiometabolic perturbations and using the GPx4^{+/-} mouse to understand the extent to which these characteristics maybe attributed to elevated levels of carbonyl stress. There were no significant differences between WTs and GPx4^{+/-} mice with diet or treatment in weight gain (**Figure 1a**), terminal body weight (**Figure 1b**) or adiposity (**Table 1**). Glycemic control as assessed following an oral glucose challenge at 16 weeks (**Figure 1c**) following intervention CAR rescues glucose tolerance to levels similar in WT CNTL group. However, AUC for GPx4^{+/-} on a HFHS is greater than WTs (**Figure 1d**) and this is only slightly improved with CAR treatment. Insulin sensitivity improves insulin sensitivity however this

effect is more pronounced in the EDL (**Figure 1f**) compared to the Soleus (**Figure 1g**). Serum Insulin levels (**Figure 1h**) reveal a trend of increased insulin in GPx4 on diet compared to WT and across genotypes CAR treatment decreases fasted insulin levels, although this does not yield statistical significance.

3.2 Whole Body Indirect Calorimetry Changes in VO_2 , CO_2 and RER values are shown in (**Figure 2a-c**), the average of these values is presented for light and dark cycles in (**Figure 2d-f**). There were slight differences within genotypes for VO_2 (**Figure 2d**) during the dark cycle otherwise whole body energy expenditure remained unchanged.

3.3 Carnosinol treatment reduces lipid peroxidation and ameliorates hepatic steatosis. GPx4 enzyme levels were increased with both the diet but even more so with CAR treatment (**Figure 3a.**). The effect was greater in WT compared to GPx4 mice. Levels of 4-HNE adducts are shown in (**Figure 3b**). HNE-adducts are increased with the diet, even more so in GPx4^{+/-} HFHS group. Levels of 4-HNE adducts are reduced with CAR treat in both WTs and GPx4^{+/-} mice. Hepatic liver steatosis is presented in (**Figure 3c**). In WTs CAR appears to reduce the size and increase dispersion of lipid droplets in the liver. However, this effect is absent in GPx4^{+/-} mice. This is reflected changes in liver triglycerides shown in (**Figure 3e**). There were only marginal changes in fibrosis (**Figure 3d**)

3.4-5 Cardiac remodeling Morphology of cardiomyocytes is presented in **Figure 4**. As expected, HFHS induced an increase in cardiomyocyte diameter (**Figure 4a**). This was mitigated with CAR treatment. Cardiac fibrosis is presented in (**Figure 4b**). HFHS diet resulted in cardiac hypertrophy (**Figure 5a**), which was slightly decreased in WT with CAR. However cardiomyocyte diameter remained unchanged in WT but was reduced in GPx4^{+/-} mice (**Figure**

5b). There were no or only marginal changes in Mean arterial pressure (**Figure 5c**), heart rate (**Figure 5d**), systolic blood pressure (**Figure 5e**), diastolic blood pressure (**Figure 5f**).

3.6 Cardiac GPx4 protein levels and 4-HNE adducts Levels of GPx4 protein in heart tissue are presented in (**Figure 6a**). CAR treatment appears to have a greater effect on increasing GPx4 expression in GPx4^{+/-} mice compared to WTs. 4-HNE levels are globally increased with HFHS diet, however CAR treatment has a greater effect on reduction of 4-HNE adducts in WTs compared to GPx4s (**Figure 6b**).

3.7 Mitochondrial efficiency improved and levels of carbonyl adducts reduced with carnosinol treatment. Mitochondrial parameters are presented in (**Figure 7**). Mitochondrial respiration with pyruvate/ malate as a substrate is presented in (**Figure 7a**). HFHS diet is associated with a decrease slight increase in respiration in WTs but an increase in GPx4^{+/-} mice. Surprisingly CAR treatment appears to result in a reduction in respiration in WTs. Conversely in GPx4 mitochondria CAR treatment results with increased mitochondrial respiration. ATP production is presented in (**Figure 7b**) reveals with the HFHS diet, ATP generation is decreased however, CAR treatment improves ATP production. Mitochondrial efficiency presented as the ATP/O ratio in (**Figure 7c**) shows CAR improves ATP/O ratio in WT but not in GPx4^{+/-} mice. Mitochondrial dysfunction as measured by H₂O₂ emission production capacity was measured and presented in (**Figure 7d**) in the presence and absence of auranofin the thioredoxin reductase-2 (TxnRd2) inhibitor. H₂O₂ emission was slightly reduced in the HFHS diet however H₂O₂ levels in CAR treatment were similar to CNTL. In the presence of auranofin, H₂O₂ was only slightly higher in the HFHS group compared to CNTLs. Levels of H₂O₂ are reduced almost by 25% in the CAR treated group. In contrast, H₂O₂ levels are increased with the HFHS diet in GPx4^{+/-} mice and CAR treatment only marginally decreased H₂O₂ emission. In the presence of auranofin, H₂O₂ emission was increased in the GPx4^{+/-} HFHS diet group, CAR

treatment reduced H₂O₂ emission by ~30% compared to the HFHS group. The levels of HNE adducts in the mitochondrial fraction are presented in (**Figure 7e**). The mitochondria of GPx4^{+/-} mice contain significantly higher levels of HNE adducts almost comparable to WT HFHS group. CAR reduces the levels of HNE adducts in the mitochondrial fraction, however level of HNE adducts are only marginally increased in GPx4^{+/-} HFHS CAR group.

4. DISCUSSION

Carnosinol is a novel histidine-containing dipeptide alcohol that is highly reactive with lipid-derived aldehydes, and is capable of sequestering reactive aldehydes such as HNE, malondialdehyde and acrolein, thereby reducing their steady-state concentrations *in vivo*. The objective of the present study was to use this compound as an intervention to determine whether reducing aldehyde levels in a HFHS diet-induced model of obesity, would mitigate the deleterious effects of obesity on cardiometabolic disease parameters. In particular, the effect of CAR on cardiac hypertrophy/fibrosis, and mitochondrial oxidative phosphorylation (OxPhos) efficiency was examined. In a recent study of human skeletal muscle, there was a positive correlation between levels of carbonylated proteins and intramyocellular lipid content (235). Together these parameters were inversely related to glycemic control. In a study that assessed the effects of 4-HNE treatment on skeletal muscle insulin sensitivity, the effect of 4-HNE was time and dose dependent reduction in insulin signaling at levels that had cytotoxic effect (236). In an elegant study conducted by Cohen et al., HNE was shown to exaggerate glucose – stimulated insulin secretion through direct action as a ligand for peroxisome proliferator-activated receptor- δ (PPAR- δ) (237).

Our study coincides with other studies that show that increased carbonyl adducts with insulin resistance in both murine and human models. These findings lend empirical support to the idea that carnosine analogs may neutralize aldehydes and analogs. The capacity of CAR to

rescue insulin resistance may occur through a number of mechanisms. In high fat fed mice, GPx4 overexpression protected from insulin resistance and β - cell dysfunction (238). It is plausible that CAR, as an exogenous agent, is working in a similar manner. The effect of carnosine analogs on insulin resistance appears to be highly dependent on the model used to induce steatosis. For instance, with high fructose diet, carnosine had no effect on insulin resistance and triglyceride levels, whereas in a model fed a 60% HF lard diet these parameters were improved (239, 240).

Preceding studies support the observation that CAR mitigates hepatic steatosis. In a study where rats were fed a 60% fructose diet and treated with 2g/L carnosine in their drinking water, hepatic steatosis and LPPs levels measured by MDA and diene conjugates were reduced. The addition of α -tocopherol had a synergistic effect (239). One possible explanation for the reduction in hepatic steatosis is a down regulation of lipogenic enzymes in the liver. In mice fed a 60% high fat diet with 1g/L carnosine for 8 weeks, carnosine reduced the activity and mRNA expression key enzymes such as malic enzyme, fatty acid synthase, 3-hydroxy-3-methylglutaryl coenzyme A (HMG-CoA) as well as sterol regulatory element-binding proteins (SREBPs) in liver and adipose tissue (240).

Mitochondrial dysfunction has been implicated in the etiology of insulin resistance and T2DM (15, 24). Numerous studies have demonstrated that aldehydes reduce mitochondrial “bioenergetics reserve” (191). The decline in mitochondrial efficiency may also be explained by decline in efficiency of mitochondrial components. Carbonyl modification of uncoupling proteins has been shown to increase their permeability of protons, thus reducing mitochondrial efficiency (241). LPPs directly inhibit the adenine nucleotide translocase (242). Alternatively, increased respiration in GPx4^{+/-} HFHS mice may be due to induction of mitochondrial biogenesis (243). The findings of our studies may also be explained by mitochondrial uncoupling in the GPx4^{+/-} mice. This is in line with studies in the Db/Db model in which mitochondrial proliferation was increased and oxidative phosphorylation was impaired. In this model these changes were

mediated by uncoupling proteins, which may explain our observations (244). One limitation of this study is that a detailed assessment of diastolic function in the mice was not obtained.

There is little doubt in our mind that diastolic function is impaired in these mice, however, given the findings of Colucci's group and Taegtmeyer's group (185, 245) using identical diet-induced obese models. It is important to note that HNE has been shown independently to impair ion homeostasis leading to increased intracellular Ca^{2+} in neurons. It is plausible that HNE may impair diastolic function through similar mechanisms (246). Previous studies have shown that treatment of cardiomyocytes with HNE also reduce cardiomyocyte contractility (247).

Our study provides evidence that CAR treatment induces the expression of GPx4 in the liver and heart. This suggests that CAR treatment may induce beneficial effects not only directly through the scavenging of LPPs, but indirectly through increasing the antioxidant capacity of tissues. In several studies of CAR treatment in xenobiotic toxicity models of extreme antioxidant stress, levels of glutathione (GSH), antioxidant enzymes including superoxide dismutase, glutathione peroxidase expression and activity were either increased or restored to basal levels (248).

It is important to acknowledge the exploratory nature of this study and the limitations of this pilot study. This study did not evaluate mitochondrial structure (e.g. fission/fusion parameters, electron microscopy), or how these parameters may be altered with carnosinol treatment. Although this was outside the scope of this study, we acknowledge the contribution of lipid peroxidation to membrane fluidity (249) and structure, which is a critical component to membrane integrity. Markers of cellular turnover and autophagy were not measured in this study however HNE was been shown to activate autophagy. (75, 215).

In conclusion, here we present a novel therapeutic CAR that mitigates the metabolic syndrome in a model of obesity in WT and GPx4^{+/-} mice. Previous studies have demonstrated that the metabolism of HNE is influenced by age, NAD⁺ metabolism and complex I activity. Therefore, we can anticipate that older patients with metabolic syndrome may benefit more from

CAR treatment (250). Further studies are required to identify underlying cell signaling mechanisms.

TABLE 1: Body composition and metabolic parameters.

Variables	WT	WT	WT	<i>GPx4</i> ^{+/-}	<i>GPx4</i> ^{+/-}	<i>GPx4</i> ^{+/-}	p- value
	CNTL	HFHS	HFHS +CAR	CNTL	HFHS	HFHS +CAR	
Terminal Body							
Weight (g)	30.1±1.2	49.7±1.0*	45.7±2.3*	29.7±0.9	48.5±2.4 [§]	46.8±3.1 [§]	<0.0001
Fat Mass (g)	6.2±0.9	5.5±0.7*	19.8±1.3*	5.5±0.7	18.2±1.2 [§]	18.2±1.3 [§]	<0.0001
Lean Mass (g)	22.0±0.4	25.7±0.9*	24.6±1.1*	21.5±0.3	24.4±1.2 [§]	24.1±1.4 [§]	0.003
Body fat (%)	19.7±2.1	42.7±0.7*	42.7±1.4*	18.2±1.7	41.8±1.2 [§]	42.2±1.8 [§]	<0.0001

All values expressed as mean ± S.E.M., n = 6-8. * P<0.05 vs. WT-CNTL vs. [‡] P<0.05 vs. WT-HFHS. [§] P<0.05 vs. *GPx4*^{+/-} CNTL.

[†]P<0.05 vs. *GPx4*^{+/-} HFHS.

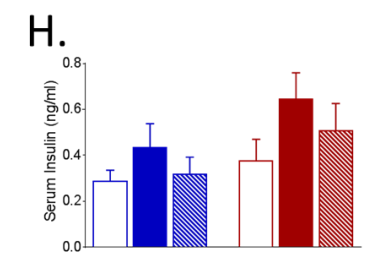
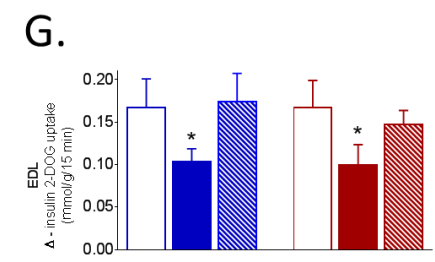
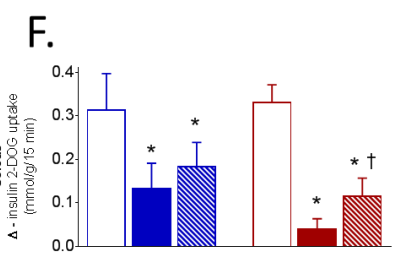
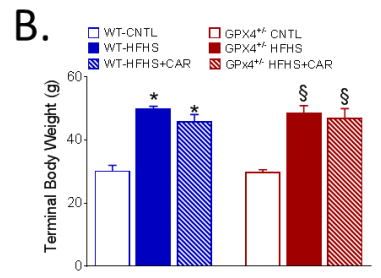
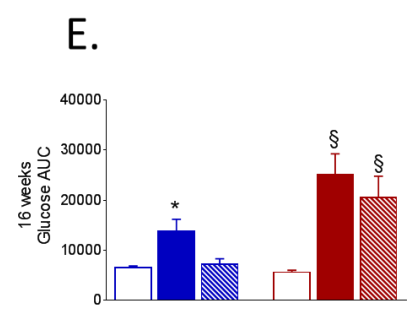
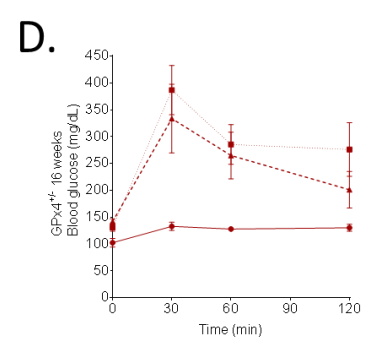
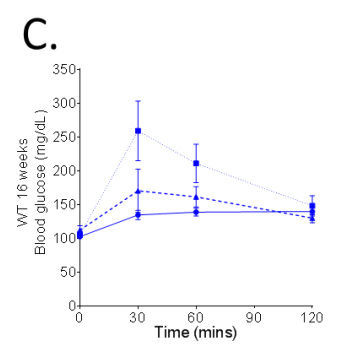
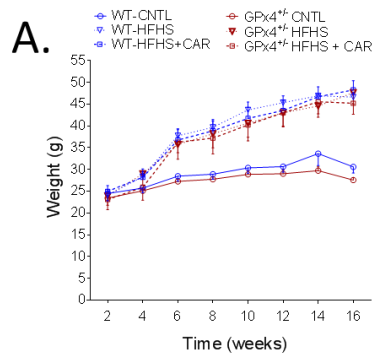


Figure 1. Body composition, glycemic control and insulin resistance. Weight change over 16 weeks is presented in **A** with terminal body weight at the end of the study in **B**. Oral glucose tolerance is shown at 16 weeks, 8 weeks after carnosinol intervention for **C** WTs and **D** GPx4^{+/-} mice. AUC is quantified in **E**. The total uptake of 2-DOG following an insulin exposure in whole, intact soleus **F** and Extensor Digitorum Longus **G** skeletal muscles prepared from the cohorts of mice in this study (n=5-6). Serum insulin levels are presented in **H**. Data are shown as \pm S.E.M. using two-way ANOVA followed by Sidak's multiple comparison test. *P<0.05 vs. WT-CNTL, ** vs. WT-HFHS. § P<0.05 vs. GPx4^{+/-} CNTL, † vs. GPx4^{+/-} HFHS

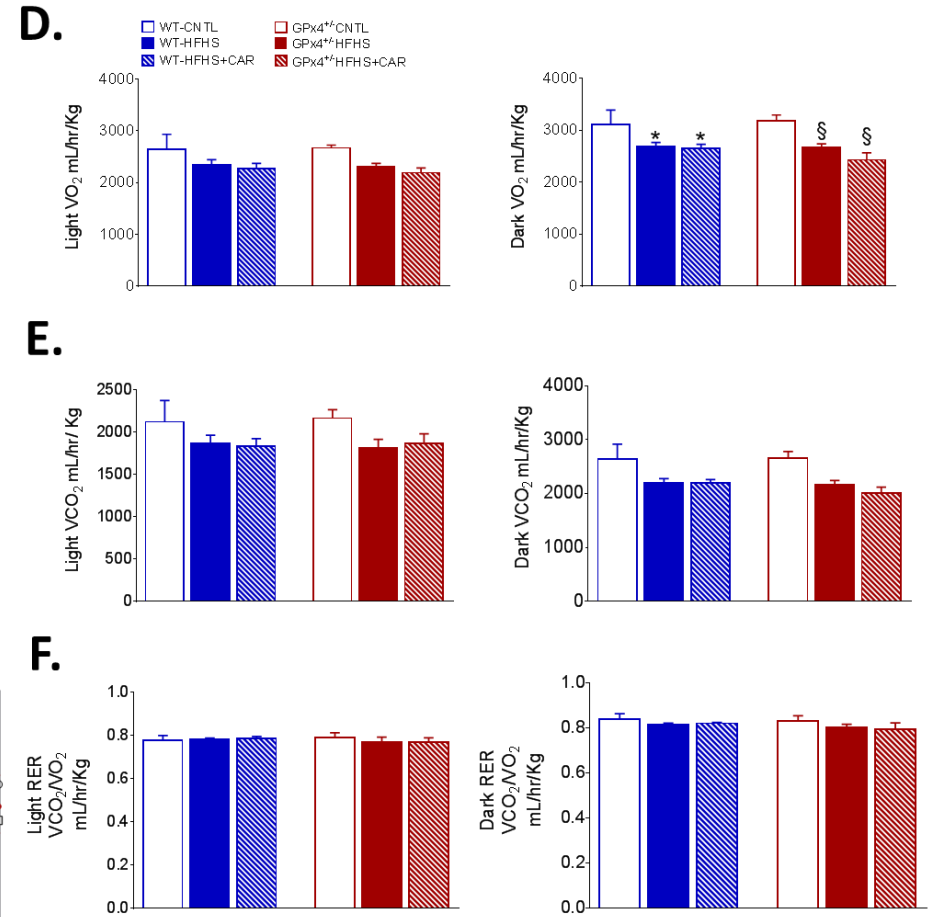
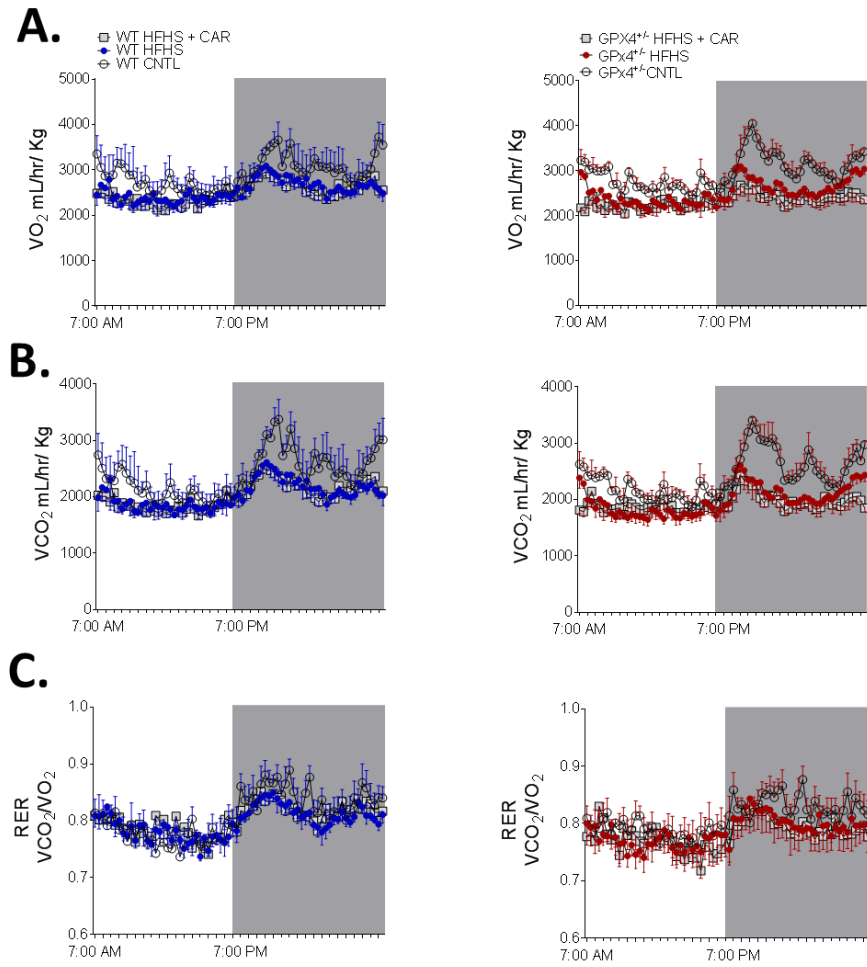


Figure 2. Whole body O₂ and CO₂ exchange. Metabolic activity was measured via indirect calorimetry of **A)** maximal O₂ consumption (VO₂) and **B)** CO₂ consumption (VCO₂) **C)** RER was calculated as VCO₂/O₂ are presented as a function of time over the dark and light cycles. **D)** VO₂ **E)** VCO₂ and **F)** RER show average mL of gas consumed/ expelled per hour normalized to body weight. Data are shown as ± S.E.M. two-way ANOVA followed by Sidak's multiple comparison tests. *P<0.05 vs. WT-CNTL, ** vs. WT-HFHS. § P<0.05 vs. GPx4^{+/-} CNTL, † vs. GPx4^{+/-} HFHS

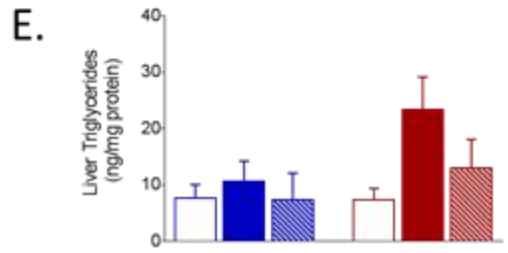
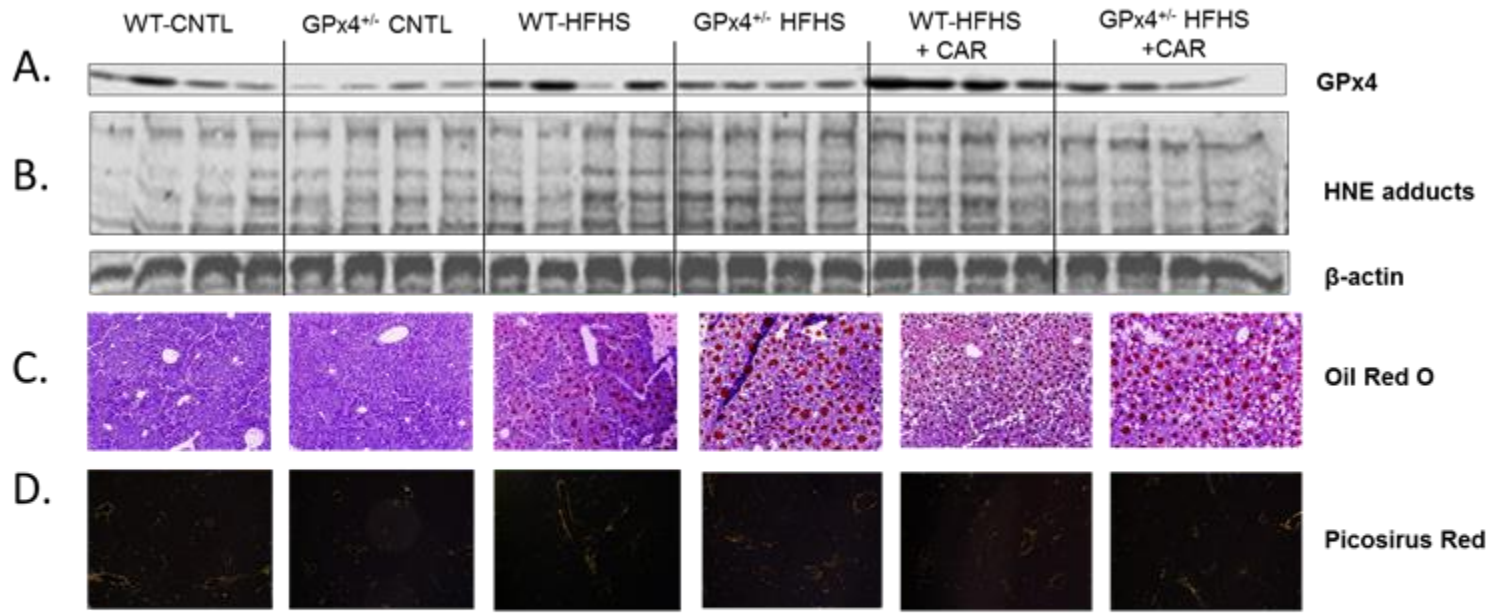
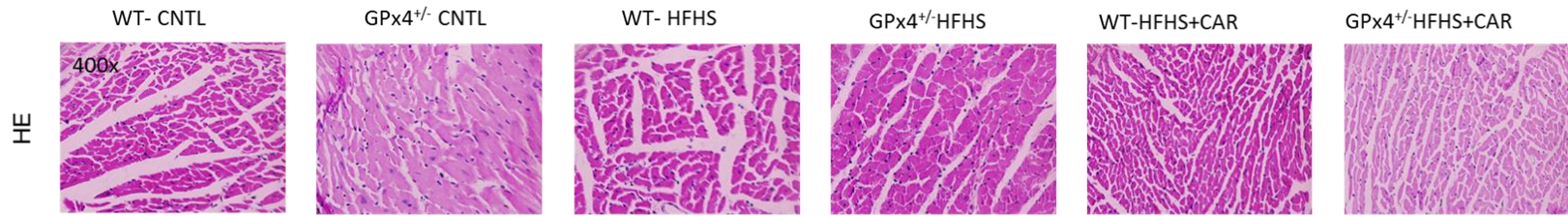


Figure 3. Liver Histology. Shown in **A** is a representative immunoblot of GPx4 and **B**. HNE-adducts in liver with B actin as the loading control (n=4). **C**. Representative images of liver stained with Oil Red O for triglycerides C and collagen stained with picosirus red under polarized light **D** is shown for each group. **E**. Levels of liver tissue triglycerides. Data are shown as \pm 7S.E.M. two-way ANOVA followed by Sidak's multiple comparison test.

A.



B.

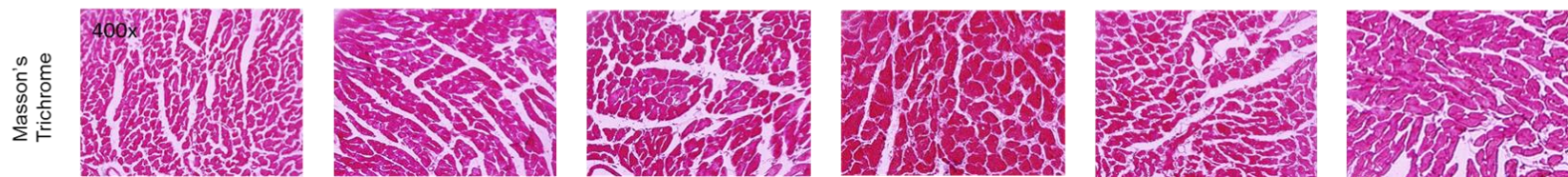


Figure 4. Cardiac Histology. Panels shown are representative images of cardiac section stained with Hematoxylin and Eosin **A** and Masson's trichrome stain **B**.(n=2)

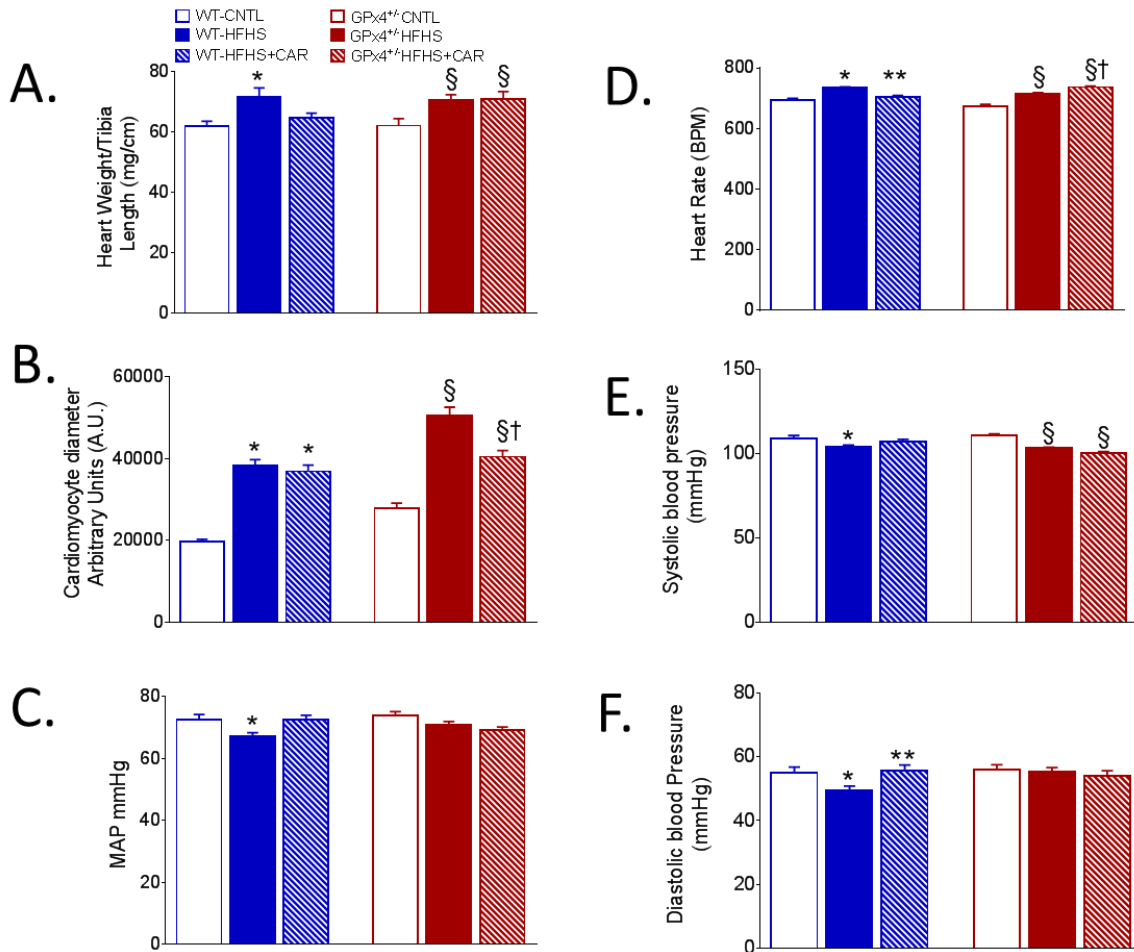


Figure 5. Cardiac function parameters. **A.** Cardiac hypertrophy as measured by heart weight/ tibia ratio. **B.** Cardiomyocyte diameter quantified from slides of cardiac tissue. Parameters of heart function are shown **C.** Mean Arterial Pressure. **D.** Heart rate, **E.** Systolic Blood Pressure, **F.** Diastolic Blood Pressure. Data are shown as \pm S.E.M. Analysis two-way ANOVA followed by Sidak's multiple comparison test. *P<0.05 vs. WT-CNTL, ** vs. WT-HFHS. § P<0.05 vs. GPx4^{+/-} CNTL, † vs. GPx4^{+/-} HFHS

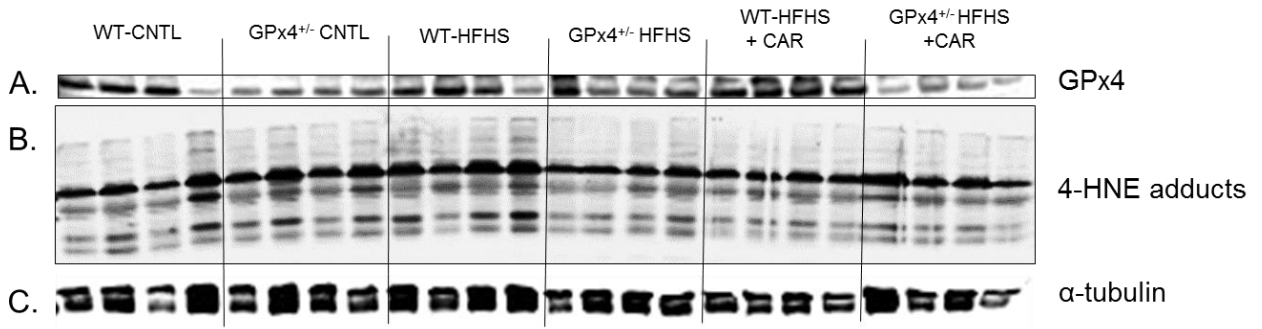


Figure 6. Cardiac GPx4 and protein carbonylation. Shown in **A.** is a representative image of GPx4 protein content and **B.** HNE-adducts with α -tubulin as a loading control in **C.**

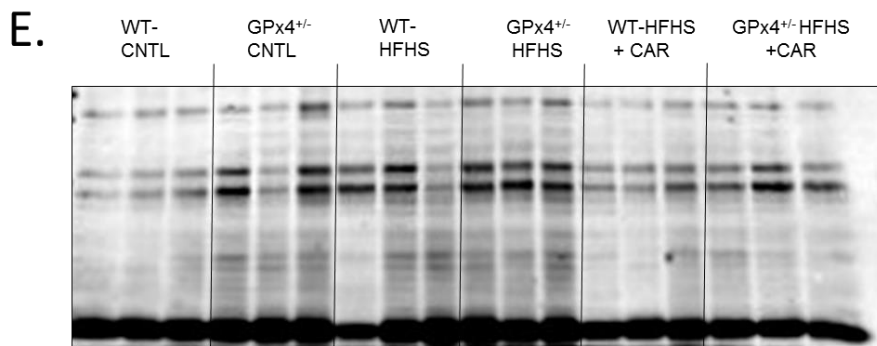
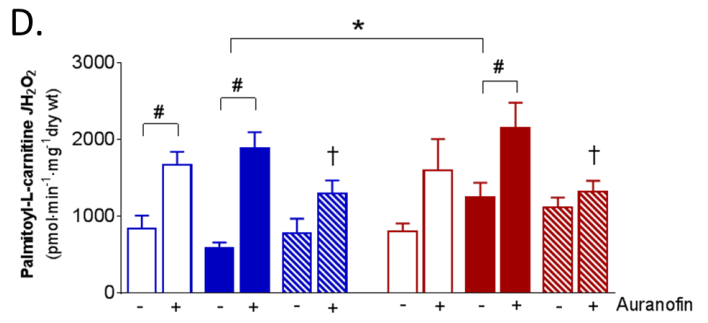
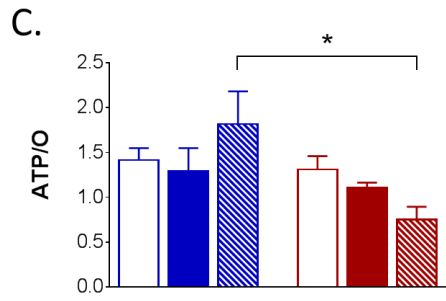
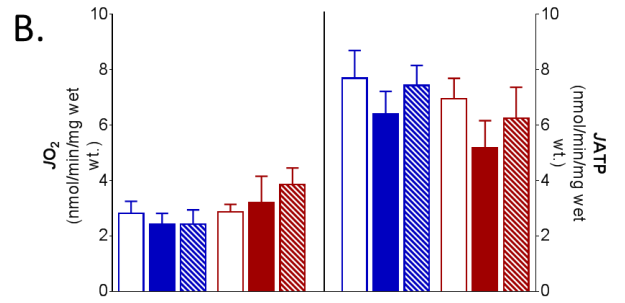
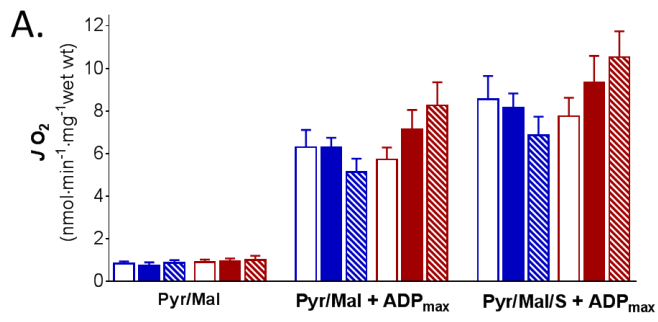


Figure 7. Mitochondrial respiratory capacity and function in cardiac muscle following HFHS diet. Rates of mitochondrial O₂ consumption ($\dot{V}O_2$) in maximal ADP-stimulated conditions are shown for cardiac tissue supported by complex I and II substrates pyruvate/malate and succinate are shown in **A**. **B** Rates of mitochondrial O₂ consumption at submaximal ADP (75mM) and corresponding levels of ATP generated. **C**. Mitochondrial efficiency as represented by the ratio of ATP generated to oxygen consumed ATP/O ratio is presented **D**. Rates of mitochondrial H₂O₂ emission (mito- $\dot{V}H_2O_2$) in the presence of succinate are shown for cardiac tissue in the presence and absence of Thioredoxin Reductase inhibitor auranofin (n=6). **E** Representative immunoblot of mitochondrial HNE adducts. Data are shown as \pm S.E.M. #P<0.05 for Auranofin effect with Paired t-test. Two way ANOVA followed by Sidak's multiple comparison test. *P<0.05 for Genotype effect within treatment, †P<0.05 for Carnosinol effect vs. HFHS alone.

FINAL DISCUSSION

The prevalence of global cardiovascular disease is increasing exponentially. Accordingly, there is an urgent need from both a clinical and public health perspective to improve our understanding of the underlying etiology of this disease. It is widely accepted that oxidative stress is a major driving mechanism in heart disease. For decades, levels of lipid-derived aldehydes such as HNE and MDA have served as biomarkers of oxidative stress, however the contribution that these signaling molecules make as specific causal factors in the development of disease was unclear. Collectively, the body of work presented in this dissertation sought to begin to address this gap in knowledge. The overall objective of this dissertation was to determine the role of LPPs in the development of cardio-metabolic perturbations observed in the obese insulin resistant heart.

In the first study, the GPx4^{+/-} mouse was employed as model of increased LPP production. This was the first time that the effects of nutrient overload were assessed in this mouse model. The findings of this study support that elevated LPPs are indeed significant etiological factors in the progression of cardio-metabolic disease. Furthermore, we provide evidence of the significance of the GPx4 as a cardio-protective enzyme in the human heart. Prior to our work, GPx4 was implicated to play a role in through inferences made in Kashin-beck heart patients but this is the first time that its role has been demonstrated in a subset of clinical patients. Thus these findings make constitute a significant contribution to the existing knowledge base.

Together these data served to validate the GPx4^{+/-} mice HFHS fed mouse as a model to evaluate the influence of elevated LPPS on signaling mechanisms involved in cardio-metabolic disease. In addition, this study described a novel protective role of GPx4 in cardiometabolic disease in obesity.

The mitochondria from GPx4^{+/-} mice possessed a higher H2O2 emission capacity, which would be expected to result in greater initiation events in lipid peroxidation ultimately resulting in carbonyl stress. The association between poor glycemic control and lower activity of mitochondrial enzymes due LPP modification was widely reported. This had never been described in the HFHS-fed GPx4^{+/-} model and this provides data highlighting new mechanisms that provide possible explanations of how these changes occur.

The protective role of GPx4 in cardio-metabolic disease is highlighted by the worsened metabolic phenotype in GPx4^{+/-} mice on a HFHS diet. After a long-term HFHS diet, GPx4^{+/-} mice were significantly more insulin resistant with worsened hepatic steatosis. This highlights a previously unidentified role for GPx4 in preventing metabolic syndrome. Chronic low-grade inflammation also known as meta-inflammation is a hallmark of metabolic syndrome. Messenger RNA data that shows higher levels of pro-inflammatory markers in GPx4^{+/-} HFHS fed mice. Although a role for GPx4 in the regulation of inflammation has been proposed this is the first time it has been validated in a model of metabolic disease.

Histological assessment of the hearts of GPx4^{+/-} mice show increased collagen deposition and cardiomyocyte hypertrophy. In a translational step of this study, we examined whether these mechanisms occurred in human atrial appendage tissue of diabetic patients undergoing coronary artery bypass surgery. Numerous groups have reported increased HNE modifications in the hearts of diabetic patients. GPx4 levels had never been reported in the hearts of diabetic patients. Here we report for the first time an association between cardiac GPx4, cardiac HNE-adducts and diabetes status. This study provides a foundation for the identification of a novel sub-set of patients that may benefit from a novel therapeutic strategy to quench LPPs. These findings served as a foundation for a second series of studies that employed the use of carnosinol, a novel LPP scavenging compound in cardio-metabolic disease.

A number of studies have explored the use of carnosine analogs in metabolic syndrome. However, the endpoints of these experiments have been on renal and atherosclerosis. Our study presents a comprehensive report of cardiometabolic endpoints using the novel compound carnosinol in a model of obesity. Carnosinol improved glycemic control and insulin sensitivity in WT mice on a HFHS diet. The effect of carnosine analogs on insulin sensitivity had not been reported before. These beneficial effects were marginal or not present in GPx4^{+/-} mice on the drug. Carnosinol treatment improved hepatic steatosis by reducing the levels of triglycerides. An intriguing finding of this study was that carnosinol reduced cardiomyocyte and whole heart hypertrophy in WT and GPx4^{+/-} mice respectively. As expected levels of 4-HNE adducts were reduced in mitochondrial fraction as well as heart and liver tissues. These data also show that carnosinol is capable of penetrating the mitochondrial compartment. Diminished 4-HNE adducts in the mitochondria were accompanied by changes in mitochondrial function. In WT mice, carnosinol treatment improved mitochondrial efficiency in heart, however in obese GPx4^{+/-} mice there was an increase in respiration with little change in ATP production. This is the first time that the effect of a carnosine analog on mitochondrial function in a model of metabolic syndrome has been reported. This study also revealed an additional mechanism through which carnosine analogs may improve redox capacity by increasing the expression of antioxidant enzymes including GPx4.

In conclusion, the body of work presented in this dissertation provides evidence for a specific role of LPPs in the etiology cardio-metabolic disease, and that the use of a novel class of aldehyde-scavenging compounds may have unique therapeutic benefit obese/diabetic patients. Together these data provide a foundation for future pharmacological and experimental studies into the role of carbonyl species as etiologic agents of cardio-metabolic disease.

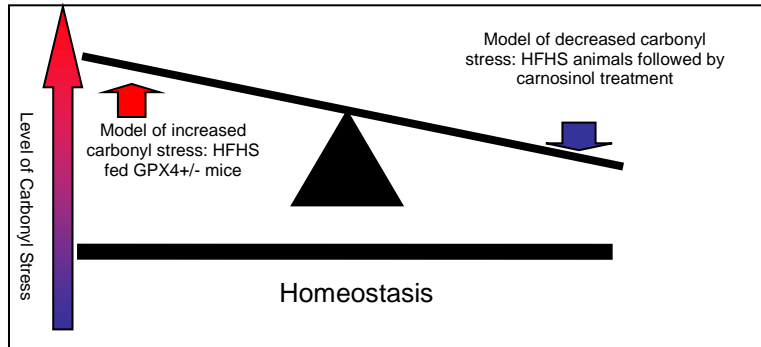


Figure 4.0: This schematic of the two approaches used to test the effect of LPPS on the heart in diet-induced obesity.

REFERENCES

1. Ng, M.; Fleming, T.; Robinson, M.; Thomson, B.; Graetz, N.; Margono, C.; Mullany, E. C.; Biryukov, S.; Abbafati, C.; Abera, S. F.; Abraham, J. P.; Abu-Rmeileh, N. M.; Achoki, T.; AlBuhairan, F. S.; Alemu, Z. A.; Alfonso, R.; Ali, M. K.; Ali, R.; Guzman, N. A.; Ammar, W.; Anwari, P.; Banerjee, A.; Barquera, S.; Basu, S.; Bennett, D. A.; Bhutta, Z.; Blore, J.; Cabral, N.; Nonato, I. C.; Chang, J. C.; Chowdhury, R.; Courville, K. J.; Criqui, M. H.; Cundiff, D. K.; Dabhadkar, K. C.; Dandona, L.; Davis, A.; Dayama, A.; Dharmaratne, S. D.; Ding, E. L.; Durrani, A. M.; Esteghamati, A.; Farzadfar, F.; Fay, D. F.; Feigin, V. L.; Flaxman, A.; Forouzanfar, M. H.; Goto, A.; Green, M. A.; Gupta, R.; Hafezi-Nejad, N.; Hankey, G. J.; Harewood, H. C.; Havmoeller, R.; Hay, S.; Hernandez, L.; Hussein, A.; Idrisov, B. T.; Ikeda, N.; Islami, F.; Jahangir, E.; Jassal, S. K.; Jee, S. H.; Jeffreys, M.; Jonas, J. B.; Kabagambe, E. K.; Khalifa, S. E.; Kengne, A. P.; Khader, Y. S.; Khang, Y. H.; Kim, D.; Kimokoti, R. W.; Kinge, J. M.; Kokubo, Y.; Kosen, S.; Kwan, G.; Lai, T.; Leinsalu, M.; Li, Y.; Liang, X.; Liu, S.; Logroscino, G.; Lotufo, P. A.; Lu, Y.; Ma, J.; Mainoo, N. K.; Mensah, G. A.; Merriman, T. R.; Mokdad, A. H.; Moschandreas, J.; Naghavi, M.; Naheed, A.; Nand, D.; Narayan, K. M.; Nelson, E. L.; Neuhouser, M. L.; Nisar, M. I.; Ohkubo, T.; Oti, S. O.; Pedroza, A.; Prabhakaran, D.; Roy, N.; Sampson, U.; Seo, H.; Sepanlou, S. G.; Shibuya, K.; Shiri, R.; Shiue, I.; Singh, G. M.; Singh, J. A.; Skirbekk, V.; Stapelberg, N. J.; Sturua, L.; Sykes, B. L.; Tobias, M.; Tran, B. X.; Trasande, L.; Toyoshima, H.; van de Vijver, S.; Vasankari, T. J.; Veerman, J. L.; Velasquez-Melendez, G.; Vlassov, V. V.; Vollset, S. E.; Vos, T.; Wang, C.; Wang,

X.; Weiderpass, E.; Werdecker, A.; Wright, J. L.; Yang, Y. C.; Yatsuya, H.; Yoon, J.; Yoon, S. J.; Zhao, Y.; Zhou, M.; Zhu, S.; Lopez, A. D.; Murray, C. J.; Gakidou, E. Global, regional, and national prevalence of overweight and obesity in children and adults during 1980-2013: a systematic analysis for the Global Burden of Disease Study 2013. *Lancet* 2014, *384*, 766-781.

2. Danaei, G.; Finucane, M. M.; Lu, Y.; Singh, G. M.; Cowan, M. J.; Paciorek, C. J.; Lin, J. K.; Farzadfar, F.; Khang, Y. H.; Stevens, G. A.; Rao, M.; Ali, M. K.; Riley, L. M.; Robinson, C. A.; Ezzati, M.; Global Burden of Metabolic Risk Factors of Chronic Diseases Collaborating Group (Blood Glucose) National, regional, and global trends in fasting plasma glucose and diabetes prevalence since 1980: systematic analysis of health examination surveys and epidemiological studies with 370 country-years and 2.7 million participants. *Lancet* 2011, *378*, 31-40.

3. Gaziano, T. A.; Opie, L. H. Body-mass index and mortality. *Lancet* 2009, *374*, 113-4; author reply 114.

4. Popkin, B. M.; Adair, L. S.; Ng, S. W. Global nutrition transition and the pandemic of obesity in developing countries. *Nutr. Rev.* 2012, *70*, 3-21.

5. Grundy, S. M.; Cleeman, J. I.; Daniels, S. R.; Donato, K. A.; Eckel, R. H.; Franklin, B. A.; Gordon, D. J.; Krauss, R. M.; Savage, P. J.; Smith, S. C., Jr; Spertus, J. A.; Costa, F.; American Heart Association; National Heart, Lung, and Blood Institute Diagnosis and management of the metabolic syndrome: an American Heart Association/National Heart, Lung, and Blood Institute Scientific Statement. *Circulation* 2005, *112*, 2735-2752.

6. Park, Y. W.; Zhu, S.; Palaniappan, L.; Heshka, S.; Carnethon, M. R.; Heymsfield, S. B. The metabolic syndrome: prevalence and associated risk factor findings in the US population from the Third National Health and Nutrition Examination Survey, 1988-1994. *Arch. Intern. Med.* 2003, *163*, 427-436.
7. Muntner, P.; He, J.; Chen, J.; Fonseca, V.; Whelton, P. K. Prevalence of non-traditional cardiovascular disease risk factors among persons with impaired fasting glucose, impaired glucose tolerance, diabetes, and the metabolic syndrome: analysis of the Third National Health and Nutrition Examination Survey (NHANES III). *Ann. Epidemiol.* 2004, *14*, 686-695.
8. Kim, S. H.; Liu, A.; Ariel, D.; Abbasi, F.; Lamendola, C.; Grove, K.; Tomasso, V.; Reaven, G. Pancreatic beta cell function following liraglutide-augmented weight loss in individuals with prediabetes: analysis of a randomised, placebo-controlled study. *Diabetologia* 2014, *57*, 455-462.
9. Kahn, S. E.; Hull, R. L.; Utzschneider, K. M. Mechanisms linking obesity to insulin resistance and type 2 diabetes. *Nature* 2006, *444*, 840-846.
10. Weyer, C.; Bogardus, C.; Mott, D. M.; Pratley, R. E. The natural history of insulin secretory dysfunction and insulin resistance in the pathogenesis of type 2 diabetes mellitus. *J. Clin. Invest.* 1999, *104*, 787-794.
11. Fontbonne, A. Insulin-resistance syndrome and cardiovascular complications of non-insulin-dependent diabetes mellitus. *Diabetes Metab.* 1996, *22*, 305-313.
12. Leahy, J. L. Natural history of beta-cell dysfunction in NIDDM. *Diabetes Care* 1990, *13*, 992-1010.

13. Shah, A. S.; Gao, Z.; Urbina, E. M.; Kimball, T. R.; Dolan, L. M. Pre-diabetes: The Effects on Arterial Thickness and Stiffness in Obese Youth. *J. Clin. Endocrinol. Metab.* 2014, jc20133519.
14. Voulgari, C.; Papadogiannis, D.; Tentolouris, N. Diabetic cardiomyopathy: from the pathophysiology of the cardiac myocytes to current diagnosis and management strategies. *Vasc. Health. Risk Manag.* 2010, 6, 883-903.
15. Boudina, S.; Bugger, H.; Sena, S.; O'Neill, B. T.; Zaha, V. G.; Ilkun, O.; Wright, J. J.; Mazumder, P. K.; Palfreyman, E.; Tidwell, T. J.; Theobald, H.; Khalimonchuk, O.; Wayment, B.; Sheng, X.; Rodnick, K. J.; Centini, R.; Chen, D.; Litwin, S. E.; Weimer, B. E.; Abel, E. D. Contribution of impaired myocardial insulin signaling to mitochondrial dysfunction and oxidative stress in the heart. *Circulation* 2009, 119, 1272-83.
16. Fontes-Carvalho, R.; Ladeiras-Lopes, R.; Bettencourt, P.; Leite-Moreira, A.; Azevedo, A. Diastolic dysfunction in the diabetic continuum : association with insulin resistance, metabolic syndrome and type 2 diabetes. *Cardiovasc. Diabetol.* 2015, 14, 4.
17. Schilling, J. D.; Mann, D. L. Diabetic cardiomyopathy: bench to bedside. *Heart Fail. Clin.* 2012, 8, 619-631.
18. Kiencke, S.; Handschin, R.; von Dahlen, R.; Muser, J.; Brunner-Larocca, H. P.; Schumann, J.; Felix, B.; Berneis, K.; Rickenbacher, P. Pre-clinical diabetic cardiomyopathy: prevalence, screening, and outcome. *Eur. J. Heart Fail.* 2010, 12, 951-957.

19. Fowlkes, V.; Clark, J.; Fix, C.; Law, B. A.; Morales, M. O.; Qiao, X.; Ako-Asare, K.; Goldsmith, J. G.; Carver, W.; Murray, D. B.; Goldsmith, E. C. Type II diabetes promotes a myofibroblast phenotype in cardiac fibroblasts. *Life Sci.* 2013, *92*, 669-676.
20. Kane, G. C.; Karon, B. L.; Mahoney, D. W.; Redfield, M. M.; Roger, V. L.; Burnett, J. C., Jr; Jacobsen, S. J.; Rodeheffer, R. J. Progression of left ventricular diastolic dysfunction and risk of heart failure. *JAMA* 2011, *306*, 856-863.
21. Montaigne, D.; Marechal, X.; Coisne, A.; Debry, N.; Modine, T.; Fayad, G.; Potelle, C.; El Arid, J. M.; Mouton, S.; Sebti, Y.; Duez, H.; Preau, S.; Remy-Jouet, I.; Zerimech, F.; Koussa, M.; Richard, V.; Neviere, R.; Edme, J. L.; Lefebvre, P.; Staels, B. Myocardial contractile dysfunction is associated with impaired mitochondrial function and dynamics in type 2 diabetic but not in obese patients. *Circulation* 2014, *130*, 554-564.
22. Anderson, E. J.; Neuffer, P. D. Type II skeletal myofibers possess unique properties that potentiate mitochondrial H₂O₂ generation. *Am J Physiol Cell Physiol* 2006, *290*, C844-51.
23. Anderson, E. J.; Rodriguez, E.; Anderson, C. A.; Thayne, K.; Chitwood, W. R.; Kypson, A. P. Increased propensity for cell death in diabetic human heart is mediated by mitochondrial-dependent pathways. *Am. J. Physiol. Heart Circ. Physiol.* 2011, *300*, H118-24.
24. Anderson, E. J.; Lustig, M. E.; Boyle, K. E.; Woodlief, T. L.; Kane, D. A.; Lin, C. T.; Price, J. W., 3rd; Kang, L.; Rabinovitch, P. S.; Szeto, H. H.; Houmard, J. A.; Cortright, R. N.; Wasserman, D. H.; Neuffer, P. D. Mitochondrial H₂O₂ emission and

- cellular redox state link excess fat intake to insulin resistance in both rodents and humans. *J. Clin. Invest.* 2009, 119, 573-581.
25. Negre-Salvayre, A.; Coatrieux, C.; Ingueneau, C.; Salvayre, R. Advanced lipid peroxidation end products in oxidative damage to proteins. Potential role in diseases and therapeutic prospects for the inhibitors. *Br. J. Pharmacol.* 2008, 153, 6-20.
 26. Poli, G.; Schaur, R. J.; Siems, W. G.; Leonarduzzi, G. 4-Hydroxynonenal: a Membrane Lipid Oxidation Product of Medicinal Interest. *Med. Res. Rev.* 2008, 28, 569-631.
 27. Mattson, M. P. Modification of ion homeostasis by lipid peroxidation: roles in neuronal degeneration and adaptive plasticity. *Trends Neurosci.* 1998, 21, 53-57.
 28. Riahi, Y.; Cohen, G.; Shamni, O.; Sasson, S. Signaling and cytotoxic functions of 4-hydroxyalkenals. *Am. J. Physiol. Endocrinol. Metab.* 2010, 299, E879-86.
 29. Jezek, P.; Hlavata, L. Mitochondria in homeostasis of reactive oxygen species in cell, tissues, and organism. *Int J Biochem Cell Biol* 2005, 37, 2478-503.
 30. Paradies, G.; Petrosillo, G.; Paradies, V.; Ruggiero, F. M. Role of cardiolipin peroxidation and Ca²⁺ in mitochondrial dysfunction and disease. *Cell Calcium* 2009, 45, 643-50.
 31. Paradies, G.; Petrosillo, G.; Paradies, V.; Ruggiero, F. M. Oxidative stress, mitochondrial bioenergetics, and cardiolipin in aging. *Free Radic Biol Med* 2010, 48, 1286-95.
 32. Boveris, A.; Chance, B. The mitochondrial generation of hydrogen peroxide. General properties and effect of hyperbaric oxygen. *Biochem J* 1973, 134, 707-16.

33. Andreyev, A. Y.; Kushnareva, Y. E.; Starkov, A. A. Mitochondrial metabolism of reactive oxygen species. *Biochemistry (Mosc)* 2005, 70, 200-14.
34. Brand, M. D.; Buckingham, J. A.; Esteves, T. C.; Green, K.; Lambert, A. J.; Miwa, S.; Murphy, M. P.; Pakay, J. L.; Talbot, D. A.; Echtay, K. S. Mitochondrial superoxide and aging: uncoupling-protein activity and superoxide production. *Biochem. Soc. Symp.* 2004, (71), 203-213.
35. Turrens, J. F. Mitochondrial formation of reactive oxygen species. *J Physiol* 2003, 552, 335-44.
36. Hauptmann, N.; Grimsby, J.; Shih, J. C.; Cadenas, E. The Metabolism of Tyramine by Monoamine Oxidase A/B Causes Oxidative Damage to Mitochondrial DNA. *Arch. Biochem. Biophys.* 1996, 335, 295-304.
37. Kaludercic, N.; Takimoto, E.; Nagayama, T.; Feng, N.; Lai, E. W.; Bedja, D.; Chen, K.; Gabrielson, K. L.; Blakely, R. D.; Shih, J. C.; Pacak, K.; Kass, D. A.; Di Lisa, F.; Paolocci, N. Monoamine oxidase A-mediated enhanced catabolism of norepinephrine contributes to adverse remodeling and pump failure in hearts with pressure overload. *Circ. Res.* 2010, 106, 193-202.
38. Cohen, G.; Kesler, N. Monoamine Oxidase and Mitochondrial Respiration. *J. Neurochem.* 1999, 73, 2310-2315.
39. Berman, S. B.; Hastings, T. G. Dopamine oxidation alters mitochondrial respiration and induces permeability transition in brain mitochondria. *J. Neurochem.* 1999, 73, 1127-1137.
40. Kaludercic, N.; Carpi, A.; Menabò, R.; Di Lisa, F.; Paolocci, N. Monoamine oxidases (MAO) in the pathogenesis of heart failure and ischemia/reperfusion injury.

- Biochimica et Biophysica Acta (BBA) - Molecular Cell Research* 2011, 1813, 1323-1332.
41. Ascenzi, P.; di Masi, A.; Sciorati, C.; Clementi, E. Peroxynitrite-An ugly biofactor? *Biofactors* 2010, 36, 264-73.
 42. Ghafourifar, P.; Asbury, M. L.; Joshi, S. S.; Kincaid, E. D. Determination of mitochondrial nitric oxide synthase activity. *Methods Enzymol* 2005, 396, 424-44.
 43. Lacza, Z.; Pankotai, E.; Csordas, A.; Gero, D.; Kiss, L.; Horvath, E. M.; Kollai, M.; Busija, D. W.; Szabo, C. Mitochondrial NO and reactive nitrogen species production: does mtNOS exist? *Nitric Oxide* 2006, 14, 162-8.
 44. Lesnefsky, E. J.; Hoppel, C. L. Cardiolipin as an oxidative target in cardiac mitochondria in the aged rat. *Biochim Biophys Acta* 2008, 1777, 1020-7.
 45. Montero, J.; Mari, M.; Colell, A.; Morales, A.; Basanez, G.; Garcia-Ruiz, C.; Fernandez-Checa, J. C. Cholesterol and peroxidized cardiolipin in mitochondrial membrane properties, permeabilization and cell death. *Biochim Biophys Acta* 2010, 1797, 1217-24.
 46. Kagan, V. E.; Bayir, A.; Bayir, H.; Stoyanovsky, D.; Borisenko, G. G.; Tyurina, Y. Y.; Wipf, P.; Atkinson, J.; Greenberger, J. S.; Chapkin, R. S.; Belikova, N. A. Mitochondria-targeted disruptors and inhibitors of cytochrome c/cardiolipin peroxidase complexes: a new strategy in anti-apoptotic drug discovery. *Mol Nutr Food Res* 2009, 53, 104-14.
 47. Esterbauer, H.; Schaur, R. J.; Zollner, H. Chemistry and biochemistry of 4-hydroxynonenal, malonaldehyde and related aldehydes. *Free Radic. Biol. Med.* 1991, 11, 81-128.

48. Starkov, A. A. The role of mitochondria in reactive oxygen species metabolism and signaling. *Ann N Y Acad Sci* 2008, 1147, 37-52.
49. Jones, D. P. Radical-free biology of oxidative stress. *Am J Physiol Cell Physiol* 2008, 295, C849-68.
50. Berndt, C.; Lillig, C. H.; Holmgren, A. Thiol-based mechanisms of the thioredoxin and glutaredoxin systems: implications for diseases in the cardiovascular system. *Am J Physiol Heart Circ Physiol* 2007, 292, H1227-36.
51. Anderson, E. J.; Katunga, L. A.; Willis, M. S. Mitochondria as a source and target of lipid peroxidation products in healthy and diseased heart. *Clin. Exp. Pharmacol. Physiol.* 2012, 39, 179-193.
52. Bacot, S.; Bernoud-Hubac, N.; Baddas, N.; Chantegrel, B.; Deshayes, C.; Doutheau, A.; Lagarde, M.; Guichardant, M. Covalent binding of hydroxy-alkenals 4-HDDE, 4-HHE, and 4-HNE to ethanolamine phospholipid subclasses. *J. Lipid Res.* 2003, 44, 917-926.
53. Osman, C.; Voelker, D. R.; Langer, T. Making heads or tails of phospholipids in mitochondria. *J. Cell Biol.* 2011, 192, 7-16.
54. Fry, M.; Green, D. E. Cardiolipin requirement for electron transfer in complex I and III of the mitochondrial respiratory chain. *J. Biol. Chem.* 1981, 256, 1874-1880.
55. Paradies, G.; Petrosillo, G.; Pistolese, M.; Di Venosa, N.; Serena, D.; Ruggiero, F. M. Lipid peroxidation and alterations to oxidative metabolism in mitochondria isolated from rat heart subjected to ischemia and reperfusion. *Free Radic. Biol. Med.* 1999, 27, 42-50.

56. Chicco, A. J.; Sparagna, G. C. Role of cardiolipin alterations in mitochondrial dysfunction and disease. *Am. J. Physiol. Cell. Physiol.* 2007, 292, C33-44.
57. Siems, W.; Grune, T. Intracellular metabolism of 4-hydroxynonenal. *Mol. Aspects Med.* 2003, 24, 167-175.
58. Motohashi, H.; Katsuoka, F.; Engel, J. D.; Yamamoto, M. Small Maf proteins serve as transcriptional cofactors for keratinocyte differentiation in the Keap1-Nrf2 regulatory pathway. *Proc Natl Acad Sci U S A* 2004, 101, 6379-84.
59. Chapple, S. J.; Cheng, X.; Mann, G. E. Effects of 4-hydroxynonenal on vascular endothelial and smooth muscle cell redox signaling and function in health and disease. *Redox Biol.* 2013, 1, 319-331.
60. Zhang, Y. K.; Yeager, R. L.; Tanaka, Y.; Klaassen, C. D. Enhanced expression of Nrf2 in mice attenuates the fatty liver produced by a methionine- and choline-deficient diet. *Toxicol Appl Pharmacol* 2010, 245, 326-34.
61. Sykiotis, G. P.; Bohmann, D. Stress-activated cap'n'collar transcription factors in aging and human disease. *Sci. Signal.* 2010, 3, re3.
62. Chartoumpakis, D. V.; Kensler, T. W. New player on an old field; the keap1/Nrf2 pathway as a target for treatment of type 2 diabetes and metabolic syndrome. *Curr. Diabetes Rev.* 2013, 9, 137-145.
63. Tkachev, V. O.; Menshchikova, E. B.; Zenkov, N. K. Mechanism of the Nrf2/Keap1/ARE signaling system. *Biochemistry (Mosc)* 2011, 76, 407-422.
64. Toyama, T.; Nakamura, H.; Harano, Y.; Yamauchi, N.; Morita, A.; Kirishima, T.; Minami, M.; Itoh, Y.; Okanoue, T. PPARalpha ligands activate antioxidant enzymes

- and suppress hepatic fibrosis in rats. *Biochem. Biophys. Res. Commun.* 2004, 324, 697-704.
65. Abdelmegeed, M. A.; Moon, K. H.; Hardwick, J. P.; Gonzalez, F. J.; Song, B. J. Role of peroxisome proliferator-activated receptor-alpha in fasting-mediated oxidative stress. *Free Radic. Biol. Med.* 2009, 47, 767-778.
66. Guelzim, N.; Huneau, J. F.; Mathe, V.; Quignard-Boulangue, A.; Martin, P. G.; Tome, D.; Hermier, D. Consequences of PPAR(alpha) Invalidation on Glutathione Synthesis: Interactions with Dietary Fatty Acids. *PPAR Res.* 2011, 2011, 256186.
67. Inoue, G.; Koh, M.; Nakao, K. [High fat diet and lipotoxicity]. *Nippon Rinsho* 2002, 60 Suppl 7, 626-31.
68. Inoue, I.; Goto, S.; Matsunaga, T.; Nakajima, T.; Awata, T.; Hokari, S.; Komoda, T.; Katayama, S. The ligands/activators for peroxisome proliferator-activated receptor alpha (PPARalpha) and PPARgamma increase Cu²⁺, Zn²⁺-superoxide dismutase and decrease p22phox message expressions in primary endothelial cells. *Metabolism* 2001, 50, 3-11.
69. Anderson, E. J.; Thayne, K. A.; Harris, M.; Shaikh, S. R.; Darden, T. M.; Lark, D. S.; Williams, J. M.; Chitwood, W. R.; Kypson, A. P.; Rodriguez, E. Do Fish Oil Omega-3 Fatty Acids Enhance Antioxidant Capacity and Mitochondrial Fatty Acid Oxidation in Human Atrial Myocardium via PPARgamma Activation? *Antioxid. Redox Signal.* 2014.
70. Rigobello, M. P.; Folda, A.; Baldoin, M. C.; Scutari, G.; Bindoli, A. Effect of auranofin on the mitochondrial generation of hydrogen peroxide. Role of thioredoxin reductase. *Free Radic Res* 2005, 39, 687-95.

71. Stanley, W. C.; Dabkowski, E. R.; Ribeiro, R. F., Jr; O'Connell, K. A. Dietary fat and heart failure: moving from lipotoxicity to lipoprotection. *Circ. Res.* 2012, *110*, 764-776.
72. Fisher-Wellman, K. H.; Mattox, T. A.; Thayne, K.; Katunga, L. A.; La Favor, J. D.; Neuffer, P. D.; Hickner, R. C.; Wingard, C. J.; Anderson, E. J. Novel role for thioredoxin reductase-2 in mitochondrial redox adaptations to obesogenic diet and exercise in heart and skeletal muscle. *J. Physiol.* 2013, *591*, 3471-3486.
73. Gurusamy, N.; Das, D. K. Autophagy, redox signaling, and ventricular remodeling. *Antioxid. Redox Signal.* 2009, *11*, 1975-1988.
74. Lee, J.; Giordano, S.; Zhang, J. Autophagy, mitochondria and oxidative stress: cross-talk and redox signalling. *Biochem. J.* 2012, *441*, 523-540.
75. Rahman, M.; Mofarrahi, M.; Kristof, A. S.; Nkengfac, B.; Harel, S.; Hussain, S. N. Reactive oxygen species regulation of autophagy in skeletal muscles. *Antioxid. Redox Signal.* 2014, *20*, 443-459.
76. Budas, G. R.; Disatnik, M. H.; Mochly-Rosen, D. Aldehyde dehydrogenase 2 in cardiac protection: a new therapeutic target? *Trends Cardiovasc. Med.* 2009, *19*, 158-164.
77. Ursini, F.; Maiorino, M.; Valente, M.; Ferri, L.; Gregolin, C. Purification from pig liver of a protein which protects liposomes and biomembranes from peroxidative degradation and exhibits glutathione peroxidase activity on phosphatidylcholine hydroperoxides. *Biochim. Biophys. Acta* 1982, *710*, 197-211.

78. McCray, P. B.; Gibson, D. D.; Fong, K. L.; Hornbrook, K. R. Effect of glutathione peroxidase activity on lipid peroxidation in biological membranes. *Biochim. Biophys. Acta* 1976, 431, 459-468.
79. Ursini, F.; Maiorino, M.; Gregolin, C. Phospholipid hydroperoxide glutathione peroxidase. *Int. J. Tissue React.* 1986, 8, 99-103.
80. Brigelius-Flohe, R. Tissue-specific functions of individual glutathione peroxidases. *Free Radic. Biol. Med.* 1999, 27, 951-965.
81. Imai, H.; Koumura, T.; Nakajima, R.; Nomura, K.; Nakagawa, Y. Protection from inactivation of the adenine nucleotide translocator during hypoglycaemia-induced apoptosis by mitochondrial phospholipid hydroperoxide glutathione peroxidase. *Biochem. J.* 2003, 371, 799-809.
82. Yant, L. J.; Ran, Q.; Rao, L.; Van Remmen, H.; Shibatani, T.; Belter, J. G.; Motta, L.; Richardson, A.; Prolla, T. A. The selenoprotein GPX4 is essential for mouse development and protects from radiation and oxidative damage insults. *Free Radic. Biol. Med.* 2003, 34, 496-502.
83. Brigelius-Flohe, R.; Maiorino, M. Glutathione peroxidases. *Biochim. Biophys. Acta* 2012.
84. Ursini, F.; Maiorino, M.; Gregolin, C. The selenoenzyme phospholipid hydroperoxide glutathione peroxidase. *Biochim. Biophys. Acta* 1985, 839, 62-70.
85. Maiorino, M.; Roveri, A.; Ursini, F.; Gregolin, C. Enzymatic determination of membrane lipid peroxidation. *J. Free Radic. Biol. Med.* 1985, 1, 203-207.
86. Maiorino, M.; Roveri, A.; Gregolin, C.; Ursini, F. Different effects of Triton X-100, deoxycholate, and fatty acids on the kinetics of glutathione peroxidase and

- phospholipid hydroperoxide glutathione peroxidase. *Arch. Biochem. Biophys.* 1986, 251, 600-605.
87. Regev-Rudzki, N.; Pines, O. Eclipsed distribution: a phenomenon of dual targeting of protein and its significance. *Bioessays* 2007, 29, 772-782.
88. Imai, H.; Hirao, F.; Sakamoto, T.; Sekine, K.; Mizukura, Y.; Saito, M.; Kitamoto, T.; Hayasaka, M.; Hanaoka, K.; Nakagawa, Y. Early embryonic lethality caused by targeted disruption of the mouse PHGPx gene. *Biochem. Biophys. Res. Commun.* 2003, 305, 278-286.
89. Chen, J.; Henderson, G. I.; Freeman, G. L. Role of 4-hydroxynonenal in modification of cytochrome c oxidase in ischemia/reperfused rat heart. *J. Mol. Cell. Cardiol.* 2001, 33, 1919-1927.
90. Dabkowski, E. R.; Williamson, C. L.; Bukowski, V. C.; Chapman, R. S.; Leonard, S. S.; Peer, C. J.; Callery, P. S.; Hollander, J. M. Diabetic cardiomyopathy-associated dysfunction in spatially distinct mitochondrial subpopulations. *Am. J. Physiol. Heart Circ. Physiol.* 2009, 296, H359-69.
91. Hollander, J. M.; Lin, K. M.; Scott, B. T.; Dillmann, W. H. Overexpression of PHGPx and HSP60/10 protects against ischemia/reoxygenation injury. *Free Radic. Biol. Med.* 2003, 35, 742-751.
92. Dabkowski, E. R.; Williamson, C. L.; Hollander, J. M. Mitochondria-specific transgenic overexpression of phospholipid hydroperoxide glutathione peroxidase (GPx4) attenuates ischemia/reperfusion-associated cardiac dysfunction. *Free Radic. Biol. Med.* 2008, 45, 855-865.

93. Liang, H.; Van Remmen, H.; Frohlich, V.; Lechleiter, J.; Richardson, A.; Ran, Q.
Gpx4 protects mitochondrial ATP generation against oxidative damage. *Biochem. Biophys. Res. Commun.* 2007, 356, 893-898.
94. Ufer, C.; Wang, C. C.; Fahling, M.; Schiebel, H.; Thiele, B. J.; Billett, E. E.; Kuhn, H.; Borchert, A. Translational regulation of glutathione peroxidase 4 expression through guanine-rich sequence-binding factor 1 is essential for embryonic brain development. *Genes Dev.* 2008, 22, 1838-1850.
95. Imai, H.; Saito, M.; Kirai, N.; Hasegawa, J.; Konishi, K.; Hattori, H.; Nishimura, M.; Naito, S.; Nakagawa, Y. Identification of the positive regulatory and distinct core regions of promoters, and transcriptional regulation in three types of mouse phospholipid hydroperoxide glutathione peroxidase. *J. Biochem.* 2006, 140, 573-590.
96. Ran, Q.; Liang, H.; Gu, M.; Qi, W.; Walter, C. A.; Roberts, L. J., 2nd; Herman, B.; Richardson, A.; Van Remmen, H. Transgenic mice overexpressing glutathione peroxidase 4 are protected against oxidative stress-induced apoptosis. *J. Biol. Chem.* 2004, 279, 55137-55146.
97. Nakagawa, Y. Role of mitochondrial phospholipid hydroperoxide glutathione peroxidase (PHGPx) as an antiapoptotic factor. *Biol. Pharm. Bull.* 2004, 27, 956-960.
98. Liang, H.; Ran, Q.; Jang, Y. C.; Holstein, D.; Lechleiter, J.; McDonald-Marsh, T.; Musatov, A.; Song, W.; Van Remmen, H.; Richardson, A. Glutathione peroxidase 4 differentially regulates the release of apoptogenic proteins from mitochondria. *Free Radic. Biol. Med.* 2009, 47, 312-320.

99. Ran, Q.; Liang, H.; Ikeno, Y.; Qi, W.; Prolla, T. A.; Roberts, L. J., 2nd; Wolf, N.; Van Remmen, H.; Richardson, A. Reduction in glutathione peroxidase 4 increases life span through increased sensitivity to apoptosis. *J Gerontol A Biol Sci Med Sci* 2007, 62, 932-42.
100. Villette, S.; Kyle, J. A.; Brown, K. M.; Pickard, K.; Milne, J. S.; Nicol, F.; Arthur, J. R.; Hesketh, J. E. A novel single nucleotide polymorphism in the 3' untranslated region of human glutathione peroxidase 4 influences lipoxygenase metabolism. *Blood Cells Mol. Dis.* 2002, 29, 174-178.
101. Huang, H. S.; Chen, C. J.; Suzuki, H.; Yamamoto, S.; Chang, W. C. Inhibitory effect of phospholipid hydroperoxide glutathione peroxidase on the activity of lipoxygenases and cyclooxygenases. *Prostaglandins Other Lipid Mediat.* 1999, 58, 65-75.
102. Zhang, L. P.; Maiorino, M.; Roveri, A.; Ursini, F. Phospholipid hydroperoxide glutathione peroxidase: specific activity in tissues of rats of different age and comparison with other glutathione peroxidases. *Biochim. Biophys. Acta* 1989, 1006, 140-143.
103. Villette, S.; Kyle, J. A.; Brown, K. M.; Pickard, K.; Milne, J. S.; Nicol, F.; Arthur, J. R.; Hesketh, J. E. A novel single nucleotide polymorphism in the 3' untranslated region of human glutathione peroxidase 4 influences lipoxygenase metabolism. *Blood Cells Mol. Dis.* 2002, 29, 174-178.
104. Crosley, L. K.; Bashir, S.; Nicol, F.; Arthur, J. R.; Hesketh, J. E.; Sneddon, A. A. The single-nucleotide polymorphism (GPX4c718t) in the glutathione peroxidase 4

- gene influences endothelial cell function: interaction with selenium and fatty acids. *Mol. Nutr. Food Res.* 2013, 57, 2185-2194.
105. Ruperez, A. I.; Olza, J.; Gil-Campos, M.; Leis, R.; Mesa, M. D.; Tojo, R.; Canete, R.; Gil, A.; Aguilera, C. M. Association of Genetic Polymorphisms for Glutathione Peroxidase Genes with Obesity in Spanish Children. *J. Nutrigenet Nutrigenomics* 2014, 7, 130-142.
106. Hayes, J. D.; Pulford, D. J. The glutathione S-transferase supergene family: regulation of GST and the contribution of the isoenzymes to cancer chemoprotection and drug resistance. *Crit. Rev. Biochem. Mol. Biol.* 1995, 30, 445-600.
107. Daniel, V. Glutathione S-transferases: gene structure and regulation of expression. *Crit. Rev. Biochem. Mol. Biol.* 1993, 28, 173-207.
108. Hartley, D. P.; Ruth, J. A.; Petersen, D. R. The hepatocellular metabolism of 4-hydroxynonenal by alcohol dehydrogenase, aldehyde dehydrogenase, and glutathione S-transferase. *Arch. Biochem. Biophys.* 1995, 316, 197-205.
109. Ambroziak, W.; Pietruszko, R. Human aldehyde dehydrogenase. Activity with aldehyde metabolites of monoamines, diamines, and polyamines. *J. Biol. Chem.* 1991, 266, 13011-13018.
110. Rooke, N.; Li, D. J.; Li, J.; Keung, W. M. The mitochondrial monoamine oxidase-aldehyde dehydrogenase pathway: a potential site of action of daidzin. *J. Med. Chem.* 2000, 43, 4169-4179.

111. Marchitti, S. A.; Brocker, C.; Stagos, D.; Vasiliou, V. Non-P450 aldehyde oxidizing enzymes: the aldehyde dehydrogenase superfamily. *Expert Opin. Drug Metab. Toxicol.* 2008, 4, 697-720.
112. Bian, Y.; Chen, Y. G.; Xu, F.; Xue, L.; Ji, W. Q.; Zhang, Y. The polymorphism in aldehyde dehydrogenase-2 gene is associated with elevated plasma levels of high-sensitivity C-reactive protein in the early phase of myocardial infarction. *Tohoku J. Exp. Med.* 2010, 221, 107-112.
113. Chang, Y. C.; Chiu, Y. F.; Lee, I. T.; Ho, L. T.; Hung, Y. J.; Hsiung, C. A.; Quertermous, T.; Donlon, T.; Lee, W. J.; Lee, P. C.; Chen, C. H.; Mochly-Rosen, D.; Chuang, L. M. Common ALDH2 genetic variants predict development of hypertension in the SAPPHIRe prospective cohort: gene-environmental interaction with alcohol consumption. *BMC Cardiovasc. Disord.* 2012, 12, 58.
114. Rosemond, M. J.; Walsh, J. S. Human carbonyl reduction pathways and a strategy for their study in vitro. *Drug Metab. Rev.* 2004, 36, 335-361.
115. Srivastava, S. K.; Ramana, K. V.; Srivastava, S.; Bhatnagar, A. In *Aldose Reductase Detoxifies Lipid Aldehydes and Their Glutathione Conjugates*; ACS Symposium Series; American Chemical Society: Washington, DC., 2003; Vol. 865, pp 37-48.
116. Srivastava, S.; Chandra, A.; Wang, L. F.; E., S. W., Jr; DaGue, B. B.; Ansari, N. H.; Srivastava, S. K.; Bhatnagar, A. Metabolism of the lipid peroxidation product, 4-hydroxy-trans-2-nonenal, in isolated perfused rat heart. *J Biol Chem* 1998, 273, 10893-900.

117. Aronson, D. Cross-linking of glycated collagen in the pathogenesis of arterial and myocardial stiffening of aging and diabetes. *J. Hypertens.* 2003, 21, 3-12.
118. Ciulla, M. M.; Paliotti, R.; Carini, M.; Aldini, G. Fibrosis, enzymatic and non-enzymatic cross-links in hypertensive heart disease. *Cardiovasc. Hematol. Disord. Drug Targets* 2011.
119. Fang, Z. Y.; Prins, J. B.; Marwick, T. H. Diabetic cardiomyopathy: evidence, mechanisms, and therapeutic implications. *Endocr. Rev.* 2004, 25, 543-567.
120. Yuen, H. K. Factors associated with preventive care practice among adults with diabetes. *Prim. Care. Diabetes* 2012, 6, 75-78.
121. Hutchinson, K. R.; Lord, C. K.; West, T. A.; Stewart, J. A., Jr Cardiac fibroblast-dependent extracellular matrix accumulation is associated with diastolic stiffness in type 2 diabetes. *PLoS One* 2013, 8, e72080.
122. Weber, K. T.; Pick, R.; Jalil, J. E.; Janicki, J. S.; Carroll, E. P. Patterns of myocardial fibrosis. *J. Mol. Cell. Cardiol.* 1989, 21 Suppl 5, 121-131.
123. Dobaczewski, M.; Gonzalez-Quesada, C.; Frangogiannis, N. G. The extracellular matrix as a modulator of the inflammatory and reparative response following myocardial infarction. *J. Mol. Cell. Cardiol.* 2010, 48, 504-511.
124. Hinz, B.; Phan, S. H.; Thannickal, V. J.; Galli, A.; Bochaton-Piallat, M. L.; Gabbiani, G. The myofibroblast: one function, multiple origins. *Am. J. Pathol.* 2007, 170, 1807-1816.
125. Fan, D.; Takawale, A.; Lee, J.; Kassiri, Z. Cardiac fibroblasts, fibrosis and extracellular matrix remodeling in heart disease. *Fibrogenesis Tissue Repair* 2012, 5, 15-1536-5-15.

126. McDowell, K. S.; Vadakkumpadan, F.; Blake, R.; Blauer, J.; Plank, G.; Macleod, R. S.; Trayanova, N. A. Mechanistic inquiry into the role of tissue remodeling in fibrotic lesions in human atrial fibrillation. *Biophys. J.* 2013, *104*, 2764-2773.
127. Rosker, C.; Salvarani, N.; Schmutz, S.; Grand, T.; Rohr, S. Abolishing myofibroblast arrhythmogenicity by pharmacological ablation of alpha-smooth muscle actin containing stress fibers. *Circ. Res.* 2011, *109*, 1120-1131.
128. Koppel, H.; Riedl, E.; Braunagel, M.; Sauerhoefer, S.; Ehnert, S.; Godoy, P.; Sternik, P.; Dooley, S.; Yard, B. A. L-carnosine inhibits high-glucose-mediated matrix accumulation in human mesangial cells by interfering with TGF-beta production and signalling. *Nephrol. Dial. Transplant.* 2011, *26*, 3852-3858.
129. Eschalier, R.; Rossignol, P.; Kearney-Schwartz, A.; Adamopoulos, C.; Karatzidou, K.; Fay, R.; Mandry, D.; Marie, P. Y.; Zannad, F. Features of cardiac remodeling, associated with blood pressure and fibrosis biomarkers, are frequent in subjects with abdominal obesity. *Hypertension* 2014, *63*, 740-746.
130. Sparvero, L. J.; Asafu-Adjei, D.; Kang, R.; Tang, D.; Amin, N.; Im, J.; Rutledge, R.; Lin, B.; Amoscato, A. A.; Zeh, H. J.; Lotze, M. T. RAGE (Receptor for Advanced Glycation Endproducts), RAGE ligands, and their role in cancer and inflammation. *J. Transl. Med.* 2009, *7*, 17.
131. Bucciarelli, L. G.; Wendt, T.; Rong, L.; Lalla, E.; Hofmann, M. A.; Goova, M. T.; Taguchi, A.; Yan, S. F.; Yan, S. D.; Stern, D. M.; Schmidt, A. M. RAGE is a multiligand receptor of the immunoglobulin superfamily: implications for homeostasis and chronic disease. *Cell Mol. Life Sci.* 2002, *59*, 1117-1128.

132. Fritz, G. RAGE: a single receptor fits multiple ligands. *Trends Biochem. Sci.* 2011, 36, 625-632.
133. Kanwar, Y. S.; Sun, L.; Xie, P.; Liu, F. Y.; Chen, S. A glimpse of various pathogenetic mechanisms of diabetic nephropathy. *Annu. Rev. Pathol.* 2011, 6, 395-423.
134. Tessier, F. J.; Birlouez-Aragon, I. Health effects of dietary Maillard reaction products: the results of ICARE and other studies. *Amino Acids* 2012, 42, 1119-1131.
135. Peyroux, J.; Sternberg, M. Advanced glycation endproducts (AGEs): Pharmacological inhibition in diabetes. *Pathol. Biol. (Paris)* 2006, 54, 405-419.
136. Ramasamy, R.; Schmidt, A. M. Receptor for advanced glycation end products (RAGE) and implications for the pathophysiology of heart failure. *Curr. Heart Fail. Rep.* 2012, 9, 107-116.
137. Creagh-Brown, B. C.; Quinlan, G. J.; Evans, T. W.; Burke-Gaffney, A. The RAGE axis in systemic inflammation, acute lung injury and myocardial dysfunction: an important therapeutic target? *Intensive Care Med.* 2010, 36, 1644-1656.
138. Gregor, M. F.; Hotamisligil, G. S. Inflammatory mechanisms in obesity. *Annu. Rev. Immunol.* 2011, 29, 415-445.
139. Frangogiannis, N. G. Regulation of the inflammatory response in cardiac repair. *Circ. Res.* 2012, 110, 159-173.
140. Pillai, S. S.; Sugathan, J. K.; Indira, M. Selenium downregulates RAGE and NFkappaB expression in diabetic rats. *Biol. Trace Elem. Res.* 2012, 149, 71-77.

141. Biernacka, A.; Dobaczewski, M.; Frangogiannis, N. G. TGF-beta signaling in fibrosis. *Growth Factors* 2011, 29, 196-202.
142. Dobaczewski, M.; Chen, W.; Frangogiannis, N. G. Transforming growth factor (TGF)-beta signaling in cardiac remodeling. *J. Mol. Cell. Cardiol.* 2011, 51, 600-606.
143. Massague, J. How cells read TGF-beta signals. *Nat. Rev. Mol. Cell Biol.* 2000, 1, 169-178.
144. Larroque-Cardoso, P.; Mucher, E.; Graziade, M. H.; Josse, G.; Schmitt, A. M.; Nadal-Wolbold, F.; Zarkovic, K.; Salvayre, R.; Negre-Salvayre, A. 4-Hydroxynonenal impairs transforming growth factor-beta1-induced elastin synthesis via epidermal growth factor receptor activation in human and murine fibroblasts. *Free Radic. Biol. Med.* 2014, 71, 427-436.
145. Boldyrev, A. A. Retrospectives and perspectives on the biological activity of histidine-containing dipeptides. *Int. J. Biochem.* 1990, 22, 129-132.
146. O'Dowd, J. J.; Robins, D. J.; Miller, D. J. Detection, characterisation, and quantification of carnosine and other histidyl derivatives in cardiac and skeletal muscle. *Biochim. Biophys. Acta* 1988, 967, 241-249.
147. Vistoli, G.; Orioli, M.; Pedretti, A.; Regazzoni, L.; Canevotti, R.; Negrisoli, G.; Carini, M.; Aldini, G. Design, synthesis, and evaluation of carnosine derivatives as selective and efficient sequestering agents of cytotoxic reactive carbonyl species. *ChemMedChem* 2009, 4, 967-975.

148. Pedretti, A.; De Luca, L.; Marconi, C.; Negrisoli, G.; Aldini, G.; Vistoli, G. Modeling of the intestinal peptide transporter hPepT1 and analysis of its transport capacities by docking and pharmacophore mapping. *ChemMedChem* 2008, 3, 1913-1921.
149. Lenney, J. F. Carnosinase and homocarnosinosis. *J. Oslo City Hosp.* 1985, 35, 27-40.
150. DAVEY, C. L. The significance of carnosine and anserine in striated skeletal muscle. *Arch. Biochem. Biophys.* 1960, 89, 303-308.
151. Guiotto, A.; Calderan, A.; Ruzza, P.; Borin, G. Carnosine and carnosine-related antioxidants: a review. *Curr Med Chem* 2005, 12, 2293-315.
152. Orioli, M.; Vistoli, G.; Regazzoni, L.; Pedretti, A.; Lapolla, A.; Rossoni, G.; Canevotti, R.; Gamberoni, L.; Previtali, M.; Carini, M.; Aldini, G. Design, synthesis, ADME properties, and pharmacological activities of beta-alanyl-D-histidine (D-carnosine) prodrugs with improved bioavailability. *ChemMedChem* 2011, 6, 1269-1282.
153. Giris, M.; Dogru-Abbasoglu, S.; Kumral, A.; Olgac, V.; Kocak-Toker, N.; Uysal, M. Effect of carnosine alone or combined with alpha-tocopherol on hepatic steatosis and oxidative stress in fructose-induced insulin-resistant rats. *J. Physiol. Biochem.* 2014, 70, 385-395.
154. Menini, S.; Iacobini, C.; Ricci, C.; Scipioni, A.; Blasetti Fantauzzi, C.; Giaccari, A.; Salomone, E.; Canevotti, R.; Lapolla, A.; Orioli, M.; Aldini, G.; Pugliese, G. D-Carnosine octylester attenuates atherosclerosis and renal disease in ApoE null mice fed a Western diet through reduction of carbonyl stress and inflammation. *Br. J. Pharmacol.* 2012, 166, 1344-1356.

155. Brown, B. E.; Kim, C. H.; Torpy, F. R.; Bursill, C. A.; McRobb, L. S.; Heather, A. K.; Davies, M. J.; van Reyk, D. M. Supplementation with carnosine decreases plasma triglycerides and modulates atherosclerotic plaque composition in diabetic apo E(-/-) mice. *Atherosclerosis* 2014, 232, 403-409.
156. Aldini, G.; Orioli, M.; Rossoni, G.; Savi, F.; Braidotti, P.; Vistoli, G.; Yeum, K. J.; Negrisoli, G.; Carini, M. The carbonyl scavenger carnosine ameliorates dyslipidaemia and renal function in Zucker obese rats. *J. Cell. Mol. Med.* 2011, 15, 1339-1354.
157. Selvin, E.; Lazo, M.; Chen, Y.; Shen, L.; Rubin, J.; McEvoy, J. W.; Hoogeveen, R. C.; Sharrett, A. R.; Ballantyne, C. M.; Coresh, J. Diabetes mellitus, prediabetes, and incidence of subclinical myocardial damage. *Circulation* 2014, 130, 1374-1382.
158. Khan, J. N.; Wilmot, E. G.; Leggate, M.; Singh, A.; Yates, T.; Nimmo, M.; Khunti, K.; Horsfield, M. A.; Biglands, J.; Clarysse, P.; Croisille, P.; Davies, M.; McCann, G. P. Subclinical diastolic dysfunction in young adults with Type 2 diabetes mellitus: a multiparametric contrast-enhanced cardiovascular magnetic resonance pilot study assessing potential mechanisms. *Eur. Heart J. Cardiovasc. Imaging* 2014.
159. Porcar-Almela, M.; Codoner-Franch, P.; Tuzon, M.; Navarro-Solera, M.; Carrasco-Luna, J.; Ferrando, J. Left ventricular diastolic function and cardiometabolic factors in obese normotensive children. *Nutr. Metab. Cardiovasc. Dis.* 2015, 25, 108-115.
160. Catala, A. Lipid peroxidation of membrane phospholipids generates hydroxy-alkenals and oxidized phospholipids active in physiological and/or pathological conditions. *Chem. Phys. Lipids* 2009, 157, 1-11.

161. Guichardant, M.; Chantegrel, B.; Deshayes, C.; Doutheau, A.; Moliere, P.; Lagarde, M. Specific markers of lipid peroxidation issued from n-3 and n-6 fatty acids. *Biochem. Soc. Trans.* 2004, *32*, 139-140.
162. Guichardant, M.; Bacot, S.; Moliere, P.; Lagarde, M. Hydroxy-alkenals from the peroxidation of n-3 and n-6 fatty acids and urinary metabolites. *Prostaglandins Leukot. Essent. Fatty Acids* 2006, *75*, 179-182.
163. Refsgaard, H. H.; Tsai, L.; Stadtman, E. R. Modifications of proteins by polyunsaturated fatty acid peroxidation products. *Proc. Natl. Acad. Sci. U. S. A.* 2000, *97*, 611-616.
164. West, J. D.; Marnett, L. J. Alterations in gene expression induced by the lipid peroxidation product, 4-hydroxy-2-nonenal. *Chem Res Toxicol* 2005, *18*, 1642-53.
165. Uchida, K. 4-Hydroxy-2-nonenal: a product and mediator of oxidative stress. *Prog. Lipid Res.* 2003, *42*, 318-343.
166. Uchida, K. Role of reactive aldehyde in cardiovascular diseases. *Free Radic. Biol. Med.* 2000, *28*, 1685-1696.
167. LoPachin, R. M.; Gavin, T.; Petersen, D. R.; Barber, D. S. Molecular mechanisms of 4-hydroxy-2-nonenal and acrolein toxicity: nucleophilic targets and adduct formation. *Chem. Res. Toxicol.* 2009, *22*, 1499-1508.
168. Januszewski, A. S.; Alderson, N. L.; Metz, T. O.; Thorpe, S. R.; Baynes, J. W. Role of lipids in chemical modification of proteins and development of complications in diabetes. *Biochem. Soc. Trans.* 2003, *31*, 1413-1416.
169. Blair, I. A. DNA adducts with lipid peroxidation products. *J. Biol. Chem.* 2008, *283*, 15545-15549.

170. Chavez, J. D.; Wu, J.; Bisson, W.; Maier, C. S. Site-specific proteomic analysis of lipoxidation adducts in cardiac mitochondria reveals chemical diversity of 2-alkenal adduction. *J. Proteomics* 2011.
171. Minko, I. G.; Kozekov, I. D.; Harris, T. M.; Rizzo, C. J.; Lloyd, R. S.; Stone, M. P. Chemistry and biology of DNA containing 1,N(2)-deoxyguanosine adducts of the alpha,beta-unsaturated aldehydes acrolein, crotonaldehyde, and 4-hydroxynonenal. *Chem. Res. Toxicol.* 2009, 22, 759-778.
172. Maier, C. S.; Chavez, J.; Wang, J.; Wu, J. Protein adducts of aldehydic lipid peroxidation products identification and characterization of protein adducts using an aldehyde/keto-reactive probe in combination with mass spectrometry. *Methods Enzymol.* 2010, 473, 305-330.
173. Nair, J.; Barbin, A.; Velic, I.; Bartsch, H. Etheno DNA-base adducts from endogenous reactive species. *Mutat. Res.* 1999, 424, 59-69.
174. Shimozu, Y.; Hirano, K.; Shibata, T.; Shibata, N.; Uchida, K. 4-Hydroperoxy-2-nonenal is not just an intermediate but a reactive molecule that covalently modifies proteins to generate unique intramolecular oxidation products. *J. Biol. Chem.* 2011, 286, 29313-29324.
175. Maiorino, M.; Thomas, J. P.; Girotti, A. W.; Ursini, F. Reactivity of phospholipid hydroperoxide glutathione peroxidase with membrane and lipoprotein lipid hydroperoxides. *Free Radic. Res. Commun.* 1991, 12-13 Pt 1, 131-135.
176. Maiorino, M.; Gregolin, C.; Ursini, F. Phospholipid hydroperoxide glutathione peroxidase. *Methods Enzymol.* 1990, 186, 448-457.

177. Scimeca, M. S.; Lisk, D. J.; Prolla, T.; Lei, X. G. Effects of gpx4 haploid insufficiency on GPx4 activity, selenium concentration, and paraquat-induced protein oxidation in murine tissues. *Exp. Biol. Med. (Maywood)* 2005, 230, 709-714.
178. Morgan, E. E.; Faulx, M. D.; McElfresh, T. A.; Kung, T. A.; Zawaneh, M. S.; Stanley, W. C.; Chandler, M. P.; Hoit, B. D. Validation of echocardiographic methods for assessing left ventricular dysfunction in rats with myocardial infarction. *Am J Physiol Heart Circ Physiol* 2004, 287, H2049-53.
179. Ran, Q.; Van Remmen, H.; Gu, M.; Qi, W.; Roberts, L. J., 2nd; Prolla, T.; Richardson, A. Embryonic fibroblasts from Gpx4^{+/-} mice: a novel model for studying the role of membrane peroxidation in biological processes. *Free Radic. Biol. Med.* 2003, 35, 1101-1109.
180. Polonikov, A. V.; Vialykh, E. K.; Churnosov, M. I.; Illig, T.; Freidin, M. B.; Vasil'eva, O. V.; Bushueva, O. Y.; Ryzhaeva, V. N.; Bulgakova, I. V.; Solodilova, M. A. The C718T polymorphism in the 3'-untranslated region of glutathione peroxidase-4 gene is a predictor of cerebral stroke in patients with essential hypertension. *Hypertens. Res.* 2012, 35, 507-512.
181. Du, X. H.; Dai, X. X.; Xia Song, R.; Zou, X. Z.; Yan Sun, W.; Mo, X. Y.; Lu Bai, G.; Xiong, Y. M. SNP and mRNA expression for glutathione peroxidase 4 in Kashin-Beck disease. *Br. J. Nutr.* 2012, 107, 164-169.
182. Villette, S.; Kyle, J. A.; Brown, K. M.; Pickard, K.; Milne, J. S.; Nicol, F.; Arthur, J. R.; Hesketh, J. E. A novel single nucleotide polymorphism in the 3' untranslated region of human glutathione peroxidase 4 influences lipoxygenase metabolism. *Blood Cells Mol. Dis.* 2002, 29, 174-178.

183. Houstis, N.; Rosen, E. D.; Lander, E. S. Reactive oxygen species have a causal role in multiple forms of insulin resistance. *Nature* 2006, *440*, 944-948.
184. Meplan, C.; Crosley, L. K.; Nicol, F.; Horgan, G. W.; Mathers, J. C.; Arthur, J. R.; Hesketh, J. E. Functional effects of a common single-nucleotide polymorphism (GPX4c718t) in the glutathione peroxidase 4 gene: interaction with sex. *Am. J. Clin. Nutr.* 2008, *87*, 1019-1027.
185. Qin, F.; Siwik, D. A.; Luptak, I.; Hou, X.; Wang, L.; Higuchi, A.; Weisbrod, R. M.; Ouchi, N.; Tu, V. H.; Calamaras, T. D.; Miller, E. J.; Verbeuren, T. J.; Walsh, K.; Cohen, R. A.; Colucci, W. S. The polyphenols resveratrol and S17834 prevent the structural and functional sequelae of diet-induced metabolic heart disease in mice. *Circulation* 2012, *125*, 1757-64, S1-6.
186. Burgmaier, M.; Sen, S.; Philip, F.; Wilson, C. R.; Miller, C. C.,3rd; Young, M. E.; Taegtmeyer, H. Metabolic adaptation follows contractile dysfunction in the heart of obese Zucker rats fed a high-fat "Western" diet. *Obesity (Silver Spring)* 2010, *18*, 1895-1901.
187. Wilson, C. R.; Tran, M. K.; Salazar, K. L.; Young, M. E.; Taegtmeyer, H. Western diet, but not high fat diet, causes derangements of fatty acid metabolism and contractile dysfunction in the heart of Wistar rats. *Biochem. J.* 2007, *406*, 457-467.
188. Hoffmann, F. W.; Hashimoto, A. S.; Lee, B. C.; Rose, A. H.; Shohet, R. V.; Hoffmann, P. R. Specific antioxidant selenoproteins are induced in the heart during hypertrophy. *Arch. Biochem. Biophys.* 2011, *512*, 38-44.
189. Curtis, J. M.; Hahn, W. S.; Stone, M. D.; Inda, J. J.; Drouillard, D. J.; Kuzmicic, J. P.; Donoghue, M. A.; Long, E. K.; Armien, A. G.; Lavandero, S.; Arriaga, E.; Griffin,

- T. J.; Bernlohr, D. A. Protein carbonylation and adipocyte mitochondrial function. *J. Biol. Chem.* 2012, 287, 32967-32980.
190. Frohnert, B. I.; Bernlohr, D. A. Protein carbonylation, mitochondrial dysfunction, and insulin resistance. *Adv. Nutr.* 2013, 4, 157-163.
191. Hill, B. G.; Dranka, B. P.; Zou, L.; Chatham, J. C.; Darley-Usmar, V. M. Importance of the bioenergetic reserve capacity in response to cardiomyocyte stress induced by 4-hydroxynonenal. *Biochem. J.* 2009, 424, 99-107.
192. Lashin, O. M.; Szweda, P. A.; Szweda, L. I.; Romani, A. M. Decreased complex II respiration and HNE-modified SDH subunit in diabetic heart. *Free Radic. Biol. Med.* 2006, 40, 886-896.
193. Sverdlov, A. L.; Elezaby, A.; Behring, J. B.; Bachschmid, M. M.; Luptak, I.; Tu, V. H.; Siwik, D. A.; Miller, E. J.; Liesa, M.; Shirihai, O. S.; Pimentel, D. R.; Cohen, R. A.; Colucci, W. S. High fat, high sucrose diet causes cardiac mitochondrial dysfunction due in part to oxidative post-translational modification of mitochondrial complex II. *J. Mol. Cell. Cardiol.* 2015, 78, 165-173.
194. Li, Q.; Sadhukhan, S.; Berthiaume, J. M.; Ibarra, R. A.; Tang, H.; Deng, S.; Hamilton, E.; Nagy, L. E.; Tochtrop, G. P.; Zhang, G. F. 4-Hydroxy-2(E)-nonenal (HNE) catabolism and formation of HNE adducts are modulated by beta oxidation of fatty acids in the isolated rat heart. *Free Radic. Biol. Med.* 2013, 58, 35-44.
195. Rindler, P. M.; Plafker, S. M.; Szweda, L. I.; Kinter, M. High dietary fat selectively increases catalase expression within cardiac mitochondria. *J. Biol. Chem.* 2013, 288, 1979-1990.

196. Bhatt, N. M.; Aon, M. A.; Tocchetti, C. G.; Shen, X.; Dey, S.; Ramirez-Correa, G.; O'Rourke, B.; Gao, W. D.; Cortassa, S. Restoring redox balance enhances contractility in heart trabeculae from type 2 diabetic rats exposed to high glucose. *Am. J. Physiol. Heart Circ. Physiol.* 2015, 308, H291-302.
197. Xie, J.; Mendez, J. D.; Mendez-Valenzuela, V.; Aguilar-Hernandez, M. M. Cellular signalling of the receptor for advanced glycation end products (RAGE). *Cell. Signal.* 2013, 25, 2185-2197.
198. Thorpe, S. R.; Baynes, J. W. Maillard reaction products in tissue proteins: new products and new perspectives. *Amino Acids* 2003, 25, 275-281.
199. Frangogiannis, N. G. Matricellular proteins in cardiac adaptation and disease. *Physiol. Rev.* 2012, 92, 635-688.
200. Anderson, E. J.; Kypson, A. P.; Rodriguez, E.; Anderson, C. A.; Lehr, E. J.; Neuffer, P. D. Substrate-specific derangements in mitochondrial metabolism and redox balance in the atrium of the type 2 diabetic human heart. *J Am Coll Cardiol* 2009, 54, 1891-8.
201. LoPachin, R. M.; Gavin, T. Molecular mechanisms of aldehyde toxicity: a chemical perspective. *Chem. Res. Toxicol.* 2014, 27, 1081-1091.
202. Behring, J. B.; Kumar, V.; Whelan, S. A.; Chauhan, P.; Siwik, D. A.; Costello, C. E.; Colucci, W. S.; Cohen, R. A.; McComb, M. E.; Bachschmid, M. M. Does reversible cysteine oxidation link the Western diet to cardiac dysfunction? *FASEB J.* 2014, 28, 1975-1987.
203. Liang, H.; Ran, Q.; Jang, Y. C.; Holstein, D.; Lechleiter, J.; McDonald-Marsh, T.; Musatov, A.; Song, W.; Van Remmen, H.; Richardson, A. Glutathione peroxidase 4

- differentially regulates the release of apoptogenic proteins from mitochondria. *Free Radic. Biol. Med.* 2009, 47, 312-320.
204. Liang, H.; Yoo, S. E.; Na, R.; Walter, C. A.; Richardson, A.; Ran, Q. Short form glutathione peroxidase 4 is the essential isoform required for survival and somatic mitochondrial functions. *J. Biol. Chem.* 2009, 284, 30836-30844.
205. Cole-Ezea, P.; Swan, D.; Shanley, D.; Hesketh, J. Glutathione peroxidase 4 has a major role in protecting mitochondria from oxidative damage and maintaining oxidative phosphorylation complexes in gut epithelial cells. *Free Radic. Biol. Med.* 2012, 53, 488-497.
206. Baseler, W. A.; Dabkowski, E. R.; Jagannathan, R.; Thapa, D.; Nichols, C. E.; Shepherd, D. L.; Croston, T. L.; Powell, M.; Razunguzwa, T. T.; Lewis, S. E.; Schnell, D. M.; Hollander, J. M. Reversal of mitochondrial proteomic loss in Type 1 diabetic heart with overexpression of phospholipid hydroperoxide glutathione peroxidase. *Am. J. Physiol. Regul. Integr. Comp. Physiol.* 2013, 304, R553-65.
207. Liang, H.; Yoo, S. E.; Na, R.; Walter, C. A.; Richardson, A.; Ran, Q. Short form glutathione peroxidase 4 is the essential isoform required for survival and somatic mitochondrial functions. *J. Biol. Chem.* 2009, 284, 30836-30844.
208. Conrad, M. Transgenic mouse models for the vital selenoenzymes cytosolic thioredoxin reductase, mitochondrial thioredoxin reductase and glutathione peroxidase 4. *Biochim. Biophys. Acta* 2009, 1790, 1575-1585.
209. Loscalzo, J. Keshan disease, selenium deficiency, and the selenoproteome. *N. Engl. J. Med.* 2014, 370, 1756-1760.

210. Ghosh, S.; Rodrigues, B. Cardiac cell death in early diabetes and its modulation by dietary fatty acids. *Biochim. Biophys. Acta* 2006, *1761*, 1148-1162.
211. Borisov, A. B.; Ushakov, A. V.; Zagorulko, A. K.; Novikov, N. Y.; Selivanova, K. F.; Edwards, C. A.; Russell, M. W. Intracardiac lipid accumulation, lipotrophy of muscle cells and expansion of myocardial infarction in type 2 diabetic patients. *Micron* 2008, *39*, 944-951.
212. Sharma, S.; Adroge, J. V.; Golfman, L.; Uray, I.; Lemm, J.; Youker, K.; Noon, G. P.; Frazier, O. H.; Taegtmeyer, H. Intramyocardial lipid accumulation in the failing human heart resembles the lipotoxic rat heart. *FASEB J* 2004, *18*, 1692-700.
213. Stanley, W. C.; Recchia, F. A. Lipotoxicity and the development of heart failure: moving from mouse to man. *Cell Metab* 2010, *12*, 555-6.
214. Opie, L. H.; Knutti, J. The adrenergic-fatty acid load in heart failure. *J. Am. Coll. Cardiol.* 2009, *54*, 1637-1646.
215. Hill, B. G.; Haberzettl, P.; Ahmed, Y.; Srivastava, S.; Bhatnagar, A. Unsaturated lipid peroxidation-derived aldehydes activate autophagy in vascular smooth-muscle cells. *Biochem. J.* 2008, *410*, 525-534.
216. Okada, K.; Wangpoengtrakul, C.; Osawa, T.; Toyokuni, S.; Tanaka, K.; Uchida, K. 4-Hydroxy-2-nonenal-mediated impairment of intracellular proteolysis during oxidative stress. Identification of proteasomes as target molecules. *J. Biol. Chem.* 1999, *274*, 23787-23793.
217. Imai, H. Biological significance of lipid hydroperoxide and its reducing enzyme, phospholipid hydroperoxide glutathione peroxidase, in mammalian cells. *Yakugaku Zasshi* 2004, *124*, 937-957.

218. Nakamura, T.; Imai, H.; Tsunashima, N.; Nakagawa, Y. Molecular cloning and functional expression of nucleolar phospholipid hydroperoxide glutathione peroxidase in mammalian cells. *Biochem. Biophys. Res. Commun.* 2003, *311*, 139-148.
219. Sneddon, A. A.; Wu, H. C.; Farquharson, A.; Grant, I.; Arthur, J. R.; Rotondo, D.; Choe, S. N.; Wahle, K. W. Regulation of selenoprotein GPx4 expression and activity in human endothelial cells by fatty acids, cytokines and antioxidants. *Atherosclerosis* 2003, *171*, 57-65.
220. Frustaci, A.; Francone, M.; Petrosillo, N.; Chimenti, C. High prevalence of myocarditis in patients with hypertensive heart disease and cardiac deterioration. *Eur. J. Heart Fail.* 2013, *15*, 284-291.
221. Kass, D. A.; Shapiro, E. P.; Kawaguchi, M.; Capriotti, A. R.; Scuteri, A.; deGroof, R. C.; Lakatta, E. G. Improved arterial compliance by a novel advanced glycation end-product crosslink breaker. *Circulation* 2001, *104*, 1464-1470.
222. Little, W. C.; Zile, M. R.; Kitzman, D. W.; Hundley, W. G.; O'Brien, T. X.; Degroof, R. C. The effect of alagebrium chloride (ALT-711), a novel glucose cross-link breaker, in the treatment of elderly patients with diastolic heart failure. *J. Card. Fail.* 2005, *11*, 191-195.
223. Tsujita, K.; Shimomura, H.; Kaikita, K.; Kawano, H.; Hokamaki, J.; Nagayoshi, Y.; Yamashita, T.; Fukuda, M.; Nakamura, Y.; Sakamoto, T.; Yoshimura, M.; Ogawa, H. Long-term efficacy of edaravone in patients with acute myocardial infarction. *Circ. J.* 2006, *70*, 832-837.

224. Anderson EJ, Efird JT, Davies SW, O'Neal WT, Darden TM BS, Thayne KA, Katunga LA, Kindell LC, Ferguson TB, Anderson CA, Chitwood WR, Koutlas TC, Williams JM, Rodriguez E MD, Kypson AP. Monoamine oxidase is a major determinant of redox balance in human atrial myocardium and is associated with postoperative atrial fibrillation. *J. Journal of the American Heart Association (JAHA)* 2014.
225. Frezza, C.; Cipolat, S.; Scorrano, L. Organelle isolation: functional mitochondria from mouse liver, muscle and cultured fibroblasts. *Nat. Protoc.* 2007, 2, 287-295.
226. Gostimskaya, I.; Galkin, A. Preparation of highly coupled rat heart mitochondria. *J. Vis. Exp.* 2010, (43). pii: 2202. doi, 10.3791/2202.
227. Negre-Salvayre, A.; Auge, N.; Ayala, V.; Basaga, H.; Boada, J.; Brenke, R.; Chapple, S.; Cohen, G.; Feher, J.; Grune, T.; Lengyel, G.; Mann, G. E.; Pamplona, R.; Poli, G.; Portero-Otin, M.; Riahi, Y.; Salvayre, R.; Sasson, S.; Serrano, J.; Shamni, O.; Siems, W.; Siow, R. C.; Wiswedel, I.; Zarkovic, K.; Zarkovic, N. Pathological aspects of lipid peroxidation. *Free Radic. Res.* 2010, 44, 1125-1171.
228. Antunes, F.; Salvador, A.; Pinto, R. E. PHGPx and phospholipase A2/GPx: comparative importance on the reduction of hydroperoxides in rat liver mitochondria. *Free Radic. Biol. Med.* 1995, 19, 669-677.
229. Antunes, F.; Salvador, A.; Marinho, H. S.; Alves, R.; Pinto, R. E. Lipid peroxidation in mitochondrial inner membranes. I. An integrative kinetic model. *Free Radic. Biol. Med.* 1996, 21, 917-943.
230. Anderson, E. J.; Thayne, K.; Harris, M.; Carraway, K.; Shaikh, S. R. Aldehyde stress and up-regulation of Nrf2-mediated antioxidant systems accompany

- functional adaptations in cardiac mitochondria from mice fed n-3 polyunsaturated fatty acids. *Biochem. J.* 2012, *441*, 359-366.
231. Gutteridge, J. M. Lipid peroxidation and antioxidants as biomarkers of tissue damage. *Clin. Chem.* 1995, *41*, 1819-1828.
232. Boldyrev, A. A. Carnosine: new concept for the function of an old molecule. *Biochemistry (Mosc)* 2012, *77*, 313-326.
233. Gualano, B.; Everaert, I.; Stegen, S.; Artioli, G. G.; Taes, Y.; Roschel, H.; Achten, E.; Otaduy, M. C.; Junior, A. H.; Harris, R.; Derave, W. Reduced muscle carnosine content in type 2, but not in type 1 diabetic patients. *Amino Acids* 2012, *43*, 21-24.
234. Colzani, M.; Criscuolo, A.; De Maddis, D.; Garzon, D.; Yeum, K. J.; Vistoli, G.; Carini, M.; Aldini, G. A novel high resolution MS approach for the screening of 4-hydroxy-trans-2-nonenal sequestering agents. *J. Pharm. Biomed. Anal.* 2014, *91*, 108-118.
235. Ingram, K. H.; Hill, H.; Moellering, D. R.; Hill, B. G.; Lara-Castro, C.; Newcomer, B.; Brandon, L. J.; Ingalls, C. P.; Penumetcha, M.; Rupp, J. C.; Garvey, W. T. Skeletal muscle lipid peroxidation and insulin resistance in humans. *J. Clin. Endocrinol. Metab.* 2012, *97*, E1182-6.
236. Pillon, N. J.; Croze, M. L.; Vella, R. E.; Soulere, L.; Lagarde, M.; Soulage, C. O. The lipid peroxidation by-product 4-hydroxy-2-nonenal (4-HNE) induces insulin resistance in skeletal muscle through both carbonyl and oxidative stress. *Endocrinology* 2012, *153*, 2099-2111.

237. Cohen, G.; Riahi, Y.; Shamni, O.; Guichardant, M.; Chatgialloglu, C.; Ferreri, C.; Kaiser, N.; Sasson, S. Role of lipid peroxidation and PPAR-delta in amplifying glucose-stimulated insulin secretion. *Diabetes* 2011, *60*, 2830-2842.
238. Koulajian, K.; Ilovic, A.; Ye, K.; Desai, T.; Shah, A.; Fantus, I. G.; Ran, Q.; Giacca, A. Overexpression of glutathione peroxidase 4 prevents beta-cell dysfunction induced by prolonged elevation of lipids in vivo. *Am. J. Physiol. Endocrinol. Metab.* 2013, *305*, E254-62.
239. Giris, M.; Dogru-Abbasoglu, S.; Kumral, A.; Olgac, V.; Kocak-Toker, N.; Uysal, M. Effect of carnosine alone or combined with alpha-tocopherol on hepatic steatosis and oxidative stress in fructose-induced insulin-resistant rats. *J. Physiol. Biochem.* 2014, *70*, 385-395.
240. Mong, M. C.; Chao, C. Y.; Yin, M. C. Histidine and carnosine alleviated hepatic steatosis in mice consumed high saturated fat diet. *Eur. J. Pharmacol.* 2011, *653*, 82-88.
241. Echtay, K. S.; Pakay, J. L.; Esteves, T. C.; Brand, M. D. Hydroxynonenal and uncoupling proteins: a model for protection against oxidative damage. *Biofactors* 2005, *24*, 119-130.
242. Chen, J. J.; Bertrand, H.; Yu, B. P. Inhibition of adenine nucleotide translocator by lipid peroxidation products. *Free Radic. Biol. Med.* 1995, *19*, 583-590.
243. Sano, M.; Fukuda, K. Activation of mitochondrial biogenesis by hormesis. *Circ. Res.* 2008, *103*, 1191-1193.
244. Boudina, S.; Sena, S.; Theobald, H.; Sheng, X.; Wright, J. J.; Hu, X. X.; Aziz, S.; Johnson, J. I.; Bugger, H.; Zaha, V. G.; Abel, E. D. Mitochondrial energetics in the

- heart in obesity-related diabetes: direct evidence for increased uncoupled respiration and activation of uncoupling proteins. *Diabetes* 2007, 56, 2457-66.
245. Taegtmeyer, H.; Razeghi, P.; Young, M. E. Mitochondrial proteins in hypertrophy and atrophy: a transcript analysis in rat heart. *Clin Exp Pharmacol Physiol* 2002, 29, 346-50.
246. Mark, R. J.; Lovell, M. A.; Markesbery, W. R.; Uchida, K.; Mattson, M. P. A role for 4-hydroxynonenal, an aldehydic product of lipid peroxidation, in disruption of ion homeostasis and neuronal death induced by amyloid beta-peptide. *J. Neurochem.* 1997, 68, 255-264.
247. Aberle, N. S., 2nd; J., P. M., Sr; Amarnath, V.; Ren, J. Inhibition of cardiac myocyte contraction by 4-hydroxy-trans-2-nonenal. *Cardiovasc Toxicol* 2004, 4, 21-8.
248. Kim, M. Y.; Kim, E. J.; Kim, Y. N.; Choi, C.; Lee, B. H. Effects of alpha-lipoic acid and L-carnosine supplementation on antioxidant activities and lipid profiles in rats. *Nutr. Res. Pract.* 2011, 5, 421-428.
249. Chen, J. J.; Yu, B. P. Alterations in mitochondrial membrane fluidity by lipid peroxidation products. *Free Radic. Biol. Med.* 1994, 17, 411-418.
250. Meyer, M. J.; Mosely, D. E.; Amarnath, V.; J., P. M., Sr Metabolism of 4-hydroxy-trans-2-nonenal by central nervous system mitochondria is dependent on age and NAD⁺ availability. *Chem Res Toxicol* 2004, 17, 1272-9.
251. Pryde, D. C.; Dalvie, D.; Hu, Q.; Jones, P.; Obach, R. S.; Tran, T. D. Aldehyde oxidase: an enzyme of emerging importance in drug discovery. *J. Med. Chem.* 2010, 53, 8441-8460.

252. Tabrizchi, R. Edaravone Mitsubishi-Tokyo. *Curr. Opin. Investig Drugs* 2000, 1, 347-354.
253. Watanabe, T.; Yuki, S.; Egawa, M.; Nishi, H. Protective effects of MCI-186 on cerebral ischemia: possible involvement of free radical scavenging and antioxidant actions. *J. Pharmacol. Exp. Ther.* 1994, 268, 1597-1604.
254. Aldini, G.; Dalle-Donne, I.; Facino, R.; Milzani, A.; Carini, M. Intervention strategies to inhibit protein carbonylation by lipoxidation-derived reactive carbonyls. *Medicinal Research Reviews* 2007, 27, 817-868.
255. Tsujita, K.; Shimomura, H.; Kawano, H.; Hokamaki, J.; Fukuda, M.; Yamashita, T.; Hida, S.; Nakamura, Y.; Nagayoshi, Y.; Sakamoto, T.; Yoshimura, M.; Arai, H.; Ogawa, H. Effects of edaravone on reperfusion injury in patients with acute myocardial infarction. *Am. J. Cardiol.* 2004, 94, 481-484.
256. Edelstein, D.; Brownlee, M. Mechanistic studies of advanced glycosylation end product inhibition by aminoguanidine. *Diabetes* 1992, 41, 26-29.
257. Thornalley, P. J. Use of aminoguanidine (Pimagedine) to prevent the formation of advanced glycation endproducts. *Arch. Biochem. Biophys.* 2003, 419, 31-40.
258. Colzani, M.; Criscuolo, A.; De Maddis, D.; Garzon, D.; Yeum, K. J.; Vistoli, G.; Carini, M.; Aldini, G. A novel high resolution MS approach for the screening of 4-hydroxy-trans-2-nonenal sequestering agents. *J. Pharm. Biomed. Anal.* 2014, 91, 108-118.
259. Chang, K. C.; Liang, J. T.; Tsai, P. S.; Wu, M. S.; Hsu, K. L. Prevention of arterial stiffening by pyridoxamine in diabetes is associated with inhibition of the pathogenic glycation on aortic collagen. *Br. J. Pharmacol.* 2009, 157, 1419-1426.



**Animal Care and
Use Committee**

212 Ed Warren Life
Sciences Building
East Carolina University
Greenville, NC 27834

252-744-2436 office
252-744-2355 fax

November 10, 2011

Ethan Anderson, Ph.D.
Department of Pharmacology
Brody 6S-10
ECU Brody School of Medicine

Dear Dr. Anderson:

Your Animal Use Protocol entitled, "Mouse Models of Inflammation and Heart Disease" (AUP #W231) was reviewed by this institution's Animal Care and Use Committee on 11/10/11. The following action was taken by the Committee:

"Approved as submitted"

Please contact Dale Aycock at 744-2997 prior to hazard use

A copy is enclosed for your laboratory files. Please be reminded that all animal procedures must be conducted as described in the approved Animal Use Protocol. Modifications of these procedures cannot be performed without prior approval of the ACUC. The Animal Welfare Act and Public Health Service Guidelines require the ACUC to suspend activities not in accordance with approved procedures and report such activities to the responsible University Official (Vice Chancellor for Health Sciences or Vice Chancellor for Academic Affairs) and appropriate federal Agencies.

Sincerely yours,

A handwritten signature in black ink, appearing to read 'Scott E. Gordon'.

Scott E. Gordon, Ph.D.
Chairman, Animal Care and Use Committee

SEG/jd

enclosure



**Animal Care and
Use Committee**

212 Ed Warren Life
Sciences Building
East Carolina University
Greenville, NC 27834

252-744-2436 office
252-744-2355 fax

November 10, 2011

Ethan Anderson, Ph.D.
Department of Pharmacology
Brody 6S-10
ECU Brody School of Medicine

Dear Dr. Anderson:

Your Animal Use Protocol entitled, "Mouse Models of Inflammation and Heart Disease" (AUP #W231) was reviewed by this institution's Animal Care and Use Committee on 11/10/11. The following action was taken by the Committee:

"Approved as submitted"

Please contact Dale Aycock at 744-2997 prior to hazard use

A copy is enclosed for your laboratory files. Please be reminded that all animal procedures must be conducted as described in the approved Animal Use Protocol. Modifications of these procedures cannot be performed without prior approval of the ACUC. The Animal Welfare Act and Public Health Service Guidelines require the ACUC to suspend activities not in accordance with approved procedures and report such activities to the responsible University Official (Vice Chancellor for Health Sciences or Vice Chancellor for Academic Affairs) and appropriate federal Agencies.

Sincerely yours,

A handwritten signature in black ink, appearing to read 'Scott E. Gordon'.

Scott E. Gordon, Ph.D.
Chairman, Animal Care and Use Committee

SEG/jd

enclosure



**Animal Care and
Use Committee**

212 Ed Warren Life
Sciences Building
East Carolina University
Greenville, NC 27834

252-744-2436 office
252-744-2355 fax

November 10, 2011

Ethan Anderson, Ph.D.
Department of Pharmacology
Brody 6S-10
ECU Brody School of Medicine

Dear Dr. Anderson:

Your Animal Use Protocol entitled, "Mouse Models of Inflammation and Heart Disease" (AUP #W231) was reviewed by this institution's Animal Care and Use Committee on 11/10/11. The following action was taken by the Committee:

"Approved as submitted"

Please contact Dale Aycock at 744-2997 prior to hazard use

A copy is enclosed for your laboratory files. Please be reminded that all animal procedures must be conducted as described in the approved Animal Use Protocol. Modifications of these procedures cannot be performed without prior approval of the ACUC. The Animal Welfare Act and Public Health Service Guidelines require the ACUC to suspend activities not in accordance with approved procedures and report such activities to the responsible University Official (Vice Chancellor for Health Sciences or Vice Chancellor for Academic Affairs) and appropriate federal Agencies.

Sincerely yours,

A handwritten signature in black ink, appearing to read 'Scott E. Gordon'.

Scott E. Gordon, Ph.D.
Chairman, Animal Care and Use Committee

SEG/jd

enclosure